Investigation of the neural mechanisms in illusory glare perception

(主観的なグレア知覚形成の神経機序の解明)

January 2020

Doctor of philosophy(Engineering)

Yuta Suzuki

Toyohashi University of Technology

別紙４－１（課程博士（英文））

Date of Submission（month day, year）: January 10th, 2020

Department of Computer Science and Engineering	Student ID Number	D133337
Applicant's name	Yuta Suzuki	

Supervisors	Shigeki Nakauchi Tetsuto Minami

Abstract（Doctor）

Title of Thesis	Investigation of the neural mechanisms in illusory glare perception

Approx. 800 words

The perceived intensity of light coming from a given portion of an object (brightness) and the perceptual experiences of a black, grey, or white-colored surface and self-luminosity (lightness) are some of the basic aspects of visual processing. Glare illusion, which is an optical illusion, enhances the perceived brightness of a central white area surrounded by a luminance gradient without any actual change in light intensity. Our experiences of perceptual misunderstanding are sometimes caused by optical illusions that create visual images that may carry deceptive interpretations. Although it seems that optical illusions trick our brains into believing things that may or may not be real, they demonstrate how the brain makes the most probable prediction about an ambiguous visual input. This is not a retina-level process, but a serial processing occurring in the brain, which is valuable for understanding how the brain interprets visual stimuli from the external world.

The pupillary response is mainly a function of retinal illuminance owing to the amount of light energy or quanta entering the eye from the ambient environment. Although one of the main functions of pupil constriction would seem to be the protection of our eyes from being dazzled by intense physical light, previous studies using pupillometry have revealed that the pupil is also constricted by the perceived intensity of light in the absence of any change in light intensity via glare illusion. Because the visual system processes luminance information from a graphical image as if it were a natural scene, colors could play an important role in the perception of brightness. In this study, we first examined whether pupil constrictions to glare illusion are stronger for blue compared to other colors. Our results indicate that blue was subjectively evaluated by participants as the brightest condition, despite all colored stimuli being equiluminant. Moreover, glare-related pupil constrictions for each participant were correlated to each individual's subjective brightness adjustments. Together, these findings show that pupillometry constitutes an easy tool to assess individual differences in color brightness perception.

Second, we tested the hypothesis that the ecological background, where getting dazzled by light is common when one directly looks at sunlight through some occluders, can explain the larger pupil constriction to blue. Interestingly, we found the effect of blue on pupillary constriction occurs only for people with black/brown iris colors. Because the iris color relates to the macular pigment density as a marker for the adaptation to the homogeneous environment, we assumed that the pupillary constriction represents the adaptation response to a probable dazzling sunlight imitated by glare illusion, and the pupil constriction might be similar to the function of macular pigments to filter the blue light projecting to the retina.

Next, we examined two probable factors to modulate the pupil size in glare illusion by using the Kanizsa

triangle with a radial pattern of luminance gradation and a control pattern. We assumed that the pupil constriction to glare illusion represents: (a) the role of 'anticipation' or 'preparation' to probable glare situation from the Sun or scattering light, and (b) the localized stimulus pattern because the averaged luminance of the glare illusion within a small visual field is higher than its control condition, where the rotated luminance gradient pattern. Our results show a larger pupil constriction effect on the Kanizsa triangle with the radial pattern; therefore, we conclude that the pupil constriction to glare illusion is prompted by self-luminosity perception. The effect of the brightness judgment on pupil response shown in previous works is considered additionally to the effect of 'self-luminosity' to the brightness perception but via difference pathway from surface color perception.

We subsequently investigated the correlation between pupil constriction and electroencephalography (EEG) response of the amplitude of the steady-state visual evoked potential (SSVEP) on the illusory brightness enhancement with glare illusion. We found that the SSVEP amplitude was lower in glare illusion than in the control condition (no glare condition), especially under high luminance contrast conditions. The probable correlation of the inhibited SSVEP amplitude to the high luminance contrast of glare illusion accompanied by the greater pupil constriction may be because of the decreased amount of light entering the pupil. Therefore, the brightness enhancement in the glare illusion is already represented at the primary stage of visual processing linked to the larger pupil constriction.

As a conclusion, we have put together the evidence of the larger pupil constriction effect on glare illusion that can be elegantly explained by the ecology of vision that the large pupil constriction on the illusory glare perception may be a prediction of the probable strong light, especially for blue, sky-like, glare illusion makes more powerful effect in causing constrictions.

Acknowledgments

I am grateful to my supervisors, Professor Shigeki Nakauchi and Tetsuto Minami, of Toyohashi University of Technology, for providing insightful comments and discussions. I would also like to express my gratitude to Professor Bruno Laeng of Oslo University for giving me the opportunity to work at Oslo University for six months and for his enormous support to my entire thesis.

I would like to thank Associate Professor Hiroshi Higashi of Kyoto University, Dr. Hsin-I Liao of NTT CS Lab and my ph.d thesis reviewers for giving me constructive comments and warm encouragement. I am also grateful to all colleagues in the Visual Perception and Cognition Lab and RITMO and Ms. Yuki Kawai for participating to my experiments and supporting my laboratory life. Finally, I would like to express my gratitude to my parents for supporting my student life.

This work was supported by Grants-in-Aid for Scientific Research from the Japan Society for the Promotion of Science (grant number 17H01807, 17H06292, 18J11571), the grants for JSPS research fellow (DC2), and the Program for Leading Graduate Schools at Toyohashi University of Technology.

Contents

List of Figures

Chapter 1

Introduction

1.1 Brightness perception

The perceived intensity of light coming from a given portion of an object (brightness) and the perceptual experiences of a black, grey, or white-colored (lightness) surface are some of the basic aspects of visual processing. For instance, gray objects appear darker in front of a white background compared to a black background, as shown in Figure 1.1(A). This phenomenon, called simultaneous contrast, is simply explained by low-level visual processing via photoreceptors with lateral inhibition (Kingdom, 1997; Lotto et al., 1999; McCourt, 1982). In addition to simultaneous contrast, the assimilation effect is important in processing the perceived brightness of objects. In Figure 1.1(B), the gray region surrounding the black circle on the left panel appears darker than the outer gray circle on the right panel, even though both circles have the same physical luminance level. The brain interpret the rings in the figures as group objects, so-called 'assimilation', which leads to perceiving a lower overall luminance in the left figure. This indicates that the simultaneous contrast is processed by low-level visual mechanisms, such as a post-retinal mechanism, while the brightness assimilation needs to process objects for grouping in the cortex level rather than in the photoreceptors level (Wook Hong and Shevell, 2004). Figure 1.1(C) shows an optical illusion produced by lateral inhibition. The gradation consists of no-gradation white and black on both sides of the figure and luminance gradation between them. The edge between gradation and white/black appears brighter/darker than the actual luminance. This is because the lateral inhibition on the edge from the white/black to the gradation is weak (e.g., Lotto et al., 1999). Although there are many and varied examples of optical illusion explained by lateral inhibition, the mechanisms of several bright illusions remain unknown. For instance, we perceive the flickers at the grid intersections in Figure 1.1(D). This was explained by the retinal ganglion cell responses of on-center, off-surround neurons on the retina (Hermann, 1870; Ishigughi, 1987). However, it has been argued that the lateral inhibition can

completely explain the illusion because the distortion version of the grid in the right figure eliminates the illusion. If lateral inhibition creates the illusion, the flicking effect should still be in the distortion grid. In addition to the Hermann grid illusion, the illusory brightness perception in Figure 1.1(E) affects the overall object. Therefore, the bright illusion cannot be explained by lateral inhibition alone. Purves et al. (1999) explained that the Craik-O'Brien-Cornsweet effect occurs because we predict the light reflex illuminated on a target object from surrounding context based on our experience. Similarly, the visual system estimates that the left figure is poorly reflective and strongly illuminated, while the right figure is highly reflective and weakly illuminated (Cornsweet, 1970; Kingdom and Moulden, 1988; Purves et al., 2001, 1999). Figure 1.1(F) also involves cortex processing. The brightness in portion B appears brighter than in portion A owing to the effect of shadow falling on the checkerboard (Adelson, 1995). These optical illusions imply that our experiences of perceptual misunderstanding sometimes occur because of optical illusions that create visual images carrying deceptive interpretations. Although it seems that optical illusions trick our brains into believing things that may or may not be real, they demonstrate how the brain makes the most probably prediction about an ambiguous visual input. This is not a retina-level process but a serial processing occurring in the brain which is valuable for understanding how the brain interprets things from the external world.

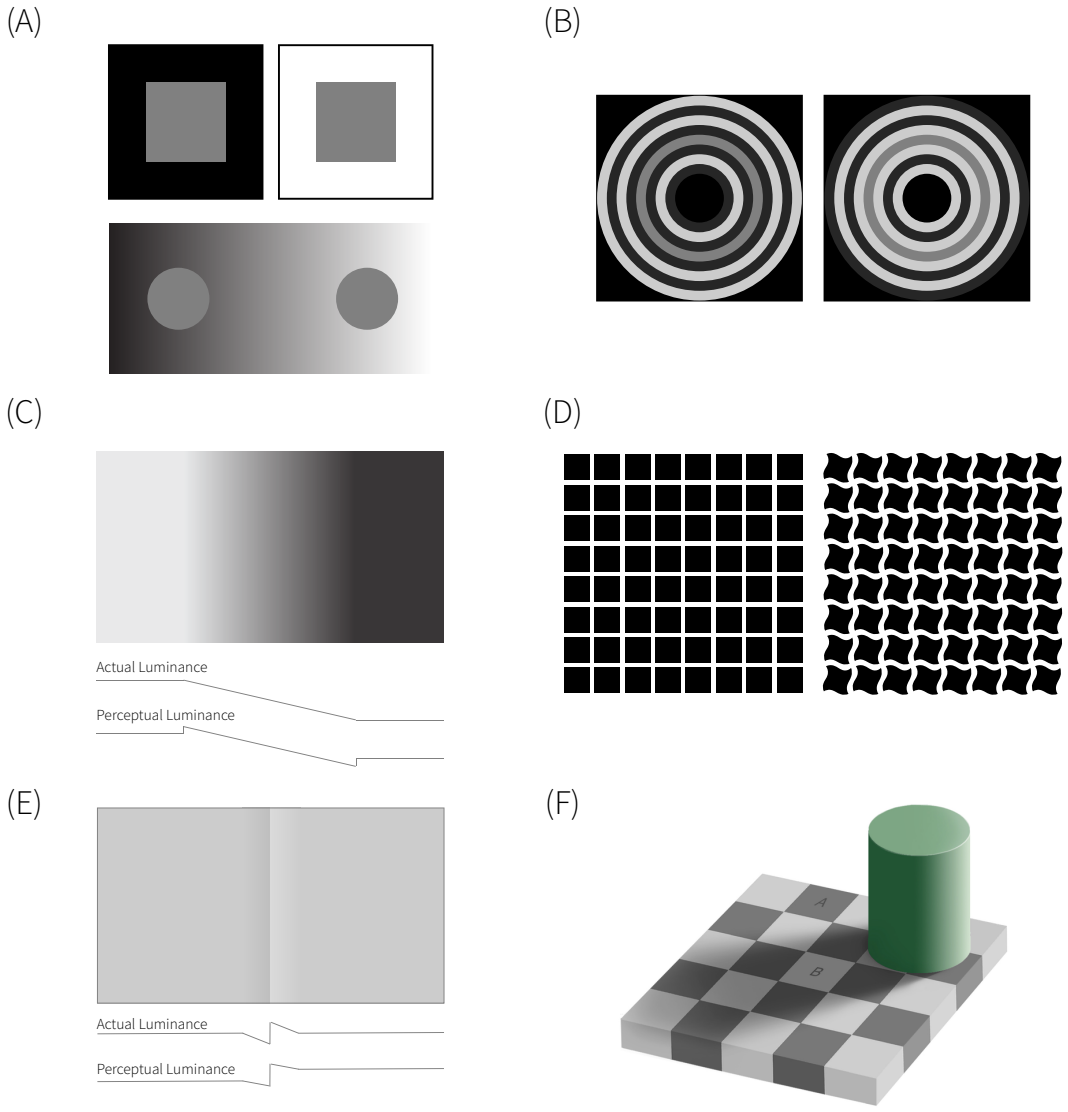

Figure 1.1 Examples of brightness illusion.

(A) Simultaneous contrast and gradation induction (Kingdom, 1997; Lotto et al., 1999; McCourt, 1982), (B) Hong-Shevell's rings (Wook Hong and Shevell, 2004), (C) Machband (Lotto et al., 1999), (D) Hermann grid illusion (Hermann, 1870; Ishigughi, 1987), (E) Craik-O'Brien-Cornsweet effect (Cornsweet, 1970; Kingdom and Moulden, 1988; Purves et al., 1999), (F) Checker-shadow illusion (Adelson, 1995)

1.2 Pupillometry

1.2.1 Pupillary light reflex and its circuit

In the human eye structure, pupils play a role in adjusting light coming into the retina. The pupil size is controlled by two incompatible muscles, the sphincter and dilator muscles; the pupil is constricted in bright situations by the sphincter muscles and is dilated in dark situations by the dilator muscles (Beatty and Lucero-Wagoner, 2000; Granholm and Steinhauer, 2004; Samuels and Szabadi, 2008). The light entering into the retina is translated to an electric signal and projected to the pretectal olivary nucleus (PON), visual cortex, and superior colliculus (SC); then, the pupillary light reflex is evoked (Gamlin, 2006). Although there is a pathway from the lateral geniculate nucleus (LGN) and visual cortex to induce the pupillary light reflex, a direct neural pathway that does not go through cortical processing exists to control the pupillary light reflex (PLR), as demonstrated by the pupil responses to flux-equated gratings in patients in the absence of V1 (Weiskrantz et al., 1998). Dilator muscles are controlled by PLR-related neural pathways and sympathetic nerve systems such as locus coeruleus (LC) (Loewenfeld, 1993; Samuels and Szabadi, 2008), while pupil constriction through the sphincter muscles is controlled by the inhibition neural circuit via the Edinger-Westphal (EW) nucleus and parasympathetic nerve systems (Lüdtke et al., 1999). Owing to the different neural systems, the velocity of change for pupil constriction is three times faster than that for pupil dilation (Bergamin et al., 1998; Ellis, 1981). In general, the pupil size changes from approximately 9 mm under dark illumination (MacLachlan and Howland, 2002) to 3 mm under bright illumination (Wyatt, 1995). Pupil size varies with human aging because of increasing sympathetic (Hotta and Uchida, 2010) and decreasing parasympathetic nervous system activities (Arnold et al., 2012). Furthermore, recent studies have reported that the average pupil size is different between genders and iris colors (e.g., Bergamin et al., 1998; Bradley et al., 2010; Dain et al., 2004).

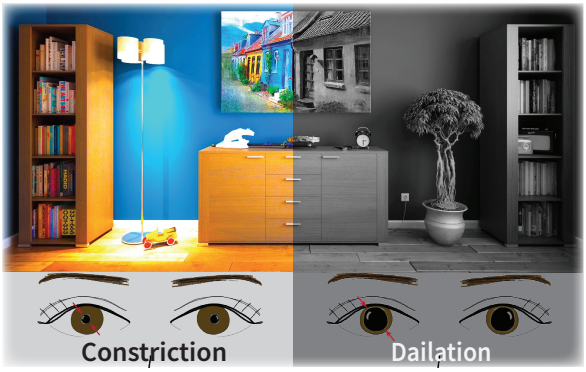

Figure 1.2 Pupil constriction and dilation.

The pupillary light reflex model is defined by Moon and Spencer (1944) as shown in Equation 1.1 and illustrated in Figure 1.3. It has been noted that there are, in general, substantial individual differences in the pupil size, latency, velocity of pupil constriction, and re-dilation toward the baseline pupil size, even to identical light intensity (Spencer and Moon, 1944; Winn et al., 1994). As mentioned above, because pupil size depends on age, Watson et al. (2012) proposed a model including the effect of

age as an independent variable (Watson and Yellott, 2012). Pamplona et al. (2009) expanded on the PLR model by including the light sensitivity based on individual differences. The model predicted the time course of pupil changes to light, as shown Equation 1.2 (Pamplona et al., 2009). These pupillary models can be applied to vision science and used to imitate the natural pupil changes on computer graphics.

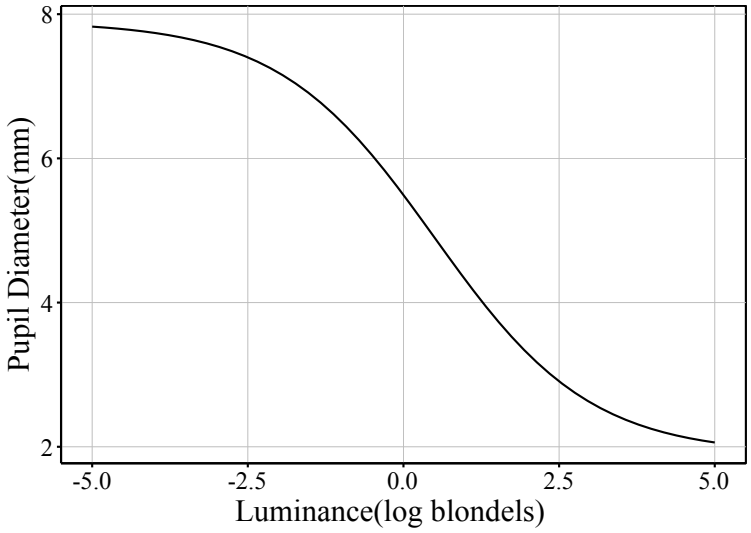

Figure 1.3 Pupil light reflex model defined by Moon and Spencer (1944).

$$D = 4.9 - 3tanh(0.4(log_{10}(L_b) - 0.5)) \tag{1.1}$$

$$\frac{dM}{dD}\frac{dD}{dt} + 2.3026atanh\left(\frac{D-4.9}{3}\right) = 5.2 - 0.45\ln\left[\frac{\phi(t-\tau)}{\hat{\phi}}\right] \tag{1.2}$$

1.2.2 LC and noradrenergic activity

The pupils also reflect the activity of the cortical mechanisms of the noradrenergic system from the LC (Aston-Jones and Cohen, 2005; Sara, 2009). Norepinephrine is a neurotransmitter from the LC related to many functions through its widespread projections, such as the cerebral cortex, cerebellum, and hippocampus to control the autonomic nerve system (ANS), the so-called locus coeruleus norepinephrine system (LC-NE system). The pupillary change is involved by the ANS according to our thoughts, emotions, and attention (Goldwater, 1972; Loewenfeld, 1993). For example, the pupil is dilated by high-arousal images, such as of spiders or snakes (Bradley et al., 2008; Sterpenich et al., 2006)), and by carrying out

difficult tasks demanding high work load because of the sympathetic nerve system, e.g., working memory tasks (Kahneman and Beatty, 1966; Klingner et al., 2011). Remarkably, pupil responses can reflect the perceived brightness on the bright illusion as well as an image of the sun (Binda et al., 2013b; Laeng and Endestad, 2012; Suzuki et al., 2019a). The pupillary response, "window as an unconsciousness and pre-consciousness processing marker", can be an easy tool to access our implicit processing or attention (e.g., Beatty, 1982; Granholm and Steinhauer, 2004; Sirois and Brisson, 2014; Suzuki et al., 2018). Although the pupil change is affected by the LC-NE system related to the perception/cognition, the changes are merely additional or side effects to control the entire brain processing, including the spinal cord, brain stem, cerebellum and hypothalamus (Beatty and Lucero-Wagoner, 2000; Samuels and Szabadi, 2008), and the extent of pupil change related to cognitive factors is a maximum of 0.5 mm (Beatty and Lucero-Wagoner, 2000).

1.2.3 A window as marker of a pre-consciousness processing

"Which is bigger, a baseball or a soccer ball?" We can easily answer this question by visualizing the objects in our mind, even if there is not an actual object in front of us. Philosophers, scientists, and especially neuroscientists have been interested in how visual images are created by involving our thinking, understanding, memory, creativity, emotion, etc. In the 17th century, Descartes (1596 - 1650), the "Father of Modern Philosophy", claimed dualism, which explained the relationship between our mind and body. Dualism proposes a strict distinction between our mind and matter (e.g., body or brain). However, common knowledge has since changed with the advances in cognitive neuroscience. The rapid progress of technology used to observe brain activities have revealed that our consciousness is created by the numerous neuron activities in the cerebral cortex. Additionally, the relationship between the mind, what we think or want, and the brain activities has been explored. Benjamin Libet (1916 - 2007), a doctor at the University of California, provided an impressive bulk of evidence that the firing neurons of the brain are preceded by our decision of voluntary motor act, the so-called "readiness potential" (Libet et al., 1983). That is, the unconscious readiness neuron activity is prior to the conscious decision making to act ourselves. This phenomenon refutes the previous theory that our free will decides what we do. Spinoza (1632 - 1677) claimed that one consequence is caused by another consequence and influences another result, an idea that is indeed consistent with the current theory. These outcomes are provided by neurophysiological methods, such as single neuron measurements, electroencephalograms and fMRI, which have made a breakthrough to understanding brain functions. Furthermore, pupillometry is a technique that can monitor our preconscious mind using the pupil size as a marker of preconscious level processing (Laeng et al., 2012). Recent studies demonstrated that subliminal reward of higher benefit cues prompted large pupil dilation similarly to supraliminal cues on decision-making tasks (Bijleveld

et al., 2009). Another study with blindsight patients reported that unseen emotional expressions evoked pupil dilation (Tamietto et al., 2009). It is thought that unconscious processing accounts for more than 90% of the entire brain processing. Therefore, these techniques can be valuable for understanding brain processing related to our perception.

1.2.4 Pupil measurement method

The history of eye-tracking measurement started when Johannes Peter Müller (1801–1858) directly observed a capillary on an iris to track the eye movement. In 1897, Huey implemented the technique for measuring the eye movement during reading using a plaster eye contact lens attached to a lever (Huey, 1898). The advancements in optical techniques in the 20th century have enabled the application of cameras for tracking the eye movement (Yarbus, 1967). Over the past several decades, advancements in eye-tracking techniques have been efficiently and broadly used in research on cognitive processes. Nowadays, the most commonly used non-intrusive eye-tracking technique is pupil center corneal reflection. As shown in Figure 1.4, a near-infrared light projected to the eyes produces a reflection point on the corneal (Purkinje images), and the camera recognizes the pupil and gaze direction by the Purkinje images and pupil of the captured eye image.

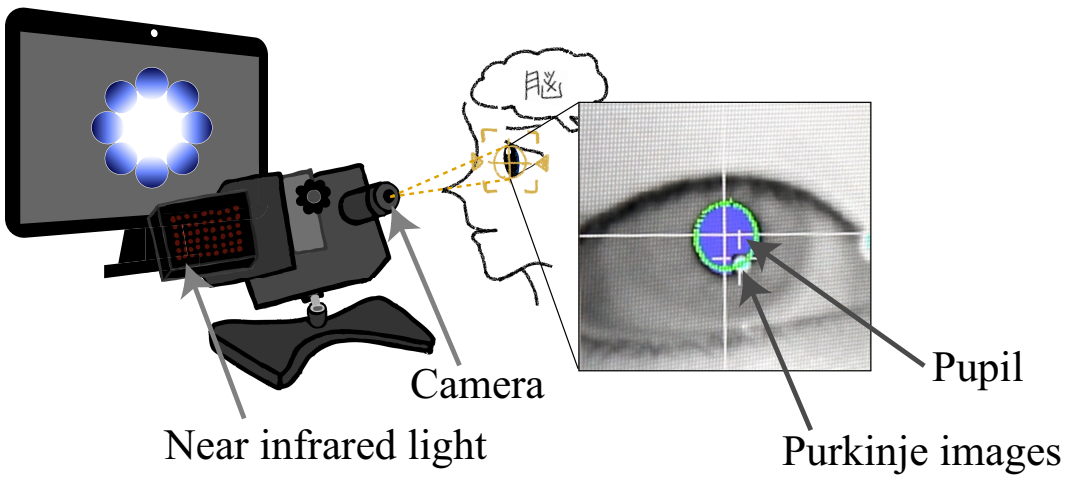

Figure 1.4 Eye-tracking system (Eyelink 1000).

1.3 Approach

Although several previous studies showed that colors per se can affect the pupil diameter (Gamlin et al., 1998; Kimura and Young, 1995; Tsujimura et al., 2001), pupillary constrictions in relation to the illusory brightness enhancement with varied stimulus properties, such as color, visual angle, and subjective brightness judgment, have been less explored. Furthermore, the relationship between the pupil constriction effect on glare illusion and brain activities remains unknown. To approach this problem, we are monitoring the pupil size with an infrared eye-tracker during the colored glare illusion, which evokes the impression of actual natural scenes presented on the screen (Chapter 2). If the pupillary response reflects the subjective brightness perception, it relates to the extent of the brightness modulated by the colors. Additionally, we measured the varied brightness and neurophysiological responses of electroencephalography (EEG) and pupil size with several luminance contrast patterns of glare illusion to address the question of whether the illusory brightness changes owing to the glare illusion process in the early visual cortex.

1.4 Overview

This thesis consists of five chapters (Figure 1.5). The first chapter presents the history of brightness perception in neuroscience and consciousness and pupillometry and gives an overview of this study. In the second chapter, we examine the causal relationship on an illusory glare perception between the pupil and brain signal by using steady-state visual evoked potentials (SSVEPs), which are one of the EEG components at early visual cortex. In the third chapter, we focus on the pupillary response to the luminosity perception, which is one of the modes of color appearance to elucidate the factor that prompts pupil constriction. In the fourth chapter, we investigate the perceived luminance (brightness) to colored glare illusion and the relationship between brightness and pupil constriction. In the fifth chapter, since we hypothesized that pupil constrictions to 'blue' reflect an ecologically-based expectation of the visual system from the experience of sky light and color, we test the pupillometry of colored glare illusion to the varied iris color participants. As a conclusion, we summarize the highlights of our study in the final chapter.

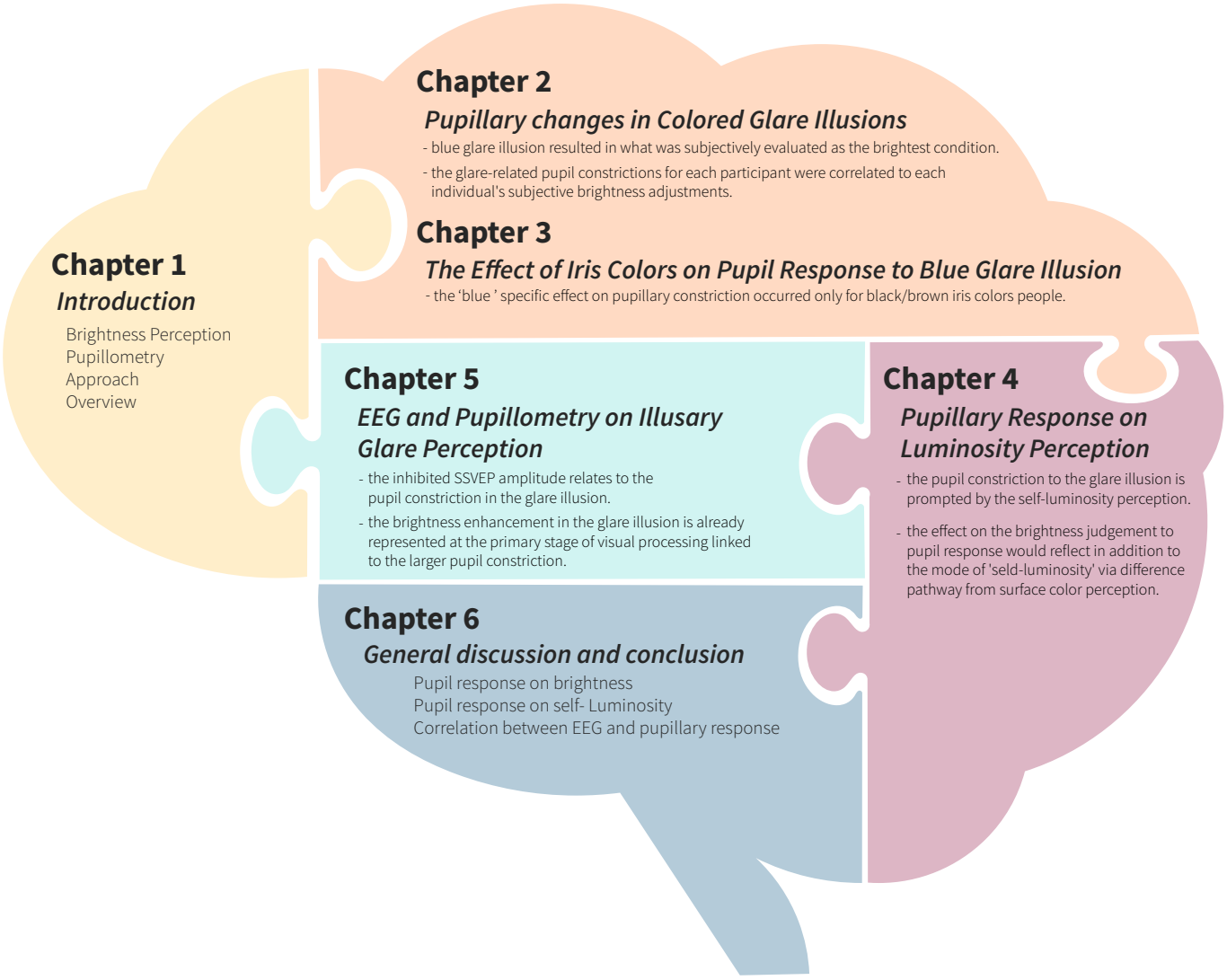

Figure 1.5 Thesis overview.

Chapter 2

Pupillary Changes in Colorful Glare Illusion

We hypothesized that pupil constrictions to the glare illusion, where converging luminance gradients subjectively enhance the perception of brightness, would be stronger for 'blue' than for other colors. Such an expectation was based on reflections about the ecology of vision, where the experience of dazzling light is common when one happens to look directly at sunlight through some occluders. Thus, we hypothesized that pupil constrictions to 'blue' reflect an ecologically-based expectation of the visual system from the experience of sky's light and color, which also leads to interpret the blue gradients of illusory glare to act as effective cues to impending probable intense light. We therefore manipulated the gradients color of glare illusions and measured changes in subjective brightness of identical shape stimuli. We confirmed that the blue resulted in what was subjectively evaluated as the brightest condition, despite all colored stimuli were equiluminant. This enhanced brightness effect was observed both in a psychophysical adjustment task and in changes in pupil size, where the maximum pupil constriction peak was observed with the 'blue' converging gradients over and above to the pupil response to blue in other conditions (i.e., diverging gradients and homogeneous patches). Moreover, glare-related pupil constrictions for each participant were correlated to each individual's subjective brightness adjustments. Homogenous blue hues also constricted the pupil more than other hues, which represents a pupillometric analog of the Helmholtz-Kohlrausch effect on brightness perception. Together, these findings show that pupillometry constitutes an easy tool to assess individual differences in color brightness perception.

2.1 Introduction

The pupillary response is mainly a function of retinal illuminance due to the amount of light energy or quanta entering the eye from the ambient environment. For example, in a bright room, the pupil constricts whereas it dilates in the darkroom via a simple subcortical reflex (Ellis, 1981; Woodhouse and Campbell, 1975). In addition to this role of physiological reflex, the pupil response can reflect several cognitive and affective factors such as mental or cognitive effort, overt and covert attentional shifts, visual awareness, emotional arousal and mental imagery (Beatty, 1982; Fahle et al., 2011; Laeng et al., 2012; Mathôt et al., 2013; Wang and Munoz, 2015). Although one of the main functions of pupil constriction would seem that of protecting our eyes from being dazzled by intense physical light, previous studies using pupillometry have revealed that the pupil is also constricted by perceived intensity of light in the absence of any change of light intensity, as in the so-called "glare illusion" (Laeng and Endestad, 2012; Laeng et al., 2018; Suzuki et al., 2018, 2019b; Zavagno et al., 2017) as well as when viewing photo images of the sun (e.g., Binda et al., 2013b; Naber and Nakayama, 2013).

The glare illusion is a "shining" example of brightness illusion evoked by luminance gradients converging onto a central white area (Agostini and Galmonte, 2002; Zavagno, 1999, see also http://www.ritsumei.ac.jp/~akitaoka/light-e.html). The typical pattern is perceived as having a luminous central region emitting light, in this case through the central hole of the pattern (see Figure 2.2). According to psychophysics studies, the perceived brightness can be enhanced up to 20–40% by the glare illusion compared to a control stimulus with homogeneous luminance (e.g., Yoshida et al., 2008). A commonly encountered example is the "glowing" effect of the sun in a computer graphics' image or in an art painting (e.g., "the Sun" by Edvard Munch, 1911).

In general, as observers, we estimate from the context what would be the luminance reflected from the depicted object, even if the object actually has neither the physical characteristics of a light source nor of a reflecting surface. The term brightness refers often in psychology and neuroscience to the perceived intensity of light coming from a given portion of an object, whereas 'lightness' to the perceived surface reflectance of an object in the scene (e.g., Purves et al., 2004). The effect of luminance on brightness and surface color perception can vary widely with the situation, context, and our own visual memories (Gilchrist, 2006; Zavagno et al., 2011). An optical illusion is a good example of how perceptions can be differently constructed from a same visual input. Importantly, perceptual illusions reveal the assumptions that the mind relies upon when 'inferring' perceptual information or the "priors" that the brain uses to recognize states and statistical regularities of the world (Brown and Friston, 2012; Purves et al., 2014). In the ecology of vision, looking up towards the sky and sunlight is likely to provoke a "dazzling" effect on the eyes, which can incapacitate vision temporarily (Bargary et al., 2014; Patterson

et al., 2015). Given that the color most associated with the sky is blue and partial occluder will typically appear as gradients of luminance converging towards sunlight, we surmise that the blue color may engender a stronger sense of brightness than any other color. In other words, we hypothesize that the visual system will tend to interpret the blue gradients of the 'glare' brightness illusion as particularly effective cues to probable intense light. In turn, a blue-related strong pupil constriction would seem to constitute an adaptive response to this ecologically-grounded expectation. In other words, past experiences in the natural environment shape the brightness and color perceptions of humans. Corney and colleagues suggested an ecological account for color perception using evidence from artificial neural networks (ANNs). Specifically, they developed models of the empirical process of learning and development from stimuli, with feedback from the environment. They were able to show that ANNs trained by various nature-like images (so-called 'dead-leaves' in a synthetic environment with similar statistical properties as natural images) result in similar brightness illusions as perceived by humans.

Importantly, in a significant number of stimuli, a layer with gaps was superimposed of the stimulus layer (under independent illumination), so as to simulate viewing background objects beyond illuminated foreground objects, like when "looking through the branches of a tree" (Corney and Lotto, 2007, p. 1791). The networks' task was to predict the source reflectance of the stimulus at the center of each scene and, with learning, these networks exhibited the same illusions of lightness that humans would report in the same situation. This finding suggests that the history of visual experience, with scenes highly similar to those resulting in enhanced perceived brightness in humans, is sufficient to generate the same illusory effect in the networks. Remarkably, pupil responses can reflect the subjective experiences better than objective properties of the stimuli (Binda et al., 2013a; Fahle et al., 2011; Naber et al., 2011, 2013). In their original study, Laeng and Endestad (2012) had observers view the glare illusion called "Asahi" figure (Kitaoka, 2005) while monitoring their pupil with an eye-tracker, which resulted in dramatic and rather long-lasting constrictions of the pupils compared to its control condition, where the same gradient elements of the Asahi pattern were rotated 180 degrees so as to destroy the central, subjective brightness enhancement while leaving unchanged the photometric levels of luminance of the whole pattern (see also Laeng et al., 2018, for a replication of the pupillary constriction with the same illusion). However, in actual natural scenes, the same objects can often take varied chromatic hues. Thus, if the visual system processes luminance information from a graphical image as if it were a natural scene (Zavagno et al., 2017), colors could play an important role in the perception of brightness.

Another situation in which brightness perception appears unrelated to the stimulus' luminance is the Helmholtz-Kohlrausch (HK) effect, where the brightness of a colored patch changes with relative saturation (i.e., its spectral purity), so that strongly colored stimuli appear brighter than the less colored ones and this also depends on the spectral distribution. That is, a hue's chroma and saturation can affect

perceived brightness of homogenous patches of color (e.g., 'greens' and 'yellows' appear less bright than 'reds' and 'blues'), despite these can all have the same luminance (Wood, 2012). Colors with greater saturation have a larger peak reflectance in the visible spectrum than equiluminant less saturated colors, which makes the saturated colors appear brighter. Interestingly, a neuroimaging study by Corney, Haynes, Rees, and Lotto (2009) showed that activation in V1 is more consistent with brightness perception than the actual luminance of a stimulus. In fact, the activation of the early visual processing to matched brightness of two different luminance colors, by using the HK effect, is nearly identical whereas matched luminance colors provide different activations in V1 (Corney et al., 2009). Finally, consistent with an ecology of vision approach, the predicted brightness of neural network learning natural images can statistically explain the HK effect (Long et al., 2006).

Although several previous studies showed that colors per se can affect the pupil diameter (Gamlin et al., 1998; Kimura and Young, 1995; Tsujimura et al., 2001), pupillary constrictions in relation to the illusory brightness enhancement with different colors have been less explored (e.g., Hanada, 2015). We therefore examined how individual differences in brightness perception, related to colors and glare illusions, are reflected in the individuals' pupillary responses. Specifically, we hypothesized that color can also affect the subjective brightness of the glare illusion and in a manner consistent with the ecology of vision. If such an ecological account plays any role, we are led to think that color should matter for the pupillary response and, in particular, those colors dominating in natural experiences where the eyes are likely to be dazzled by sunlight (e.g., the 'blue' of the sky and perhaps the 'green' of vegetation). Specifically, we hypothesize that pupillary responses will differentially reflect the subjective changes of brightness as experienced from the differently colored glare illusion patterns. Specifically, at the individual level, we expect that the extent of pupil constriction (e.g., the average and/or maximum constriction, its velocity, etc.) should reflect each individual's increased/decreased subjective sense of brightness of the differently colored stimuli. Nevertheless, several color features matter for the psychophysical and physiological responses and one can expect systematic effects of either the saturation or chromatic contrast between elements of the patterns (Barbur et al., 1992, 2004; Gamlin et al., 1998), which can have in turn systematic effects on the pupil responses. Thus, in the final experiment, we also tested the pupil responses in relation to the HK effect, using patterns similar to those of the glare stimuli, but with no gradients or homogeneous color patches.

Hence, in Experiment 1, we monitored pupil size with an infrared eye-tracker while participants viewed the same pattern consisting of gradients converging onto a central 'glare' region but that could be different colored in black, blue, cyan, green, magenta, red, and yellow. By rotating 180 degrees the same gradients, so that the gradients would be diverging from the patterns' centers, we also created a control 'halo' condition, where the illusory glare effect was greatly reduced and confined to a peripheral

halo (see Figure 2.2, second row). In Experiment 2, we sought to confirm that the subjective brightness changed with the colors of the glare illusion by using the psychophysical method of adjustment. Finally, in Experiment 3, we assessed whether hues of different saturations could differentially affect the size of the pupils, i.e., a pupillary HK effect, by showing similar patterns to those of the previous experiments are but with the same colors entirely or homogenously filling the elements (i.e., in the absence of gradients causing illusory glare). Because these separate experiments involved the same participants, we were able to relate these responses to one another and therefore make some conclusions about the effects of color hue and saturation on the illusory experience of glare and pupillary responses.

2.2 Experiment 1

In the initial experiment, we presented the illusory brightness stimuli individually on a computer screen. Each of these differently colored glare stimuli, displayed in Figure 2.2a, was presented repeatedly to each participant, each time for a few seconds and with no other instruction than simply to look at the pattern. An infrared eye-tracker registered simultaneously the spontaneous adjustment of the pupil to each pattern. Given our hypothesis, as well as previous studies' evidence that equiluminant but differently colored surfaces or objects can appear to have different brightness, we expected the pupil to adjust differentially to the seven stimuli shown in Figure 2.2a.

2.2.1 Methods

Participants

Twenty-three volunteers (18 men; 5 women; age range 20–26) took part in experiment 1. Two participants were excluded from pupil analyses due to eye blinks on $> 50\%$ of trials. All participants were undergraduate and graduate students who had a normal or correctedto-normal vision. In addition, they had a normal color vision as established by use of the Ishihara pseudo-isochromatic plates (Ishihara, 1996). All experimental procedures were in accordance with the ethical principles outlined in the Declaration of Helsinki and approved by the Committee for Human Research at the Toyohashi University of Technology. The experiment was conducted in accordance with the approved guidelines of the committee and all participants provided written informed consent. Participant data and experimental scripts are available from https://github.com/suzuki970/Experimental_data/tree/master/P03.

Stimulus and apparatus

We used as glare stimulus a circular pattern with luminance gradations converging onto a central white area. In addition to the glare stimuli, we also presented a 'halo' stimulus, with luminance gradations diverging away from the center, as a control to each of the glare stimuli (see Figure 2.2). The xy coordinates of the colors in the CIE1931 color space were as follows: Black (0.3127, 0.3290), Blue (0.3107,0.0921), Cyan (0.2330, 0.3260), Green (0.3074, 0.5827), Yellow (0.4168, 0.4963), Red (0.6132, 0.3413), Magenta (0.3159, 0.1759). The averaged color distributions of each stimulus (i.e., the central region of the gradation) are shown in Figure 2.1. The color gradation in the pattern gradients of each stimulus changed progressively from the xy values mentioned above to achromatic color (0.3127, 0.3290). The luminance of the pattern gradients also changed from 0.4116 cd/m^2 to 80.91 cd/m^2, accompanied with changing xy value in each color. For instance, in the 'blue' condition, the darkest and brightest region of CIE1931 xy coordinates were xy (0.1653, 0.0921) and xy (0.3127, 0.3290) respectively. In this case, the color gradation of CIE xy values changed linearly from 0.1653 to 0.3127 of x and 0.0921 to 0.3290 of y as well as luminance changed. Background and central region of stimulus luminance remained constant at 40.52 cd/m^2 and 80.91 cd/m^2 respectively in the achromatic color (x = 0.3127, y = 0.329). The luminance of the stimuli was calibrated using a Spectro-radiometer (SR–3AR, TOPCON, Tokyo, Japan).

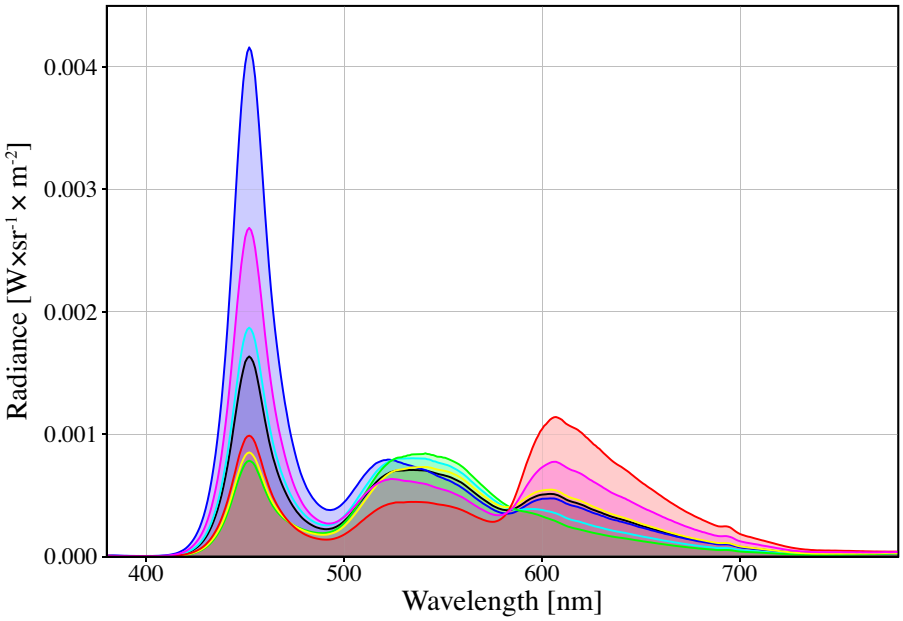

Figure 2.1 Spectral distribution of each color stimulus.

All stimuli were presented on a liquid-crystal display (LCD) monitor (Display++, Cambridge Research Systems Ltd., Kent, UK) with a resolution of 1920 × 1080 and refresh rate of 120 Hz. The radius of each circle gradient was 1.81 degrees of visual angle. Each pattern was generated by arranging 8 circle gradients in a circular shape, with each circle's center located 4.62 degrees from the center of the screen. The halo stimuli were generated from the identical elements of the glare stimuli by rotating each element of 180 degrees so that the gradients were more luminant peripherally. During each trial, there was a tiny fixation point of 0.23 degrees positioned in the center of each pattern (not shown in Figure 2.2). The experiment was conducted in a darkroom under the control of MATLAB2016a (The MathWorks, Natick, MA, USA) using Psychtoolbox (Brainard, 1997).

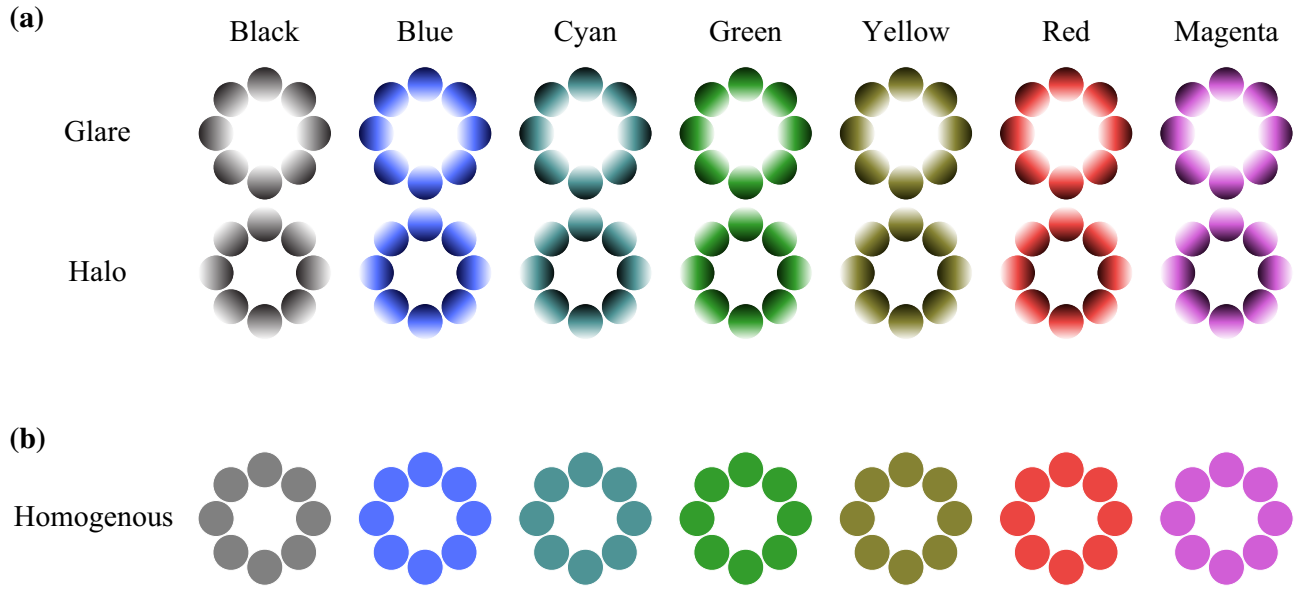

Figure 2.2 Experimental stimuli.

(a) Both the central glare illusion (above) and the peripheral halo stimuli (below) consisted of luminance gradient circles that either converged towards the pattern's center or turned towards its periphery. As a result, the central region of each glare pattern (top row) typically appears brighter than the corresponding central region of the halo stimulus (bottom row) despite both having the same photometric light intensity. Indeed, simply inspecting this figure should demonstrate that the perceived intensity of each pattern varies with the color of the inducers. (b) The homogeneous colors averaged the inducers of gradient pattern were used in Experiment 3.

Procedure

The eye tracker was calibrated prior to each session using a standard five-point calibration, following which a session was conducted for approximately 8 min. Each trial began with a fixation point presented

for 1000 ms prior to the presentation of the stimulus and, consequently, each glare and halo stimulus was presented for 4000 ms (see Figure 2.3, panel (a) for an illustration). Each trial was separated by an inter-stimulus interval (ISI) of 2000 ms. The experiment consisted of 280 trials, divided into four sessions. Each of the 14 stimuli (7 types of color $\times$ 2 gradient patterns) was presented randomly (N = 20). Participants rested their chin at a fixed viewing distance of 70cm. Participants rested for at least 5 min between successive sessions.

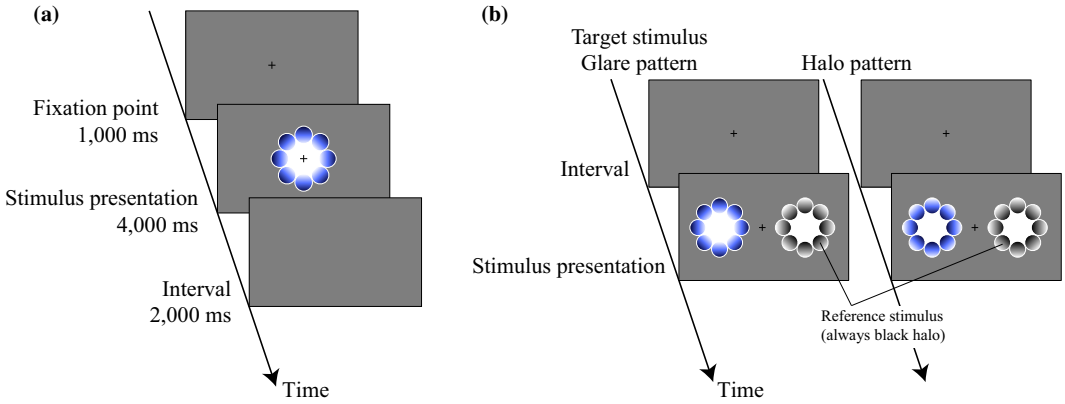

Figure 2.3 Experimental design of Experiments 1 and 2.

(a) Experiment 1: Each trial consisted in the presentation of the central fixation point for 1000 ms, followed by a stimulus presentation for 4000 ms. Each trial was separated by an inter-stimulus interval (ISI) of 2000 ms. (b) Experiment 2: Participants clicked the mouse in the initial blank screen to continue to the stimulus presentation; subsequently the participant adjusted the luminance of the canter region of the reference stimulus using a "trackball". Panel (b) illustrates the target stimuli in the blue Glare or Halo conditions. (For interpretation of the references to color in this figure legend, the reader is referred to the web version of this article.)

Recording and analysis of pupil size

Pupil size and eye movements were measured by a SensoMotoric Instruments RED500 (SMI, Berlin, Germany) eye-tracking system at a sampling rate of 250 Hz. This equipment can measure an eye movement at a resolution of about 0.01 degrees. The pupil data during eye blinks were interpolated using cubic-spline interpolation (Mathôt, 2013). Trials in which the pupils could not be detected during the beginning/ ending of the trial were excluded from the analysis. Trials with additional artifacts, revealed by using peak changes on the velocity of the pupil response, were excluded from the analysis (the average rejected trials were 4.49 $\pm$ 3.17 trials out of 280 per participant). The device outputs pupil size in mm. Baseline pupil size was computed as an average of data collected during the fixation period prior to stimulus onset from –200 ms to 0 ms (i.e., presentation onset). In the time course analysis, the pupil data in each trial was

normalized by subtracting the pupil size at stimulus onset from the baseline pupil size, following which smoothing of each data point with ± 30 ms. Across conditions, the pupillary response was averaged from the presentation period of stimulus onset until 4000 ms and evaluated by a repeated-measures analysis of variance (ANOVA).

Statistical analysis

Two-way ANOVAs were performed using pupil change (either as an average during the whole epoch or as maximum constrictions) as the dependent variable and Pattern (glare, halo) and Color (black, blue, cyan, green, yellow, red, and magenta) as within-subject factors. The level of statistical significance was set to $p < 0.05$ for all analyses. Pairwise comparisons for main effects were corrected for multiple comparisons using the modified Bonferroni (Shaffer) method. Effect sizes (partial η^2; η_p^2) were determined for the ANOVA. Greenhouse-Geisser corrections were performed when the results of Mauchly's sphericity test were significant.

2.2.2 Results

A two-way repeated-measures ANOVA on average pupil changes revealed a significant main effect of both Pattern and Color conditions on the pupil diameter ($F(1, 20) = 33.62$, $p < 0.001$, $\eta_p^2 = 0.627$, $F(2.763, 55.267) = 9.275$, $p < 0.001$, $\eta_p^2 = 0.317$, respectively). Figure 2.4a illustrates the grand-averaged time course of pupil changes among participants during the whole presentation time and for each Pattern (glare, halo) and Color conditions. We observed the occurrence of the pupillary light reflex (PLR) around 1 s from stimulus onset and then a slow dilation returning towards baseline levels. Figure 2.4b shows the averaged pupil constrictions from 0 ms to 4000 ms for each Pattern and Color condition. Most importantly, following multiple comparison for color conditions, the larger pupil constriction was observed by the 'blue' compared to the yellow, cyan, black and green ($t(20) = 3.5676$, $p = 0.0289$, $t(20) = 3.9098$, $p = 0.0130$, $t(20) = 3.7763$, $p = 0.0178$, $t(20) = 3.4061$, $p = 0.0420$, respectively). However, in this analysis, the interaction of Pattern with Color was not significant, $F(3.891, 77.823) = 0.1972$, $p = 0.936$, $\eta_p^2 = 0.009$.

Crucially, the maximum or "peak" pupil constriction was calculated across the conditions as shown in Figure 2.4c. A two-way repeated-measures ANOVA revealed a significant main effects of Pattern ($F(1, 20) = 30.55$, $p < 0.001$, $\eta_p^2 = 0.617$) and Color ($F(2.043, 40.867) = 13.57$, $p < 0.001$, $\eta_p^2 = 0.417$). Their interaction was also marginally significant (Rosnow & Rosenthal, 1989), since $F(4.032, 80.644) = 2.074$, $p = 0.0617$, $\eta_p^2 = 0.0984$. Importantly, the results of multiple comparisons for the Glare color conditions showed that the peak pupil constriction to Blue was larger than to all the other colors ($p < 0.05$), whereas comparisons of the Halo conditions revealed that the constriction to Blue was only significantly larger

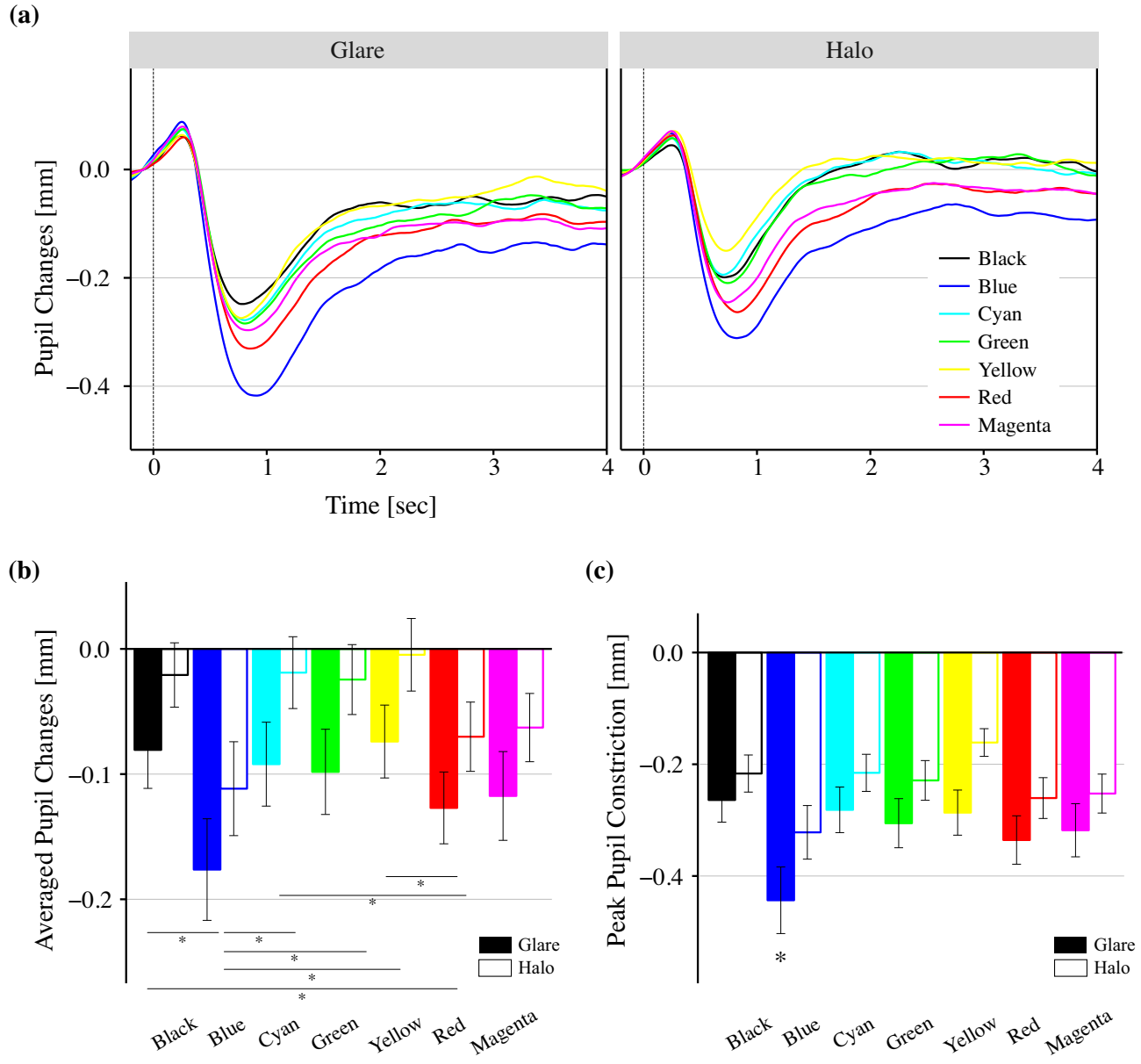

Figure 2.4 Pupillary responses in Experiment 1.

Pupillary responses in Experiment 1. The horizontal axis indicates the time (in second), while the vertical axis indicates the grand-averaged change in pupil dilation from baseline (the gray shaded area, from -200 ms to 0 ms, shows the time range of the baseline). (a) Each line color shows the result of averaged pupil diameter to the halo stimuli and colored glare. (b) The average pupil changes in 4 s of viewing (c) the peak pupil constriction for each Pattern and Color condition. The asterisks (*) indicate a statistical significance of $p < 0.05$. Error bars indicate the standard error of the mean.

than to Black and Magenta but did not differ from the other colors (e.g., green, red, etc.). In order to assess the evidence in more detail, we carried out Bayesian t-tests, which allow estimating the relative weight of the evidence in favor of H_1 (difference) but also for H_0 (i.e., no difference) using the statistical software JASP (https://jasp-stats.org/; JASP Team, 2018). A Bayesian analysis reveals whether the evidence is more in favor of H_1 whenever the obtained Bayesian Factor (BF_{10}) is > 3, inconclusive or "anecdotal" evidence if BF is comprised within 0.33 and 3, and evidence for the null hypothesis when the BF is between zero and 0.33 (Dienes, 2014; cf. Jeffreys, 1961). These analyses revealed that blue glare patterns resulted in strong evidence for pupil constrictions to blue relatively to all other colored glares (BF_{10} ranged from 9.7 to 325) but not with the halo patterns (where the BF_{10} was below 3 for the Blue versus Red comparisons and around 3 versus Magenta) as shown in Figure 2.5.

We also analyzed the averaged velocity of the peak pupil constriction in each Pattern and Color conditions (Figure 2.6a). A two-way repeated-measures ANOVA revealed that the main effect of Pattern and Color were significant $F(1, 20) = 19.64$, $p < 0.001$, $\eta_p^2 = 0.495$, $F(3.694, 73.872) = 8.148$, $p < 0.001$, $\eta_p^2 = 0.289$). Multiple comparison for color conditions showed that the constriction velocity to Blue was faster than for other colors ($p < 0.05$) and that peak pupil constrictions to Red were faster than to Black and Cyan.

However, the interaction was not significant ($F(4.031, 80.619) = 1.537$, $p = 0.199$, $\eta_p^2 = 0.0714$). The time latency of the peak pupil constriction was also calculated across the conditions (Figure 2.6b) and a two-way repeated-measures ANOVA revealed no main effects of Pattern and Color ($F(1, 20) = 0.3624$, $p = 0.554$, $\eta_p^2 = 0.0178$, $F(1.982, 39.639) = 0.7615$, $p = 0.473$, $\eta_p^2 = 0.036$) or an interaction ($F(2.509, 50.186) = 0.9462$, $p = 0.412$, $\eta_p^2 = 0.045$).

2.2.3 Discussion

The present results replicate the pupil constriction effect due to illusory glare as reported in previous studies (e.g., Bombeke et al., 2016; Laeng and Endestad, 2012; Laeng et al., 2018; Zavagno et al., 2017). That is, pupils initially constricted when a display was presented but the level of constriction was greater and sustained for all of the glare stimuli compared to their halo controls. In addition, as expected, the blue patterns resulted in a greater average and maximum peak constrictions than any of the other colors.

We also note that the 'halo' stimuli yielded constrictions in the same direction of the 'glare' stimuli. However, even these 'halo' stimuli belong to the same category of 'glare' stimuli, since they do contain the same gradients but diverging outward and consequently inducing a visible weaker effect of illusory brightness and only peripherally (as also explored in Experiment 2).

The current results support the idea that the pupil response tracks the perceived brightness across

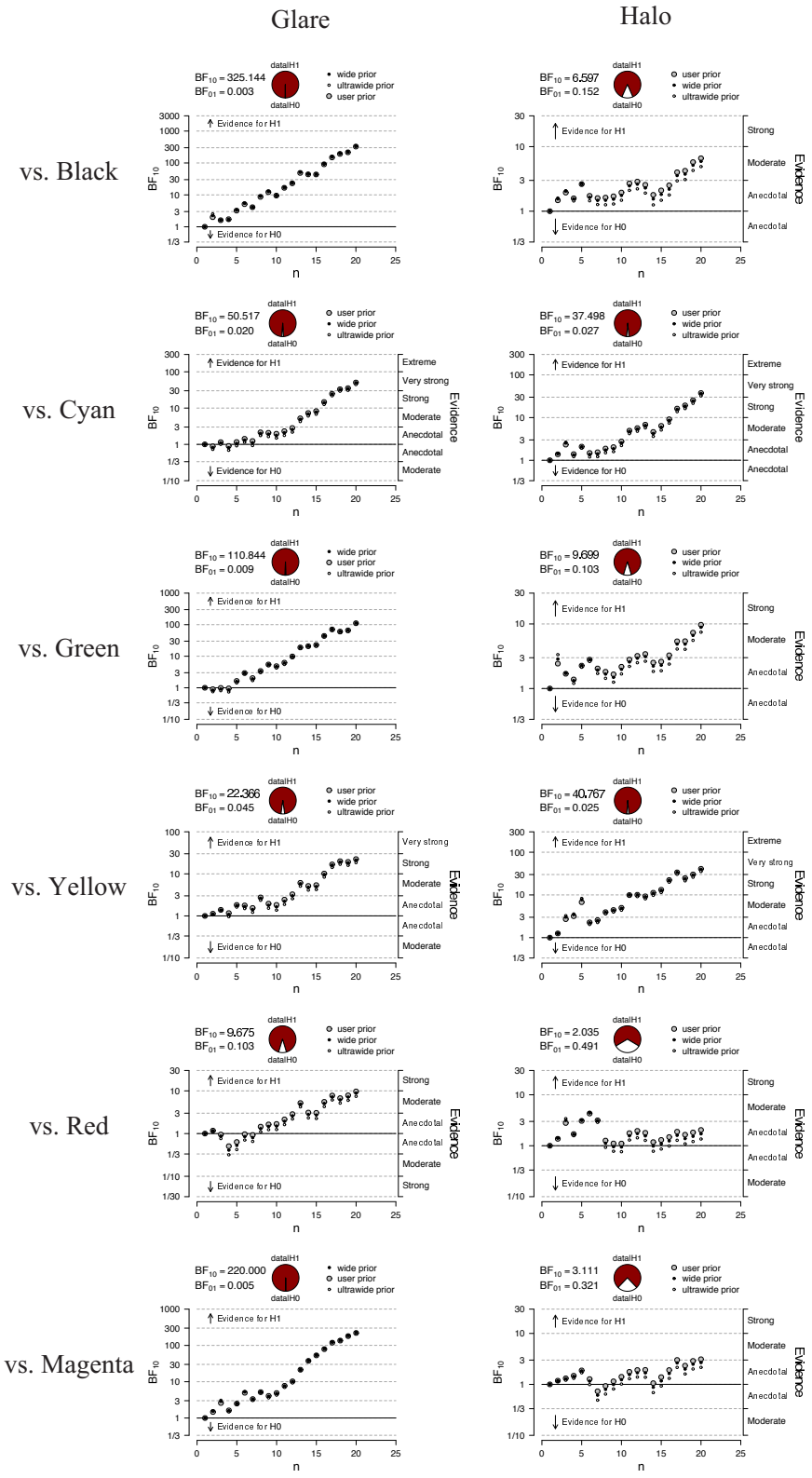

Figure 2.5 The results of Bayesian analysis.

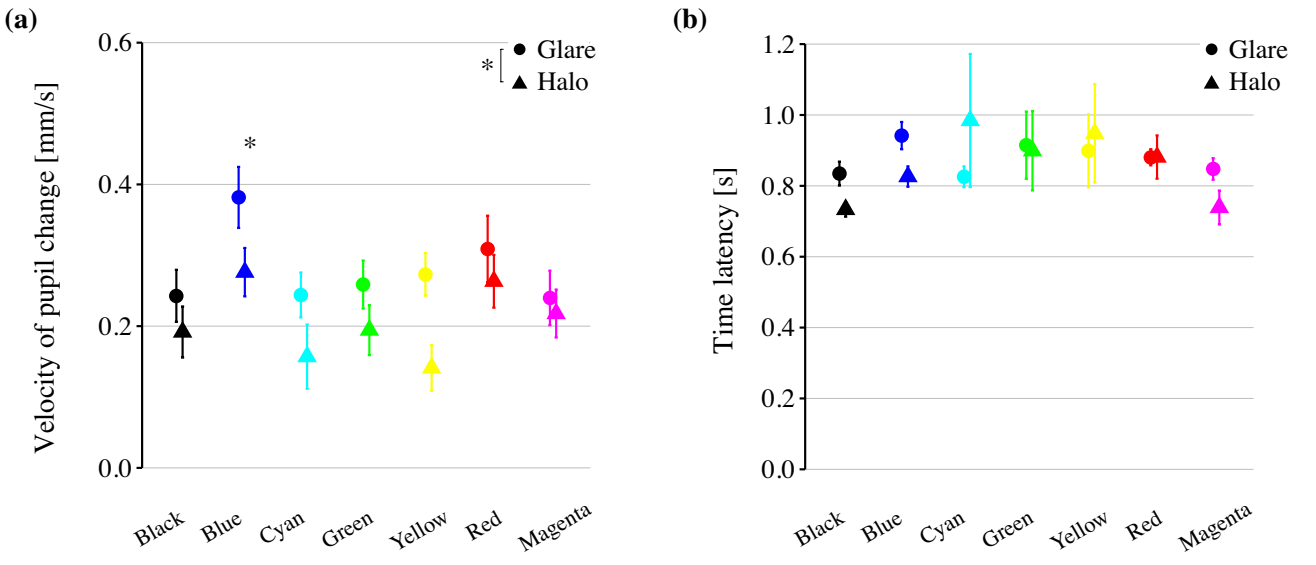

Figure 2.6 The velocity and time latency of pupil dilation in Experiment 1.

(a) The results of the velocity of pupil dilation after initial light reflex. (b) the time latency of the minimum pupil constriction after stimulus onset. The asterisks (*) indicate a statistical significance of $p < 0.05$. Error bars indicate the standard error of the mean.

colors; larger pupil constrictions to longand short-wavelength light (i.e., red and blue) were observed than to middle-wavelength light and in accordance to the brightness changes typical of the HK effect. That is, the more saturated colors appear brighter than less saturated colors, and longand short-wavelength light (i.e., blue and red) appear brighter than middle-wavelength light (i.e., yellow and green), even when stimuli have identical luminance (Fairchild, 2013).

The pupillary responses are also consistent with our hypothesis that an ecological account based on the statistics of natural images (Corney et al., 2009) since we found interactive effects on peak pupil constriction between pattern types and colors. The transient effect of such a pupillary light reflex (PLR) to 'blue glare' illusion would also seem consistent with our original ecological account, given the larger PLR in 'blue glare' than in 'blue halo' as well as compared to the other color patterns. In addition, the Bayesian analysis confirmed the presence of stronger evidence for the difference of the peak pupil constriction to the Glare condition than to the Halo condition between blue and other colors. That is, 'blue glare' might appear to be a more effective color for yielding the illusory glare effect because dazzling sunlight typically is experienced within the blue field of the sky. In turn, this effect may be also consistent with the idea that the brightness perception is generated according to the empirical frequency of the possible sources of visual stimuli. Specifically, as pointed out by Lotto & Purves (1999, p. 1012), "the empirical

information provided by color changes the relative probability of the possible sources underlying the stimuli, thus changing the perception of brightness." In general terms, perceptual illusions help to reveal the assumptions that the mind relies upon when unconsciously 'inferring' perceptual information (Brown and Friston, 2012; Clark, 2015; Hohwy, 2013).

That the pupillary response appears to be influenced by subjective brightness is also consistent with several previous studies which have reported that pupil responses better reflect subjective experiences rather than the stimulus properties (Einhäuser et al., 2010; Fahle et al., 2011; Gamlin, 2006; Naber et al., 2013). Thus, the pupil response appears to be an easy tool for assessing the individual differences in brightness perception and, generally, for increasing the range of pupil response amplitudes, and their sensitivity to the color effects.

Because we obtained a larger pupil constriction of 'blue', we may consider the possibility of a melanopsin-driven role in blue-related pupil constrictions (Brown et al., 2012; Park and McAnany, 2015). Recent findings showed the effect of interactions among melanopsincontaining retinal ganglion cells and photoreceptors on pupil constriction (Miyamoto and Murakami, 2015; Spitschan et al., 2014). Woeldersa et al. reported that increment of MS-cone activities provide an inhibitory effect on pupillary response whereas increment of L-cone and intrinsically photosensitive retinal ganglion cell (ipRGC) activities play an excitatory role (Woelders et al., 2018). The current results of the present study show less pupil constriction for the middle-wavelength light (cyan, yellow and green) than long-wavelength (Red, Magenta) and short-wavelength light (blue). The previous studies also showed that the time latency of peak pupil constriction in PLR to ipRGC-driven pupil constriction from stimulus onset is slower than the photoreceptors mediated PLR (Kardon et al., 2009; Lucas et al., 2001; Tsujimura and Tokuda, 2011). In addition, Experiment 1 revealed a difference in the velocity of pupil changes after initial PLR to blue condition, which was "faster" than to the other colors, but no statistically difference of the time latency across colors. Thus, it would seem that the observed 'blue' effect cannot be fully explained by a melanopsin-driven pupil constriction, but interactive effects among melanopsin-containing retinal ganglion cells and the cone photoreceptors remain possible.

We cannot exclude that other factors may also lead to a blue-specific stronger pupil constriction. The s-cones on which the perception of blue is dependent have previously been suggested to have access to the visual luminance pathway (Lee and Stromeyer, 1989). Thus, in Experiment 2 and 3 we assessed whether properties of color per se may affect both pupil constrictions and the subjective brightness of the colored glare illusions.

2.3 Experiment 2

In this experiment, we used the psychophysical method of adjustment to verify that observers have the phenomenological experience that gradient patterns with different colors do generate a different sense of brightness. We presented again, to a subgroup of the participants in Experiment 1, the differently colored glare stimuli paired with an achromatic identical pattern or 'reference pattern'. The task was to change manually the luminance of the reference pattern until the two looked like having identical brightness. Crucially, we also expected that participants would adjust the reference's brightness so that brightness would be negatively proportional to their pupil constrictions, as measured in Experiment 1.

2.3.1 Methods

Participants

Seventeen of the volunteers who participated in Experiment 1 (15 men; 2 women; age range 20–25) took also part in Experiment 2. Two participants were excluded from analyses because they are rejected in Experiment 1.

Stimuli and apparatus

The stimuli used during the adjustment procedure are displayed in Figure 2.3b. The participant adjusted the luminance of the central region of the reference stimulus by using a "trackball". The same equipment of Experiment 1 was used.

Procedure

At the beginning of a trial, a fixation point appeared prior to the stimulus presentation for 1000 ms. Then, two stimuli were displayed side-by-side: the target stimulus and the reference stimulus, at 6.93 degrees from the center of the monitor on either side of the center. The side (left, right) of the target and reference stimuli was determined randomly in each trial but the number of the trials for each stimulus was kept constant (N = 8). The target stimulus could be one of 14 stimuli (7 colors $\times$ 2 patterns, as shown in Figure 2.2a) and the reference stimulus was always an achromatic halo. The whole experiment therefore consisted of 112 trials (7 colors $\times$ 2 patterns $\times$ 16 trials), divided into two sessions. Participants were asked to adjust the luminance of the center region of the reference stimulus (achromatic halo stimulus) until they felt that it had the same brightness as that of the target stimulus. Each session was conducted for approximately 10 min. Participants rested for at least 5 min between each session.

Statistical analysis

A two-way repeated-measures analysis of variance (ANOVA) was conducted using the average brightness adjustments for each Pattern (glare, halo) and Color (black, blue, cyan, green, yellow, red, and magenta) as within-subject factors. To compare the mean brightness adjustments across color conditions, we used t-tests. We also used linear mixed-effects modeling (LMM) with participant as a random effect to calculate the correlation between the individuals' brightness adjustments and the pupil constrictions in Experiment 1, using the lme4 packages (Bates et al., 2015).

2.3.2 Results

In order to normalize the data, the obtained value of adjusted luminance to each condition was divided by that to the achromatic halo stimulus. This ratio indicates what amount the brightness in each condition increases/decreases relatively to the achromatic halo stimulus. After this calculation, the brightness changes were averaged among participants. A two-way repeated measures ANOVA revealed a significant interaction between Pattern and Color, ($F(3.567, 49.941) = 7.821$, $p < 0.001$, $\eta_p^2 = 0.376$) as well as significant main effects of both Pattern, $F(1, 14) = 7.813$, $p = 0.0152$, $\eta_p^2 = 0.375$, and Color, $F(2.803, 39.24) = 7.24$, $p < 0.001$, $\eta_p^2 = 0.358$. Figure 2.7a shows the grand-averaged adjusted relative luminance ratio in conditions among participants and color conditions. Multiple comparisons for Color at glare condition showed that black glare was significantly darker than the other Color condition ($p < 0.001$, Figure 2.7a). Blue glare was brighter than Red Yellow and Cyan condition ($t(14) = 4.8537$, $p = 0.0047$, $t(14) = 3.5689$, $p = 0.0377$ and $t(14) = 3.5179$, $p = 0.0416$, respectively) and Green was brighter than Red and Yellow ($t(14) = 4.4839$, $p = 0.0377$ and $t(14) = 3.5689$, $p = 0.0416$).

We further analyzed the association between the adjusted relative luminance ratios and the average pupil constrictions to the colored glare illusions measured in the previous experiment. Specifically, we used LMM and regarded brightness enhancement and participants as fixed effect and random effect. Results of the LMM for each individual's data as fixed effects in the Glare condition showed significant negative slopes ($y = –0.0063x + 0.0138$, $t(14) = –2.772$, $p = 0.0207$, $R = –0.438$), as also shown in Figure 2.7b. Importantly, in the Halo condition, we could not find the same relationship between pupil change and subjective adjustments ($y = 9e–04x + 0.0417$, $t\ (14)=0.4005$, $p=0.6898$, $R=0.076$), most likely because of the weak peripheral perception of enhanced brightness in these stimuli.

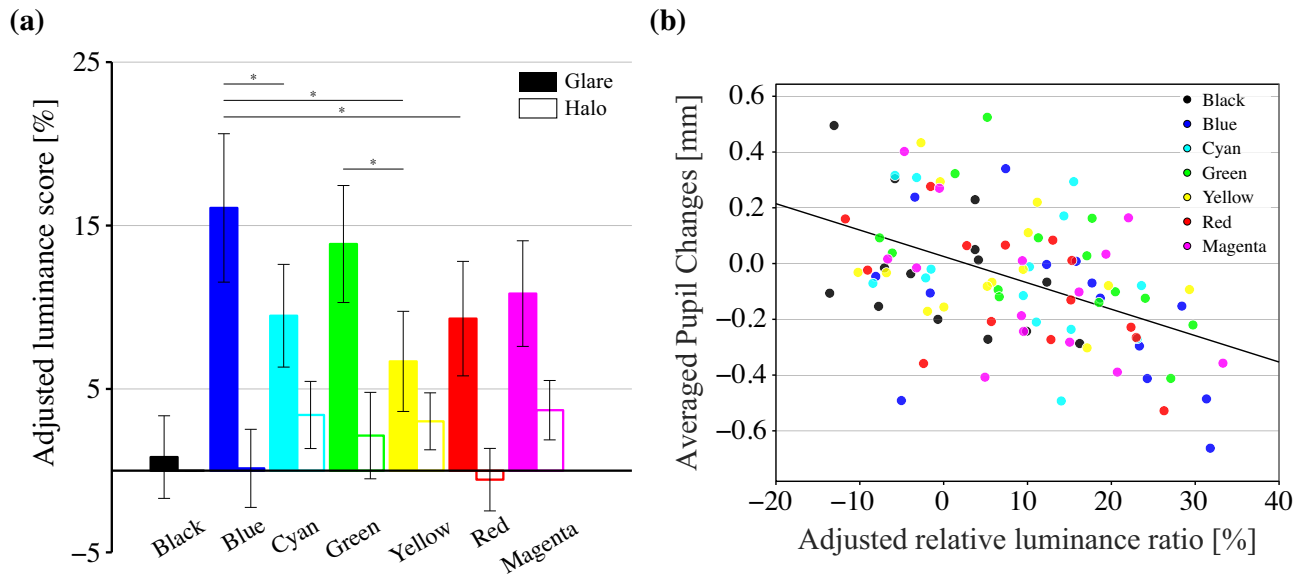

Figure 2.7 Results of adjusting luminance for each colored glare illusion.

(a) The vertical axis shows the adjusted luminosity compared to the achromatic halo condition. The colored circle indicates the averaged data among the participants in each colored glare and halo condition. (b) Scatterplot between the averaged pupil diameter in the glare condition and adjusted relative luminance ratio (each dot indicates the participants' means of the relative luminance ratio and pupil diameter). Each colored circle indicates the results of each color type of glare illusion. The interpolating black line shows the simple regression line of LMM as fixed effect.

2.3.3 Discussion

The perception of brightness was enhanced by the colored gradients and, in particular, on the basis of psychophysical adjustments, the 'blue glare' illusion was clearly perceived as having the brightest color. As expected, there was also a strong relationship between the pupil constriction in the previous Experiment 1 and the level of adjusted luminance in the present Experiment 2 for the same participants. Thus, the present result appears consistent with the idea that the pupil constrictions observed in Experiment 1 may have been triggered by each individual's sense of perceived brightness for each specific color.

We note that there are, in general, substantial individual differences of the contribution of chromatic channels to brightness (Kawada et al., 1993; Nakano et al., 1988) and the present results also indicated that what color was perceived the brightest could vary between individuals. Since a perceived intensity of light is determined by the combination of the luminance and the chromatic channels, one possible account for the individual differences may be due to the spectral absorption of the eye lens and of macular pigments (Nayatani et al., 1988; Whitehead, 2006).

Intriguingly, the stronger bright effect of 'blue glare' illusion seems consistent with psychological studies showing that the short-wavelength light is particularly effective in yielding a strong 'discomfort glare' (Bullough et al., 2002; Flannagan et al., 1994; Sivak et al., 2005a,b). Given that the spectral absorption of short-wavelength light can be higher than middle- and long-wavelength light, in terms of 'blue glare' illusion, a color property such as saturation may also account for the stronger bright effect of 'blue glare' illusion. Hence, the final experiment attempts to address this question by testing the same participants with similar colored patterns but where, crucially, there were no gradients. These stimuli allow us to test specifically the effects of the colors per se on the pupil response in the absence of the enhancement of luminance (glare effect) evoked by the gradients.

2.4 Experiment 3

The previous experiment showed that the short-wavelength light of the blue glare illusion was indeed deemed the brightest among all of the tested colors. One possibility is that the effect on the pupil of blue over the other glare stimuli simply reflects the activation of S-cones since these have access to the visual luminance pathway (Lee and Stromeyer, 1989). In fact, previous studies have shown that M-cone increments actually decrease perceived brightness, while L-cone increments in- crease it (Parry et al., 2016). Interestingly, the yellow glare illusion was adjusted to be the 'darkest' appearing color in Experiment 2.

By manipulating color while keeping luminance constant, we also aimed to assess the influence of brightness to the colors itself. For in- stance, the Helmholtz-Kohlrausch effect may provide one of the possible explanations of the 'blue' glare effects observed here and consistent with differential activation of photoreceptors, since the saturation of the colors used in the experiment were not equal. In the HK effect, blue and red appear brighter than green and yellow in equiluminant displays. Therefore, if the pupil constriction to the glare illusion in Experiment 1 and the adjusted brightness in Experiment 2 were determined by saturation and hue-based properties of the color itself, according to a HK effect, then the pupil response to homogeneous colors in the same participants should also be related with the pupil responses in Experiment 1 and the subjective sense of brightness as measured in Experiment 2.

2.4.1 Methods

Participants

Twelve of the volunteers who participated in Experiment 1 and 2 (10 men; 2 women; age range 21–26) took part in Experiment 3.

Stimuli

The individual elements of all patterns had homogeneous colors that now filled what originally were the inducers of colored glare illusions as shown in Figure 2.2b. The surface areas under the curves calculated from the spectrograph (see Figure 2.1) were the following: Black 0.265 W/sr/m^2, Blue 0.4010W/sr/m^2, Cyan 0.2700W/sr/m^2, Green 0.2056 W/sr/m^2, Yellow 0.2302 W/sr/m^2, Red 0.2833 W/sr/m^2 and Magenta 0.3466 W/sr/m^2. The average Y value of the inducer among colors was 39.41 $\pm$ 1.44 cd/m^2. The CIE xy coordinates were as follows; Black (0.3127, 0.329), Blue (0.2380, 0.2090), Cyan (0.2723, 0.3273), Green (0.3100, 0.4575), Yellow (0.3654, 0.4138), Red (0.4649, 0.3352), Magenta (0.3143, 0.2515). These CIE xy coordinates were determined by the averaged value of the circle element used as the colored glare illusion in Experiment 1 and 2. Background and central region of stimulus luminance were identical to Experiment 1. The visual angle of the stimuli and equipment were identical to Experiment 1.

Procedure

As done previously, each trial began with a central fixation point presented for 1000 ms prior to the presentation of the color field which was presented for 4000 ms. Trials were separated by an inter-stimulus interval (ISI) of 2000 ms. Participants were exposed to homogeneous color patterns while keeping gaze on the central fixation point. Each of the 7 types of the color pattern was presented randomly 20 times, divided into four sessions. Each session was conducted for approximately 8 min. Participants rested for at least 5 min between each session.

Statistical analysis

A two-way ANOVA was conducted on pupil changes for Color (black, blue, cyan, green, yellow, red, and magenta) and Pattern (Glare, Halo, and Homogeneous) as within-subject factors and Pattern. To compare the mean pupil changes across color conditions, we used t-tests and LMM with participant as random effect for calculating the correlation between the pupil constrictions in Experiment 1 and 3 of the same participants.

2.4.2 Results

As done earlier, the averaged pupil changes from –200 ms to 0 ms prior to stimulus onset was used for baseline pupil diameter. Figure 2.8a shows the grand-averaged time course of pupil changes among participants for six colors. Separate two-way repeated-measures ANOVAs were carried out for the averaged pupil changes and for the maximum constrictions.

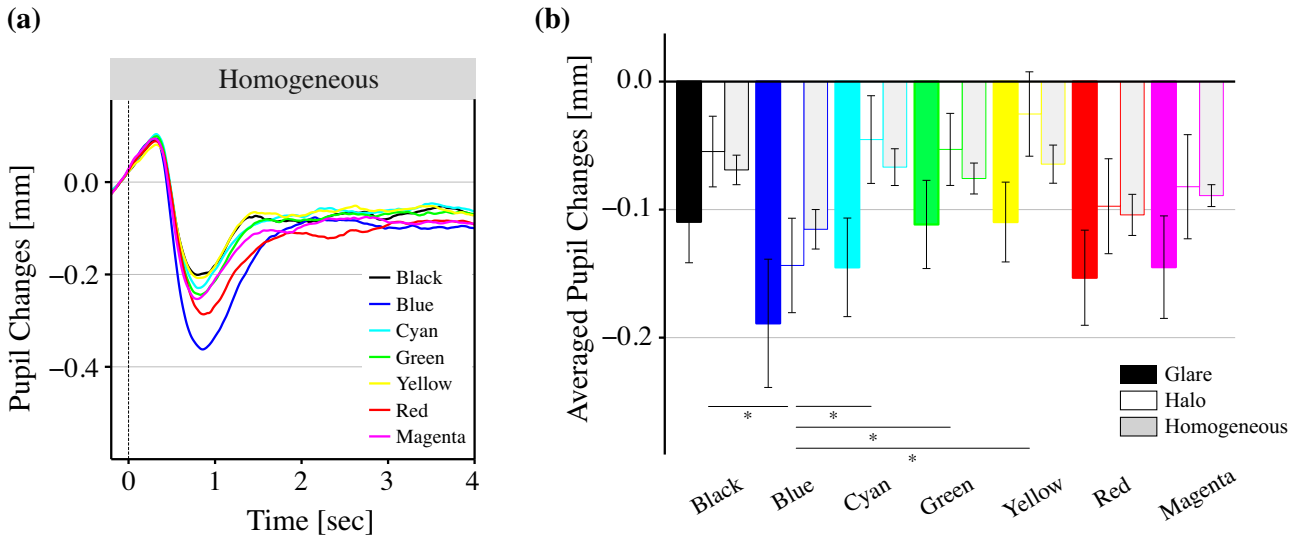

Figure 2.8 Results of pupillary response to the homogeneous colors.

(a) The horizontal axis indicates the time (in second), while the vertical axis indicates the grand-averaged change in pupil dilation changes from baseline (from -200 ms to 0 ms). The vertical, gray-shaded, areas show the time range used for baselines. Each line color shows the result of averaged pupil diameter to homogeneous color. (b) The average pupil changes in 4 s of viewing for Experiment 1 and 3 to the identical participants.

The analysis of average pupil changes from 0 ms to 4000 ms for Experiment 1 and 3 on the identical participants revealed a significant main effect of Pattern ($F(1.443, 15.876) = 4.585$, $p = 0.0365$, $\eta_p^2 = 0.294$) and Color ($F(3.953, 43.483) = 9.72$, $p < 0.001$, $\eta_p^2 = 0.469$). The interaction of Pattern with Color was not significant ($F(4.462, 49.081) = 0.9039$, $p = 0.478$, $\eta_p^2 = 0.0759$) as shown in Figure 2.8b. A two-way repeated-measures ANOVA on the "peak" pupil constriction revealed a significant main effect of Color ($F(3.783, 41.612) = 21.88$, $p < 0.001$, $\eta_p^2 = 0.665$) and of Pattern ($F(1.258, 13.835) = 5.686$, $p = 0.0261$, $\eta_p^2 = 0.341$). The interaction of Color and Pattern was not significant ($F(4.305, 47.358) = 1.321$, $p = 0.275$, $\eta_p^2 = 0.107$).

2.4.3 Discussion

We assessed whether the color itself may affect both the perceived brightness and the pupil constriction via chromatic channels. The larger pupil response for blue and red homogenous stimuli was expected on the basis of the HK effect on brightness perception as well as the color's saturation effect on the pupil response. The pupillary response was significantly correlated to the color's saturation and this effect appeared consistent with previous studies (Barbur et al., 1992, 1999). Together with the results

of Experiment 1, this pupillary HK effect further indicates, that the pupil reflects well the subjective brightness perception.

2.5 General Discussion

In the current study, we examined the phenomena of enhanced perceived brightness and pupil constrictions to colored glare illusions. We observed that all colored converging gradients or 'glare' stimuli were subjectively perceived as brighter than their control, equiluminant, divergent gradients or 'halo' patterns. As expected, the 'blue glare' illusion was specifically evaluated as the brightest color. Clearly, the pupil responses matched the subjective brightness rather than the actual stimulus properties. The peak pupil constriction for the 'blue glare' illusion in Experiment 1 was also consistent with the results of psychophysical adjustments (Experiment 2). Moreover, all experiments indicated that colors per se differentially enhanced brightness, revealing a Helmholtz-Kohlrausch effect of hue and saturation on the pupil response.

The present findings not only succeeded in replicating previous demonstrations that pupil constriction matches to the perceived brightness (Laeng and Endestad, 2012). We did confirm our expectation that the 'blue glare' illusion constricted the pupil more strongly than the same illusion with other colors; although the present findings did not present strong empirical evidence for the specificity of 'blue glare' on the observed pupillary response. However, the maximum or "peak" pupil constriction to each color was stronger for blue and more so for the converging gradients than the diverging gradients versus halo patterns. Indeed, Bayesian analyses confirmed that the evidence was more supportive for a blue enhancement of the glare effect on the pupil than when the same color was presented with reduced glare (in the halo patterns: in Experiment 1) or no glare at all (in the homogenous patterns, Experiment 3).

As hypothesized, the above set of results can be seen "in the light of" a typical natural world situation: the 'glare' from sunlight when looking up towards the sky, which can "dazzle" and incapacitate vision temporarily (Bargary et al., 2014; Patterson et al., 2015; Sivak et al., 2005b). We assume that people have learned to associate the sky color with the experience of the dazzling effects of sunlight. Zavagno et al. (2017) suggested that a physiological pupil constriction response would be consistent with the interpretation of a scene based on such a natural statistic of the world. That is, the convergent arrangement of the gradually lighter ends of the elements of the pattern primes the perceptual inference of a bright source of light at the center of the figure. Repeated observations in nature when looking up towards sunlight in the sky or through a canopy of leaves could lead to seeing similar gradient configurations are seen and especially when the gradients within a backdrop of blue color (Laeng et al., 2018). "Seen in this light", the constriction of the pupil to illusory glare stimuli would also seem to express an adaptive response

of the visual system to a probable and dangerous situation (Bargary et al., 2014; Gao and Pei, 2009). Interestingly, neural network simulations (Corney and Lotto, 2007) support the idea that the statistics of visual experience, or the natural ecology of vision, lead to illusory brightness perception. Computational research by training networks to estimate brightness of a stimulus central area, with stimuli resembling "looking through the branches of a tree", has also revealed human-like illusory effects.

Finally, we need to point out that the pupil adjustments to illusory brightness observed here and elsewhere (e.g., Laeng and Endestad, 2012; Laeng et al., 2018; Zavagno et al., 2017) or even to mental images (Laeng and Sulutvedt, 2013), typically represent a fragment of the appropriate adjustments of the pupil diameter to physical luminous intensity. It may be best to view these pupillary responses as "anticipatory" or "preparatory" to a probable perceptual scenario (Sulutvedt et al., 2018; Zavagno et al., 2017) which could still provide an adaptive response by reducing the probability of being dazzled by sudden increases in light levels.

2.6 Conclusions

The present findings indicate that blue yield a strong perception of enhanced perceived brightness than all the other colors in a variety of patterns and that the pupil measurements capture this aspect effectively. This pupillary constriction effect is enhanced with converging colored gradients but only weakly when the colored gradients diverge, so that the peripheral effect of the halo glare is negligible both in terms of perceived brightness and pupil constrictions. We had originally hypothesized that 'blue' may not only enhance the subjective sense of brightness but that a constriction of the pupil to such color could represent an adaptive response of the visual system to a probable dangerous situation of dazzling sunlight. The present findings are at least consistent with an ecological account, which specifically predicts that colors dominating in natural scenes (e.g., the 'blue' sky) should be more effective than other colors in enhancing the illusory glare effect and, in turn, trigger a preparatory, defensive, pupillary constriction.

Chapter 3

The Effect of Iris Color on Pupil Response to Blue Glare Illusion

---

Glare illusion is a brightness illusion evoked by luminance gradients converging onto a central white area. Blue glare illusion yields a brighter perception and larger pupil constriction than other hue glare illusions. We hypothesize that the specific effect of blue on pupil constriction is an adaptive response of the visual system to a probable dangerous situation of dazzling sunlight (i.e., the sun in a blue sky) in terms of triggering a preparatory, defensive, pupillary constriction. In this study, we monitored the pupil response to the colored glare illusion and the PLR. Then, we compared the pupillary response between people with black/brown and blue/hazel colored iris because we expected that the brightness perception on blue glare illusion relates to the iris color based on inherited traits. As a result, we succeeded in replicating the effect of the larger pupil constriction caused by glare illusion regardless of iris colors. The specific larger effect on pupil constriction for blue glare illusion, as originally reported, was observed only for the black/brown iris group but not for the blue/hazel group. Because the iris color relates to a macular pigment density as a marker for the adaptation to the homogeneous environment, we assumed that the pupillary constriction represented the adaptation response to a probable dazzling sunlight imitated by the glare illusion, and the pupil constriction could be similar to the function of MP to filter the blue light projection to the retina.

3.1 Introduction

The pupils are controlled by two incompatible muscles (sphincter and dilator muscles) in the retina to adjust the light entering the eyes. In addition to the role of physiological reflex to light, several cognitive factors prompt the pupillary dilation/constriction via noradrenergic activity, which is a neurotransmitter from the LC, as in the so-called LC-NE system (Beatty, 1982; Fahle et al., 2011; Laeng et al., 2012; Mathôt et al., 2013; Wang and Munoz, 2015). The pupillary changes to the illusory brightness perception also tell us that pupillary response plays an important role in the anticipation of being dazzled or temporarily incapable of receiving light by the sun (Laeng and Endestad, 2012; Zavagno et al., 2017). Moreover, the pupil constriction is correlated with the perceived brightness to glare illusion (Suzuki et al., 2019a). Glare illusion is a brightness illusion evoked by luminance gradients converging onto a central white area. Blue glare illusion yields a brighter perception and larger pupil constriction than other hue glare illusions. The specific effect of blue on pupil constriction seems to be an adaptive response of the visual system to a probable dangerous situation of dazzling sunlight (e.g., the sun in a blue sky) in terms of triggering a preparatory, defensive, pupillary constriction.

Similarly, the macular pigment (MP) has the function of protecting the eyes from strong light (e.g., the sun) because the carotenoid pigments of lutein and zeaxanthin in the macula absorb blue light. That is, MP helps in filtering the blue light that is projected to the retina. Importantly, the optical density of the MP at the paracentral fovea, as illustrated in Figure 3.1 is related to the iris color because of the pigment density on the iris stroma (Hammond et al., 1996; Sturm and Frudakis, 2004).

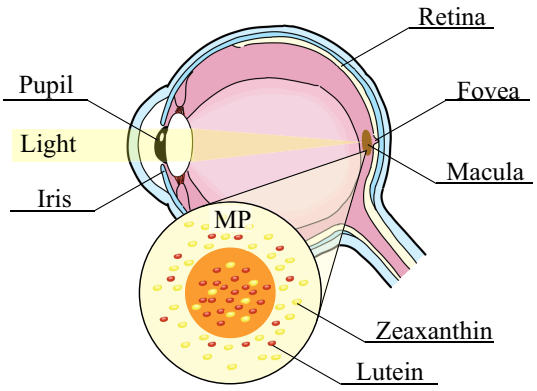

Figure 3.1 Eye structure and MP.

In general, because melanin pigments absorb the ultraviolet (UV) light to protect the skin, people originating from the near-equatorial area have a higher amount of melanin pigment. Contrarily, people in low UV areas, such as Scandinavian countries, have a lower amount of pigment. This results in varied iris colors depending on the region where people originate from. Note that the iris color is related to three types of genes in addition to the amount of melanin in the iris; EYCL1, EYCL2, and EYCL3 (Rebbeck et al., 2002). There are two major genes and several minor ones that account for the tremendous variety of human eye color. These genes are in 19 chromosomes for EYCL1 and 15 for EYCL3 out of the 23 pairs of chromosomes transferred from parents, with EYCL1 and EYCL3 relating to brown and green/blue, respectively. The number of single nucleotide polymorphism (SNP) near the oculocutaneous albinism II

(OCA2) gene on chromosome 15 determines the iris color (Duffy et al., 2007; Sturm and Frudakis, 2004). To summarize so far, iris colors are determined by inherited traits and are related to the melanin pigments and the MP to protect the skin and eyes from intense light. Ciulla et al. (2001) reported that individuals with blue-grey irises, for instance, had 19% less MP than individuals with brown-black irises, as shown in Figure 3.2 (Ciulla et al., 2001). The measurement of macular pigment optical density (MPOD) based on psychological techniques has been known as heterochromatic modulation photometry (Bone and Landrum, 2004). In this method, participants adjust a green light (typically—green, 540 nm) and blue light (typically— blue, 460 nm) which are alternately presented in equal brightness. Under the identical intensity of light, blue light appears darker to the brown iris color than green light because the light is absorbed by the macular pigment. Therefore, the brightness differences between blue and green light depend on the number of macular pigments; the differences are larger for dark iris colors (black/brown) than for bright iris colors (blue/green). Most importantly, it has been reported that MPOD depends on the differences light absorption effects related to light sensitivity, contrast sensitivity, and glare recovery (Loskutova et al., 2013; Whitehead, 2006). Hammond et al. (1996) suggested that the accumulation of the retinal pigments and ocular melanin evolve with inherited traits, such as adaptation to a similar type of environmental situation based on light or oxygen intensity (Hammond et al., 1996).

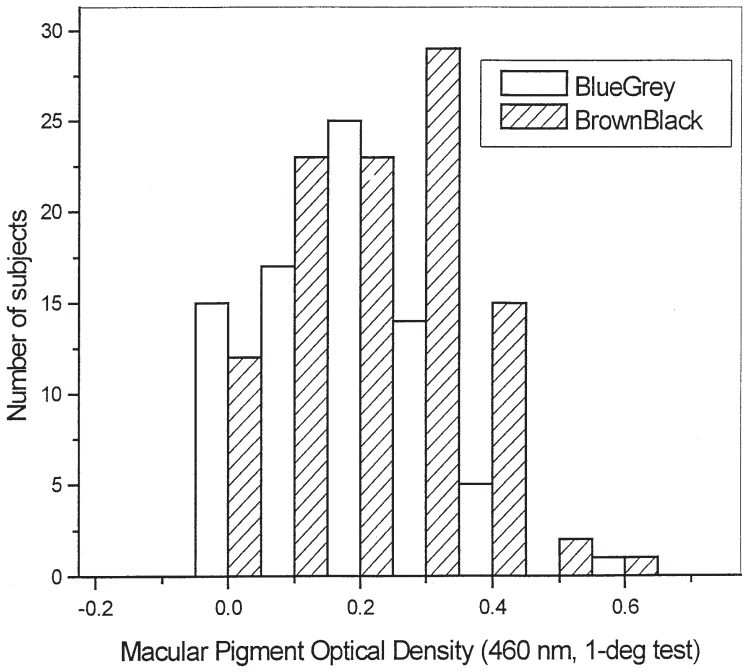

Figure 3.2 The density of MP for brown/black and blue/gray irises (Ciulla et al., 2001).

Histogram of the MP distribution for individuals with brown/black irises compared to blue/gray irises.

The previous study suggested that a) the blue glare illusion resulted in what was subjectively evaluated as the brightest condition compared to other colored stimuli, and b) the enhanced brightness effect prompts to changes in pupil size, where the maximum pupil constriction peak was observed for the blue converging gradients (Suzuki et al., 2019a). We hypothesized that if the ecological background can explain the larger pupil constriction as a means to prevent strong light from the sun, iris colors as a marker for the adaptation to the homogeneous environment would relate to pupillary response. Here, because we expected that the brightness perception of blue glare illusion relates to the iris color, we monitored pupil response to the colored glare illusion and the PLR. Then, we compared the pupillary response between people with black/brown and blue/hazel colored iris colors. First of all, we classified participants iris colors into two groups by machine learning using the k-nearest-neighbor method and an iris image database (Proença and Alexandre, 2005). Each iris image was classified in one out of four categories: dark brown, light brown, hazel, and blue. Following that, we monitored the participants' pupil size while viewing the differently colored glare stimuli and the control stimuli, which was created by rotating the same gradients by 90 degrees, so that the effect of glare illusion disappeared (see Figure 3.4).

3.2 Methods

3.2.1 Participants

18 volunteers (9 men; 9 women; age range 22–34) participated in the experiment. Three participants were excluded from pupil analysis due to eye blinks on $> 50\%$ of trials. All participants were graduate students who had a normal or corrected-normal vision. All experimental procedures were in accordance with the ethical principles outlined in the Declaration of Helsinki and approved by the Committee for Human Re- search at the Oslo University. The experiment was conducted in accordance with the approved guidelines of the committee and all participants provided written informed consent. Participant data and experimental scripts are available at https://github.com/suzuki970/Experimental_data/tree/master/P08.

3.2.2 Stimulus and apparatus

We used a circular pattern of glare stimulus with luminance gradations converging onto a central white area. Additionally, we also presented a control stimulus, which was generated by rotating by 90 degrees the luminance gradation from glare illusion, as a control to each of glare stimuli (see Figure 3.4). The xy coordinates of the colors in the CIE1931 color space were as follows: black (0.3127, 0.3290), blue (0.2590,

0.2438), cyan (0.2213, 0.3266), green (0.3093, 0.4449), yellow (0.3882, 0.4488), red (0.3998, 0.3312), and magenta (0.3150, 0.2485), as shown in Figure 3.3. We changed the control stimulus used by Suzuki et al. (2019a) to reduce the effect of localized average luminance projecting around the fovea in the visual field to pupil size. Additionally, the saturation value was aligned to any color condition (i.e., the magnitudes of vectors a* and b* were identical) to eliminate the effect on the pupil size. The color gradation in the pattern gradients of each stimulus changed progressively from the xy values mentioned above to achromatic color (0.3127, 0.3290). The luminance of the pattern gradients also changed from 0.74 cd/ m^2 to 123.4 cd/m^2, accompanied by the changing xy values in each color. For instance, for the blue condition, the darkest and brightest regions of CIE1931 were coordinates (0.2590, 0.2438) and (0.3127, 0.3290), respectively. In this case, the color gradation of CIE coordinate values changed linearly from 0.2590 to 0.3127 for x and 0.2438 to 0.3290 for y; luminance changed as well. In the measurement of PLR, we used the homogeneous white (149.4 cd/m^2) and black (0.74 cd/m^2) in the achromatic color (x = 0.3127, y = 0.329).

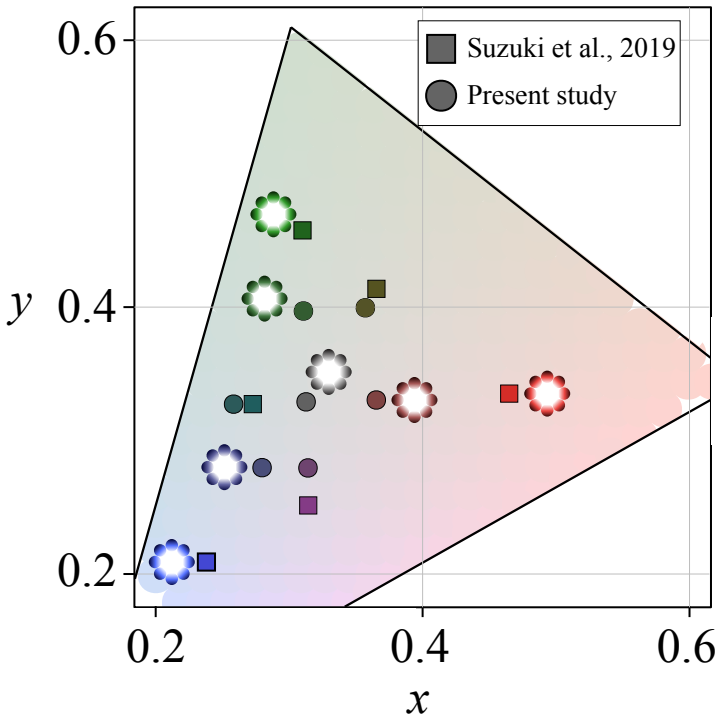

Figure 3.3 xy values of the stimuli used in this experiment.

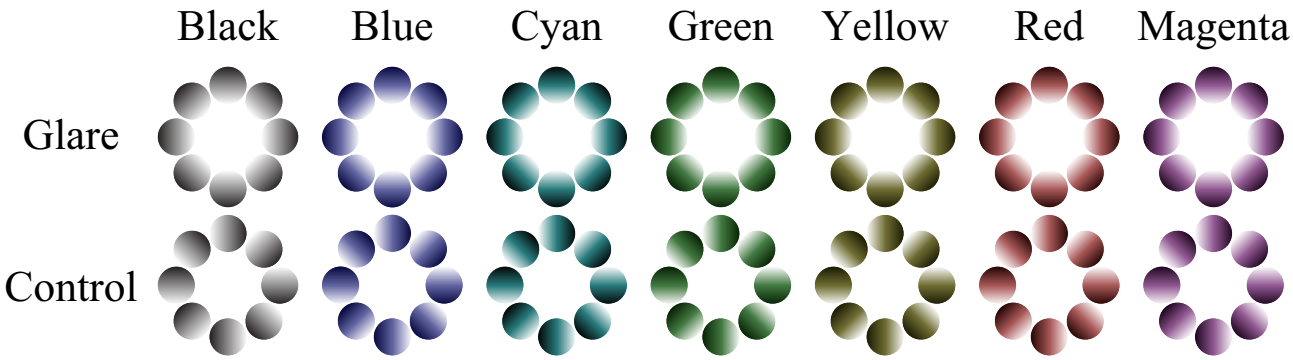

Figure 3.4 Experimental stimuli.

Both the central glare illusion (above) and the control stimuli (below) consisted of luminance gradient circles that either converged towards the pattern's center or turned towards its periphery. As a result, the central region of each glare pattern typically appears brighter than the corresponding central region of the control stimulus despite both having the same photometric light intensity. Indeed, simply inspecting this figure should demonstrate that the perceived intensity of each pattern varies with the color of the inducers.

The background and central region of the stimulus luminance remained constant at 78.5 cd/m^2 and 123.4 cd/m^2, respectively, in the achromatic color (x = 0.3127, y = 0.329). The luminance of the stimuli was calibrated using a photometer (Spyder 4 Elite, Datacolor Imaging Solutions, Lawrenceville, USA). All stimuli were presented on a liquid-crystal display (LCD) monitor (FlexScan EV 2451, EIZO, Ishikawa, Japan) with a resolution of 1920 $\times$ 1080 and refresh rate of 60 Hz. The radius of each circle gradient was 1.81 degrees of visual angle. Each pattern was generated by arranging 8 circle gradients in a circular shape, with the center of each circle located at 4.62 degrees from the center of the screen. The control stimuli were generated from identical elements of the glare stimuli by rotating each element by 90 degrees so that the gradients were more luminant peripherally. During each trial, there was a tiny fixation point of 0.23 degrees positioned at the center of each pattern. The experiment was conducted in a darkroom under the control of MATLAB2018a (The MathWorks, Natick, MA, USA) using Psychtoolbox (Brainard, 1997).

3.2.3 Procedure

Before the experiment was carried out, we measured the PLR to the bright and dark screen. After the dark screen was shown for 120 seconds, the bright screen was turned on for 10 seconds while we monitored the pupil size, as shown in Figure 3.5a. During the experiment, each trial began with a fixation point presented for 1000 ms prior to the presentation of the stimulus, and each glare and control stimulus was

presented for 4000 ms (see Figure 3.5b for an illustration). Each trial was separated by an inter-stimulus interval (ISI) of 2000 ms. The experiment consisted of 168 trials, divided into three sessions. Each of the 14 stimuli (7 types of color × 2 gradient patterns) was presented randomly (N = 12). Participants rested their chin at a fixed viewing distance of 60 cm. The eye tracker was calibrated prior to each session using a standard five-point calibration, following which a session was conducted for approximately 8 minutes.

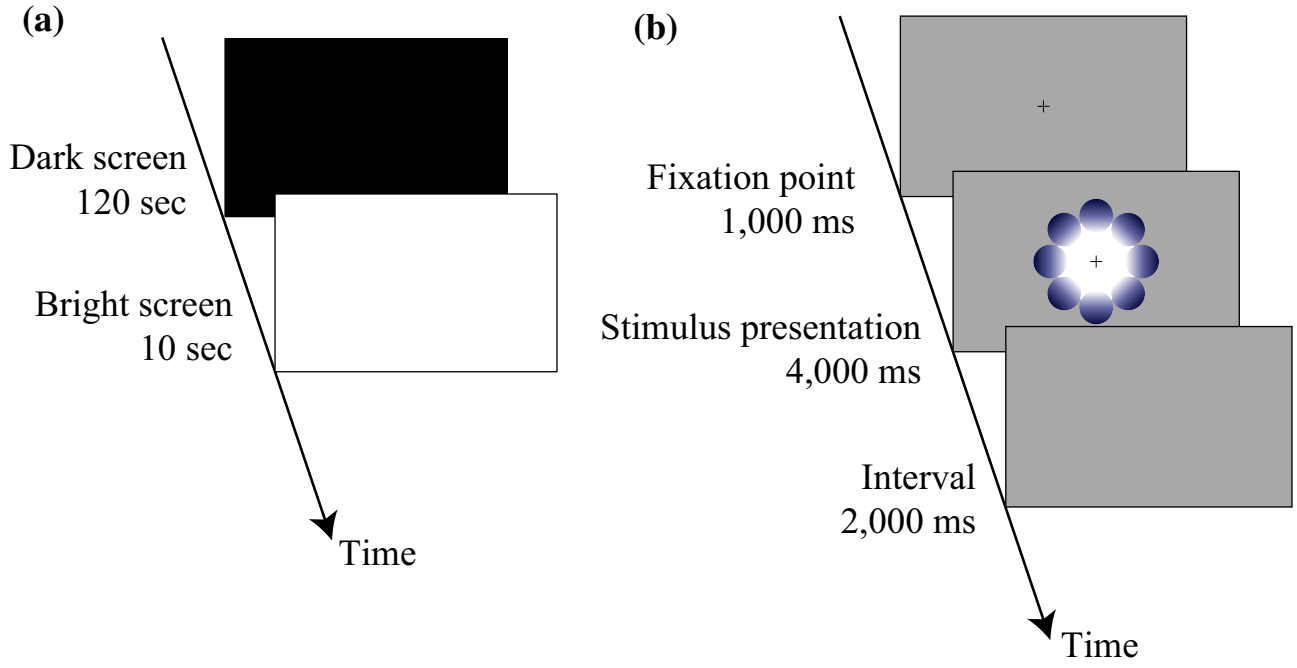

Figure 3.5 Experimental design.

(a) Pupillary light reflex test: a black screen was shown for 120 s, followed by a bright screen for 10 s. (b) Each trial consisted of the presentation of the central fixation point for 1000 ms, followed by a stimulus presentation for 4000 ms. Each trial was separated by an ISI of 2000 ms.

3.2.4 Recording and analysis of pupil size

Pupil size and eye movements were measured by a Tobii Pro Spectrum (Tobii Technology K.K., Danderyds, Sweden) eye-tracking system at a sampling rate of 600 Hz. This equipment can measure eye movement at a resolution of about 0.06 degrees. The pupil data during eye blinks were interpolated using cubic-spline interpolation. Trials in which the pupils could not be detected at the beginning/ending of the trial were excluded from the analysis. Trials with additional artifacts, revealed by using peak changes on the velocity of the pupil response, were excluded from the analysis (the average rejected trials to each condition were 1.76 ± 1.59 trials out of 12 per participant). The device outputted the pupil size in mm.

The baseline pupil size was computed as the average of the data collected during the fixation period prior to stimulus onset from 200 ms to 0 ms (i.e., presentation onset). In the time course analysis, the pupil data in each trial was normalized by subtracting the pupil size at stimulus onset from the baseline pupil size, followed by the smoothing of each data point with ± 33 ms. Across conditions, the pupillary response was averaged from the presentation period of stimulus onset until 4000 ms and evaluated by a repeated-measures analysis of variance (ANOVA).

3.2.5 Iris detection method

Here, we devised an automatic segmentation algorithm for the iris region extracted from the 1648 images of the iris database. First, we applied a Gaussian filter to the images to reduce noise (a 5 x 5 grid and σ = 1.0) as described in Equation 3.1.

$$g(x, y, \sigma) = \frac{1}{\sqrt{2\pi\sigma}} exp(-\frac{x^2 + y^2}{2\sigma^2}) \tag{3.1}$$

where x and y are the pixels of each input image.

Next, we performed edge detection using the Canny method (Canny, 1986). The vertical and horizontal direction of the edges G(x,y) are specified by the first derivative, as described in Equation 3.2.

$$G(x, y) = (f_x(x, y)^2 + f_y(x, y)^2)^{\frac{1}{2}} \tag{3.2}$$

From these two derivative images, we calculate the gradient and angle of the edges from Equation 3.3 and 3.4.

$$G = \sqrt{g_x^2 + g_y^2} \tag{3.3}$$

$$\theta = \tan^{-1}(\frac{G_x}{G_y}) \tag{3.4}$$

As a next step, pixels of derivative images containing extreme values (minimum value = 20 and maximum value = 50) were excluded from further analyses to remove pixels unrelated to edges. The threshold between the iris and pupil region was calculated from the RGB histogram of the original image to determine the circle size of the pupil, as shown in Figure 3.6. The circle positions of the pupil and iris are calculated by the Hough transform; if the pixel $P(x, y)$ on an image belongs to the disk of radius r(x_c,

y_c), Equation 3.5 is established. Figure 3.7 shows the scheme of the iris detection algorithm used in this study.

$$r^2 = (x - x_c)^2 + (y - y_c)^2 \tag{3.5}$$

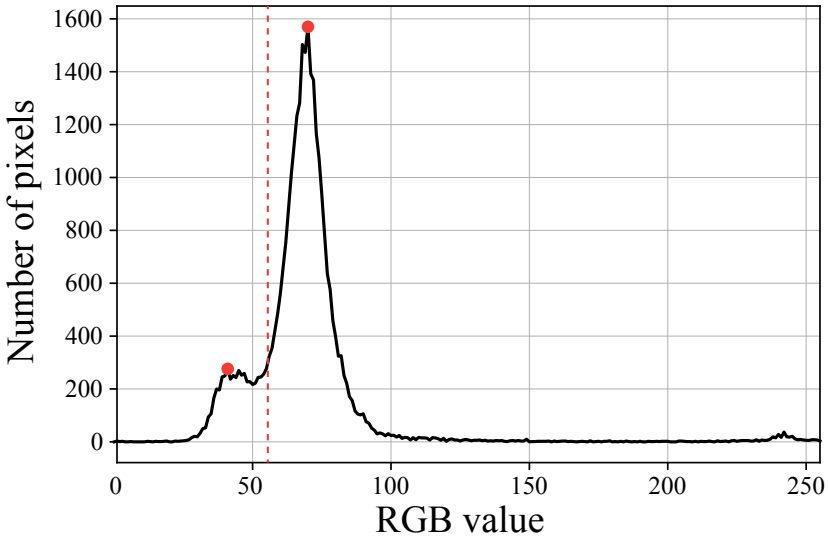

Figure 3.6 An example of RGB histogram.

The vertical line shows the number of pixel in each iris image. The threshold is determined in each image from the two-peaks, which were typically found in the histogram.

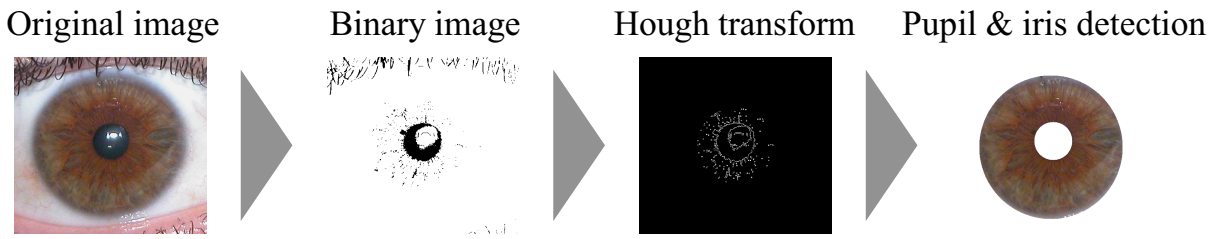

Figure 3.7 Iris detection algorism.

We first hollow out the pupil and then remove the white region of the eye, eyelashes, and skin to calculate the averaged iris color.

3.2.6 Statistical analysis

Two-way ANOVAs were performed using pupil change (either the change average during the whole epoch or the maximum value of the pupil constrictions) as a mixed design. The eye color (blue/hazel, black/brown) was used as a dependent variable between-subject factor. Pattern (glare, control) and color (black, blue, cyan, green, yellow, red, and magenta) are used as within-subject factors. The level of statistical significance was set to $p < 0.05$ for all analyses. Pairwise comparisons for the main effects were corrected for multiple comparisons using the modified Bonferroni (Shaffer) method. Effect sizes (partial η^2; η_p^2) were determined for the ANOVA. Greenhouse-Geisser corrections were performed when the results of Mauchly's sphericity test were significant.

3.3 Results

The iris colors were classified by machine learning using the k-nearest-neighbor method (see section 4.2.2) (Proença and Alexandre, 2005). Each participant's iris image was classified in one out of four categories of dark brown, light brown, hazel, and blue. The red stars indicate the input images of the participant's eye, as shown in Figure 3.8. The averaged L a* b* values were 21.49 ± 4.88, 7.95 ± 5.08, 5.09 ± 1.53 for black/brown and 36.09 ± 5.84, 5.80 ± 6.16, –1.56 ± 1.10 for blue/hazel, respectively. A one-way repeated-measures ANOVA on average L and b* value revealed that iris colors of blue/hazel were significantly brighter than of black/brown ($F(1,15) = 45.82$, $p < 0.001$, $\eta_p^2 = 0.753$). As expected, we also found the significant differences on b* value between the group ($F(1,15) = 97.53$, $p < 0.001$, $\eta_p^2 = 0.867$), while a* value was not significant ($F(1,15) = 0.5031$, $p = 0.489$, $\eta_p^2 = 0.0325$).

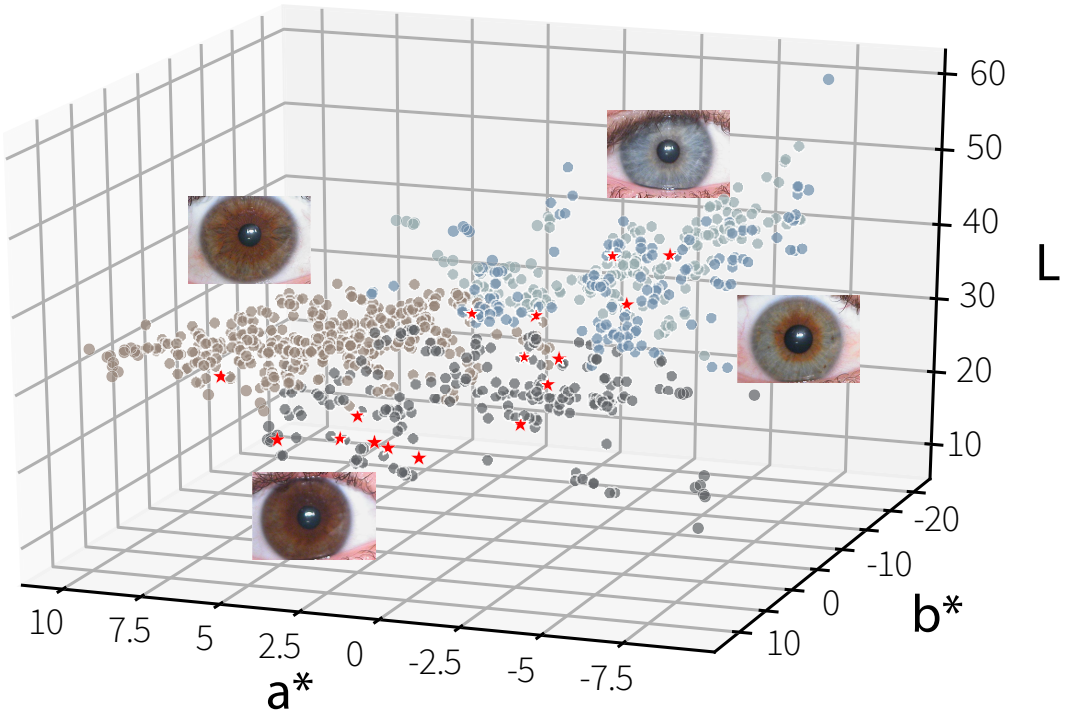

Figure 3.8 The results of iris classification.

The iris colors were categorized into four groups, which were picked from iris database. The color spaces of L a*b* were used for the classification. The red stars indicate the data of the individuals who participated in the experiment.

First, we tested two-way ANOVAs on the PLR for the bright and dark screens between classified iris color groups. Figure 3.9 shows the grand-averaged pupil changes among participants during the whole presentation time and for the bright and dark screens separately. The pupil response to the bright screen was larger than that to dark screen ($F(1,14) = 2026.056$, $p < 0.001$, $\eta_p^2 = 0.99$). Moreover, the PLR for the brown/black iris colors was larger than that for the hazel/blue iris colors ($F(1,14) = 9.30$, $p < 0.0087$, $\eta_p^2 = 0.40$). There was no significant interaction between iris color and screen luminance ($F(1, 14) = 1.46$, $p = 0.25$, $\eta_p^2 = 0.09$).

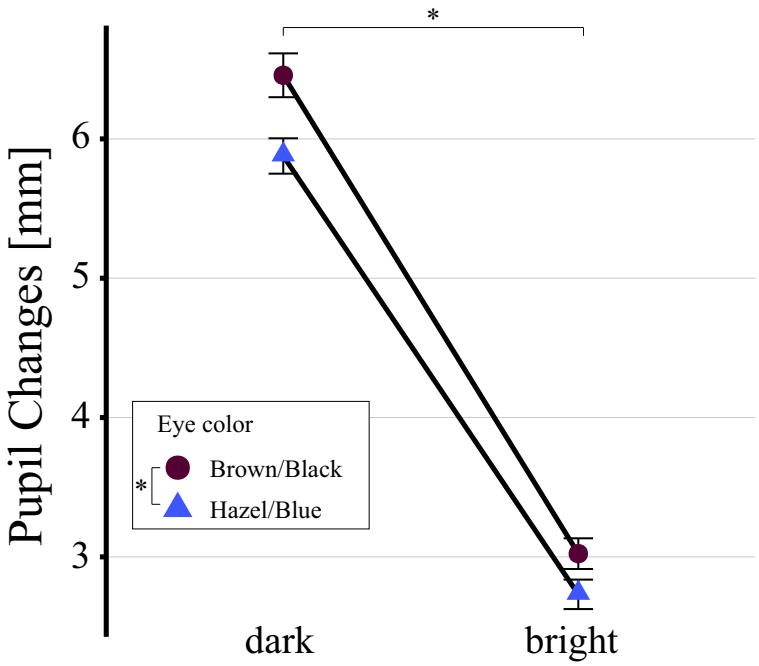

Figure 3.9 Pupillary light reflex.

The results of pupillary light reflex when dark or bright screen were presented in whole screen. Brown and blue dots indicate the averaged pupil diameter to each brown/black and hazel/blue iris group.

Figure 3.10a illustrates the time course of pupil changes for each iris color group during the whole presentation time and for each pattern (glare, control) and color conditions. Compared to previous studies, the initial pupil constriction for each color in the current data was almost aligned to each color. This may be because we used isochromatic colors as peripheral inducers of the stimuli. Note that the effect of the larger pupil constriction in the glare illusion existed under any color condition; a two-way repeated-measures ANOVA on average pupil changes revealed a significant main effect of both pattern and color condition ($F(6,14)=125.7580$, $p<0.001$, $\eta_p^2 = 0.9063$; $F(1,14)=3.1282$, $p=0.0084$, $\eta_p^2 = 0.194$, respectively). Additionally, a two-way repeated-measures ANOVA on the difference in pupil size between the glare and control conditions revealed a significant main effect on the interaction between eye color and color condition ($F(6,84)=1.99$, $p=0.076$, $\eta_p^2 = 0.12$). There was no significant main effect of both pattern and color condition ($F(6,14)=1.2908$, $p=0.2750$, $\eta_p^2 = 0.0844$; $F(1,14)=1.4199$, $p=0.2166$, $\eta_p^2 = 0.0921$, respectively). Following simple effect for the interaction indicated that the difference in pupil constriction to blue is larger in the group of black/brown iris colors than in the group of hazel/blue iris colors ($F(1,14)=7.0260$, $p=0.0190$, $\eta_p^2 = 0.3342$) , as shown in Figure 3.10b.

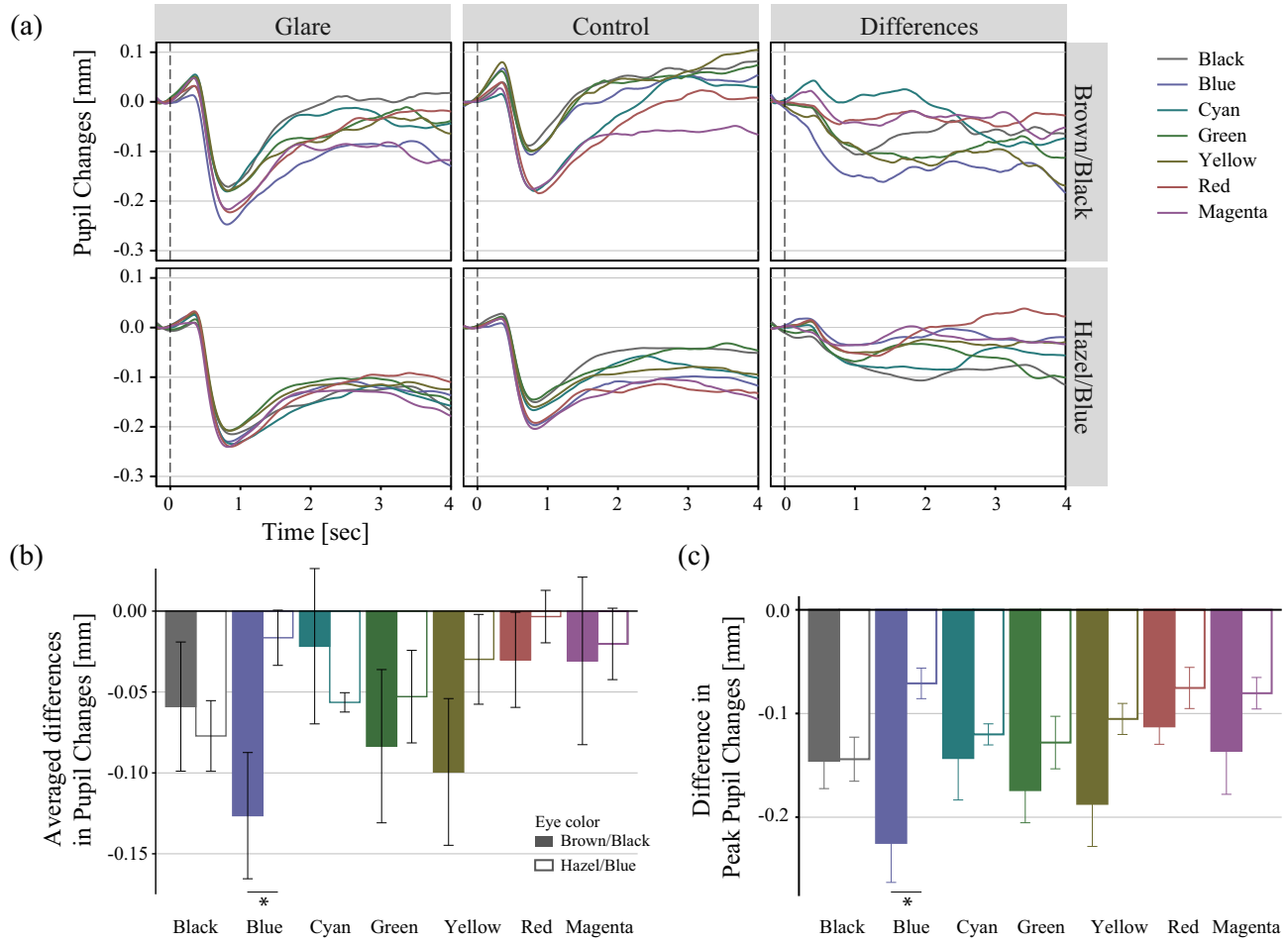

Figure 3.10 The results of the pupillary responses.

The horizontal axis indicates the time (in seconds), while the vertical axis indicates the grand-averaged change in pupil dilation from the baseline (the gray shaded area, from -200 ms to 0 ms, shows the time range of the baseline). (a) Each line color shows the result of the averaged pupil diameter to the halo stimuli and colored glare. (b) The average pupil changes in 4 s of viewing. (c) The peak pupil constriction for each pattern and color condition. The asterisks (*) indicate a statistical significance of $p < 0.05$. Error bars indicate the standard error of the mean.

We further analyzed the correlation between the PLR (Figure 3.9) and the average differences in pupil constriction (Figure 3.10b) for each participant. Here, we used a simple linear model (LM) with PLR values as independent variables to evaluate the differences in pupil response between the glare and control conditions. However, the PLR could not explain the extent of pupil constriction to the glare illusion ($t(14)= 0.029$, $p = 0.977$). We subsequently tested the correlation between the iris color values (i.e., L ab) and the average differences in pupil constriction with the colored glare illusions. The results of the LM for each color value showed that L was significantly related to pupil constriction ($y = 0.0022x$

- 0.1127, t(14) = 2.5811, p = 0.0113), indicating that the effect of pupil constriction on glare illusion was larger for dark-colored eyes than in bright-colored eyes. Additionally, the model that was used to enter the L ab values as dependent variables indicated that L, b* value, and the interaction between them was assessed by the LM (y = –0.0098 × L + 0.2248 × b* - 0.0291 × L b* + 0.001; t = –2.599, p = 0.0107 for L, t = –2.349, p=0.0207 for b* and L = 2.525, p = 0.0131 for L b*).

3.4 Discussion

In the current study, we examined the pupillary response to the colored glare illusion in participants with different iris colors. We assumed that if the pupil constriction to the glare illusion reflects the implicit response as anticipation to 'dazzling', the pupillary responses would be similar to the mechanism used by MP which involves the protection of the eyes. As we hypothesized, larger pupil constriction to blue glare illusion was observed for black/brown-colored irises, while there was no effect for blue/hazel-colored irises.

The pupillary response on the bright illusion has been reported here and elsewhere (e.g., Laeng and Endestad, 2012; Zavagno et al., 2017) or even to image of the sun (Binda et al., 2013b; Naber and Nakayama, 2013). In addition to successfully replicating the effect of the larger pupil constriction on the glare illusion regardless of iris colors, the specific larger effect on pupil constriction for blue glare illusion was observed only for the black/brown iris group but not for blue/hazel group (Suzuki et al., 2019a).

The different effect of the pupil response to blue glare illusion is at least consistent with the idea of an ecological account based on the iris color, which is related to the density of the MP. Since the iris color relates to the macular pigment density, the difference in density affects the extent of absorption of the light projected on the retina. The differences in the varied light sensitivity, contrast sensitivity, glare recovery, and color perception seem to play an important role in preventing strong light from entering the retina (Davison et al., 2011; Hammond Jr et al., 2013; Laeng et al., 2007). Additionally, the sensitivity to blue light is higher for high MP density than for low MP density (Stringham et al., 2015). In the current findings, the larger pupil constriction to blue glare illusion for black/brown eyes is likely to function in a similar way as the MP regarding the protection of the eyes from strong light.

In the correlation analysis with iris color values of L a*b*, we confirmed that the pupillary constriction effect on the glare illusion is related to the iris colors, given the correlation between the pupillary response to the glare illusions and the L b* interaction. This also supports the effect of the pupillary response on the inherited property of the accumulation of retinal pigments and ocular melanin as a marker for the adaptation to a homogeneous environment.

Chapter 4

Pupillary Response on Luminosity Perception

Previous studies reported that glare illusion, which enhances the perceived brightness of a central white area surrounded by a luminance gradient, yields a large pupil constriction. In this study, we examined two probable factors modulating the pupil size in glare illusion by using the Kanizsa triangle and no-triangle (i.e., no illusory contour) with a radial pattern of luminance gradation and control pattern, which rotates the luminance gradation by 90 degrees. We hypothesized that the pupil constriction to glare illusion reflects: (a) a perceived brightness or self-luminosity perception involved in an anticipation/ preparation for a probable dazzling, and (b) the configuration of the stimulus luminance pattern because the averaged luminance of the glare illusion used in previous studies within a small visual field is higher than its control condition. Thus, we observed the pupil responses to the Kanizsa triangle with a radial and control pattern, and their averaged luminance in any region of the visual angle matched to exclude the effect of luminance configuration of the stimulus to the pupil response. The results showed the larger pupil constriction in the Kanizsa triangle with the radial pattern was observed than in the no-triangle condition and control pattern. Interestingly, although the Kanizsa triangle with a control pattern had an effect on the brightness enhancement by an illusory contour, it did not affect the pupil responses. Therefore, we conclude that pupil constriction to glare illusion is occurred by the brightness changes which is considered additionally to the effect of 'self-luminosity'. At the same time, we deny the argument that the pupil changes related to illusory glare perception were determined by the localized luminance projected around the fovea in the visual field.

4.1 Introduction

A perceptual experience of perceived intensity of light (brightness) and surface-color categories of an object (lightness) are the basic aspects of visual processing. As described in a simultaneous contrast, a gray object in white background appears darker than that in black background simply because of the low-level visual processing by the lateral inhibition (Kingdom, 1997; Lotto et al., 1999). Our brightness/lightness judgment is determined not only by stimulus properties such as the actual luminance level, but also by various contextual factors. In the cortical visual processing to estimate the lightness from an object surface, Gilchrist proposed an anchoring theory; we re-scale the lightness of an object in the visual field based on the brightest region of the retinal image as an anchor (Gilchrist et al., 1999). In terms of brightness, higher-level pathways, such as an interpretation of the surrounding context, stimulus configuration, and memory-related processing, involve the determination of brightness perception (Adelson, 1993; Adelson and Pentland, 1996).

The mode of color appearance, which is a concept of how we perceive the surface of an object, was first suggested by Katz (Katz, 1935). One of the modes defined self-luminosity, which is described as the visual experience where a given portion of an object appears glowing or emitting light regardless of whether there is an actual light source. We can perceive self-luminosity from various scenes; the sun in a clear sky, traffic lights, and a car headlamp at night. Interestingly, we can also experience luminosity as a pictorial representation of self-lumonsity from the picture. For example, glare illusion is perceived as if the ray of light is coming from the central region, as in the so-called self-luminosity perception related to the brightness enhancement of a central white area surrounded by a luminance gradient owing to a pattern of luminance gradations converging onto a central white area, without any actual change in light intensity (Agostini and Galmonte, 2002; Zavagno, 1999). Zavagno and Caputo (2005) suggested the existence of different visual pathways between the luminosity perception to the glare illusion and surface color perception. Therefore, the perception of self-luminosity cannot be explained as the extension of white as a surface color, and white does not relate to the determination of self-luminosity.

Interestingly, several previous studies on pupillometry reported that glare illusion yielded larger pupil constriction compared to the control condition, where the same gradient elements of glare illusion were rotated by 180 degrees to eliminate the central, subjective brightness enhancement (e.g., Bombeke et al., 2016; Laeng and Endestad, 2012; Suzuki et al., 2019a,b; Zavagno et al., 2017). The pupil constriction effect on the glare illusion was observed even though the pupillary response is mainly a function of adjusting the amount of light entering the eye from the ambient environment (Ellis, 1981; Woodhouse and Campbell, 1975).

What, then, is the factor related to the large pupil constriction in glare illusion? One possibility

is the intrinsic pathway on the pupillary response for 'anticipation' or 'preparation' for glare perception. Because the glare illusion evokes the self-luminosity perception, the pupillary constriction to the glare illusion represents the adaptation response to probable dazzling sunlight imitated by the glare illusion. Another explanation is that the pupil changes just reflect the configuration of the stimulus luminance pattern as a PLR; the pupil changes may be determined by the localized stimulus luminance projected around the fovea in the visual field because the averaged luminance of the glare illusion within a small visual field is higher than its control condition.

Therefore, we examined two probable factors to modulate the pupil size in the glare illusion by using the Kanizsa triangle with a radial pattern of luminance gradation and a control pattern, where the luminance gradation is rotated by 90 degrees (see Figure 4.1a) (Kanizsa, 1979). The Kanizsa triangle with luminance gradation induces a similar effect on the brightness enhancement as the glare illusion. Importantly, the averaged luminance to those stimuli in any visual angle was identical to one another (see 4.1c) to observe the effect of the stimulus configuration on the pupil response. Hence, in Experiment 1, we monitored pupil response with infrared eye-trackers during the presentation of each Kanizsa triangle. In Experiment 2, we confirmed the subjective brightness changes with the Kanizsa triangle for a different gradation pattern by using the psychophysical adjustment method.

4.2 Methods

4.2.1 Participants

Twenty-one volunteers (21 men; age range 20 – 28) took part in Experiments 1 and 2. The sample size was determined by a priori power analysis using the G*Power (Faul et al., 2007), considering a power at 0.8, Type I error level at 0.05 and expected effect size at 0.33. These parameter settings led to a minimum sample size of 20 participants. All participants were undergraduate and graduate students who had normal or corrected-to-normal vision. Additionally, they had normal color vision as established by the use of the Ishihara pseudo-isochromatic plates (Ishihara, 1996). All experimental procedures were in accordance with the ethical principles outlined in the Declaration of Helsinki and approved by the Committee for Human Research at the Toyohashi University of Technology. The experiment was conducted under the approved guidelines of the committee, and all participants provided written informed consent. Participant data and experimental scripts are available at https://github.com/suzuki970/Experimental_data/tree/master/P04.

4.2.2 Experiment 1

Stimulus and apparatus

Figure 4.1a shows the Kanizsa triangle and no-triangle condition (i.e., no illusory contour) with a radial and control pattern used in this experiment. The xy coordinates of the each line in the CIE1931 color space were 0.3127 and 0.3290. The luminance graduation in the peripheral elements of the stimulus was changed from the xy value mentioned above to an archroma color, accompanied by a changing Y value from 0.72 cd/m^2 to 84.43 cd/m^2. The luminance of the Kanizsa triangle with uniform pattern (Figure 4.1a bottom) and peripheral triangle line was 42.62 cd/m^2. The background luminance was 84.43 cd/m^2. The luminance of the stimuli was calibrated using a spectro-radiometer (SR–3AR, TOPCON, Tokyo, Japan). The averaged luminance in the visual angle of 4, 4.71, and 6.81 degrees was 82.30 $\pm$ 1.24, 79.09 $\pm$ 1.14 and 75.24 $\pm$ 0.65 cd/m^2, respectively, as shown in Figure 4.1b.

All stimuli were presented on an LCD monitor (Display++, Cambridge Research Systems Ltd., Kent, UK) with a resolution of 1920 x 1080 and a refresh rate of 120 Hz. In the Kanizsa triangle, the diameter of each peripheral circle was 4.20 degrees, and 3 circles were located at 4.71 degrees from the center of the monitor. The equilateral triangle was put at the center of the monitor at 8.16 degrees from the side. The three different sizes of the inverted line triangles were drawn in every stimulus condition (see Figure 4.1a). The visual angle of each triangle of one side was 8.17, 6.53, and 5.23 degrees, respectively. In the control condition of the Kanizsa triangle, the three circles were rotated clockwise by 30 degrees, while the luminance gradation of peripheral elements was identical to the radial pattern. The fixation point was located at 0.1 degrees from the center. Each participant's chin was fixed at a viewing distance of 700 mm. The task was conducted in a darkroom and executed in MATLAB2016a (The MathWorks, Natick, MA, USA) using Psychtoolbox (Brainard, 1997).

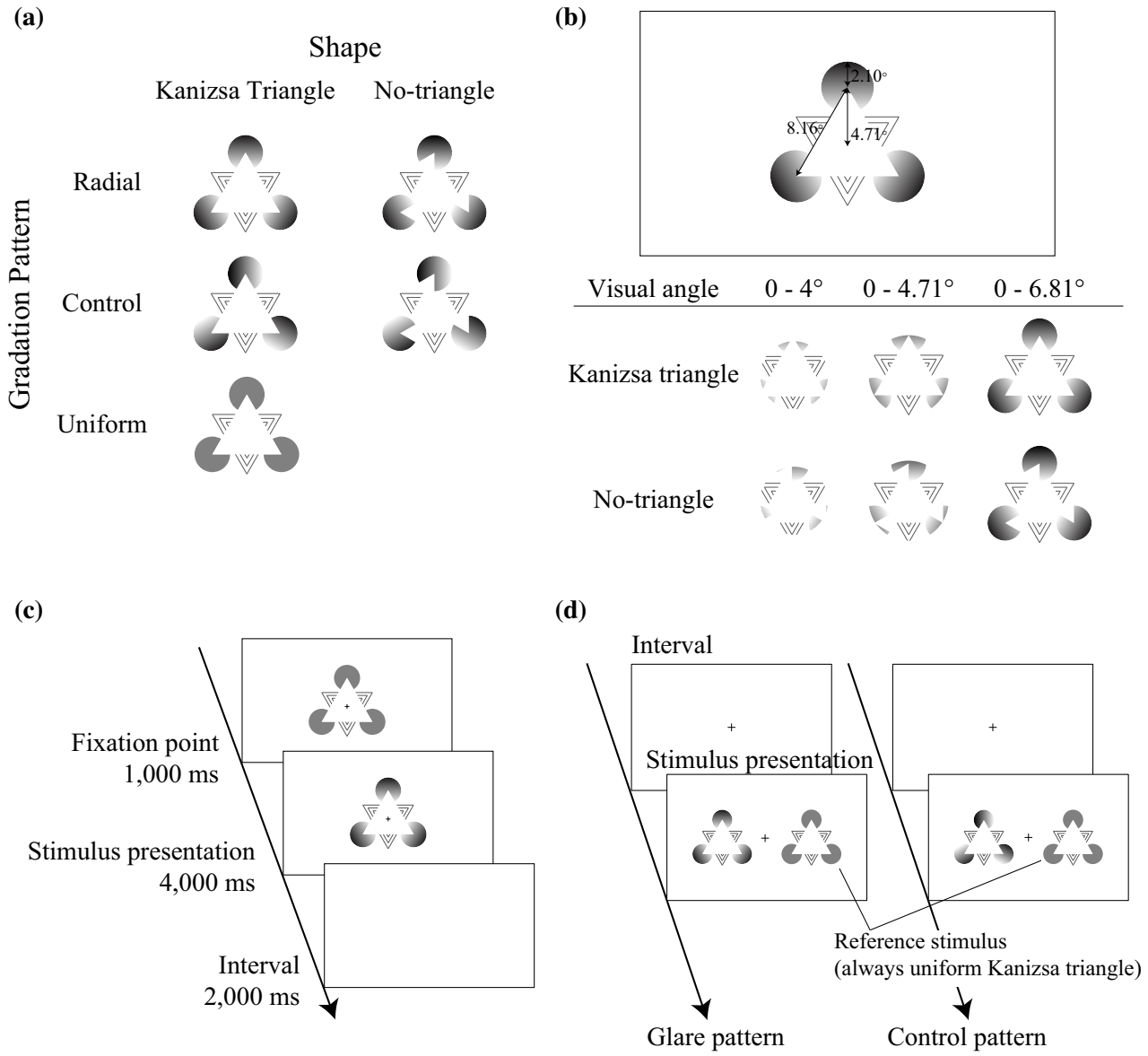

Figure 4.1 Experimental stimuli and procedure.

(a) Both the central glare illusion (above) and the control stimuli (middle) consisted of luminance gradient circles that either converged towards the center of the pattern or were turned towards its periphery. The uniform pattern had no gradation (row). The Kanizsa triangle with the luminance gradation and control condition, where elements were rotated by 90 degrees. (b) Configuration of the stimuli. The definition of the stimulus visual angle is illustrated above. (c) The procedure of Experiment 1. Each trial consisted of the presentation of the central fixation point for 1000 ms and the Kanizsa triangle with a uniform pattern, followed by a stimulus presentation for 4000 ms. Each trial was separated by an inter-stimulus interval (ISI) of 2000 ms. (d) Participants clicked the mouse in the initial blank screen to continue to the stimulus presentation; subsequently, the participant adjusted the luminance of the central region of the reference stimulus using a "trackball".

Procedure

A standard five-point calibration was performed prior to each session. Each trial started with the presentation of a uniform Kanizsa triangle (i.e., no-gradation Kanizsa triangle) with fixation cross for 1,000 ms. Then, one out of the four stimuli was displayed at the center of the monitor for 4,000 ms. Each trial was separated by the presentation of blank screen as an inter-stimulus interval (ISI) of 2,000 ms. The experiment consisted of 80 trials (2 shapes $\times$ 2 gradient patterns $\times$ 20 trials), divided into two sessions. Each of the four stimuli was presented randomly. Each session lasted for approximately 10 min.

Recording and analysis of pupil size

Pupil diameter and eye movements were measured by a Senso Motoric Instruments RED500 (SMI, Berlin, Germany) eye-tracking system at a sampling rate of 120 Hz. An measurable resolution of eye movement was at a about 0.01 degrees. The pupil data during eye blinks, detected by using peak changes on the velocity of the pupil response, were interpolated using cubic-spline interpolation. The trial, including the missing data of 50%, were excluded from the analysis. Additionally, a principal component analysis (PCA) was performed to each time point of pupil size. When the averaged first and second principal component of the trial was more than $\pm$ 3 σ, these trials were rejected (the average rejected trials were 4.65 $\pm$ 5.80 trials out of 80 per participant). Following which smoothing of each data point with $\pm$ 30 ms, baseline pupil size was calculated as an average of data measured during the presentation of a uniform Kanizsa triangle prior to stimulus onset from $-$ 200 ms to 0 ms (i.e., presentation onset). The pupil data in each trial was normalized by subtracting the baseline pupil size. Across conditions, the pupillary response was averaged from the presentation period of stimulus onset until 4,000 ms.

Statistical analysis

A two-way repeated-measures ANOVA was performed using pupil change as an average during the whole epoch using pattern and gradation as within-subject factors. The level of statistical significance was set to $p < 0.05$ for all analyses. Pairwise comparisons of the main effects were corrected through multiple comparisons using the modified Bonferroni (Shaffer) method. Effect sizes (partial η^2; η_p^2) were determined for the ANOVA. Greenhouse-Geisser corrections were performed when the results of Mauchly' s sphericity test were significant. Statistical analyses were performed using R software (Ihaka and Gentleman, 1996).

4.2.3 Experiment 2

Stimulus and apparatus

The stimuli displayed in Figure 4.1a and the same equipments of Experiment 1 were used in Experiment 2.

Procedure

At the beginning of each trial, a fixation cross appeared prior to the stimulus presentation, and participants clicked the mouse to proceed to the stimulus presentation. Then, two stimuli were displayed side-by-side: the target stimulus and the reference stimulus, at 10 degrees from the center of the monitor on either side of the center. The side (left, right) of the target and reference stimuli were determined randomly in each trial, but the number of trials for each stimulus was kept constant (N = 8). Although the fixation cross appeared on the center of the screen, they allowed to move their gaze. The target stimulus could be one of two stimuli (the Kanizsa triangle with radial or control pattern, as shown in Figure 4.1c), and the reference stimulus was always the Kanizsa triangle with a uniform pattern. Therefore, the whole experiment consisted of 32 trials (2 patterns $\times$ 16 trials). Participants were asked to adjust the luminance of the central region of the reference stimulus (the uniform Kanizsa triangle) until they felt that it had the same brightness as that of the target stimulus by using a trackball. Each session lasted approximately 10 min.

Statistical analysis

A one-way repeated-measures ANOVA was conducted using the average brightness adjustments for each pattern (radius, control) as within-subject factors. To compare the mean brightness adjustments with the uniform Kanizsa triangle, one-sample student' s t-test was carried out by comparing these values to the null hypothesis that the averaged data were the actual luminance value of the central triangle.

4.3 Results

4.3.1 Experiment 1

A two-way repeated-measures ANOVA on the average pupil changes revealed a significant main effect of both the pattern (i.e., a radius and control), shape (i.e., the Kanizsa triangle and no-triangle) and its interaction on the pupil diameter ($F(1, 20) = 6.828$, $p = 0.0167$, $\eta_p^2 = 0.255$; $F(1, 20) = 14.078$, $p = 0.0013$, $\eta_p^2 = 0.4131$; $F(1, 20) = 5.872$, $p = 0.0250$, $\eta_p^2 = 0.227$, respectively). Figure 4.2a illustrates

the grand-averaged time-course of pupil changes among participants during the whole presentation time, and Figure 4.2b shows the averaged pupil constriction from 0 ms to 4000 ms for each pattern and shape condition. We observed the occurrence of the pupil dilation around 500 ms from stimulus onset owing to the luminance difference between ISI and the baseline. Importantly, multiple comparisons showed that the pupil response to the Kanizsa triangle with a radial pattern was larger than the response to the Kanizsa triangle with a control pattern and to no-triangle with radial pattern ($F(1, 20) = 12.390$, $p = 0.0022$, $\eta_p^2 = 0.3825$; $F(1, 20) = 13.900$, $p = 0.0013$, $\eta_p^2 = 0.4100$). Furthermore, no significant difference was observed between the Kanizsa triangle and no-triangle with a control pattern ($F(1, 20) = 2.2411$, $p = 0.1500$, $\eta_p^2 = 0.1008$) and the no-triangle with a radial and control pattern ($F(1, 20) = 0.0301$, $p = 0.8641$, $\eta_p^2 = 0.0015$). Figure 4.2c shows the averaged gaze map for both the Kanizsa triangle and no-triangle with radial patterns. Because we instructed participants to pay attention to the central fixation cross, the mean duration time of the gaze fixation was focused on the central region of the stimulus. A one-way ANOVA for the mean duration time in the visual angle of 1 degree was not significant in any pair of pattern and shape ($F(1, 20) = 0.8781$, $p = 0.4423$, $\eta_p^2 = 0.0421$).

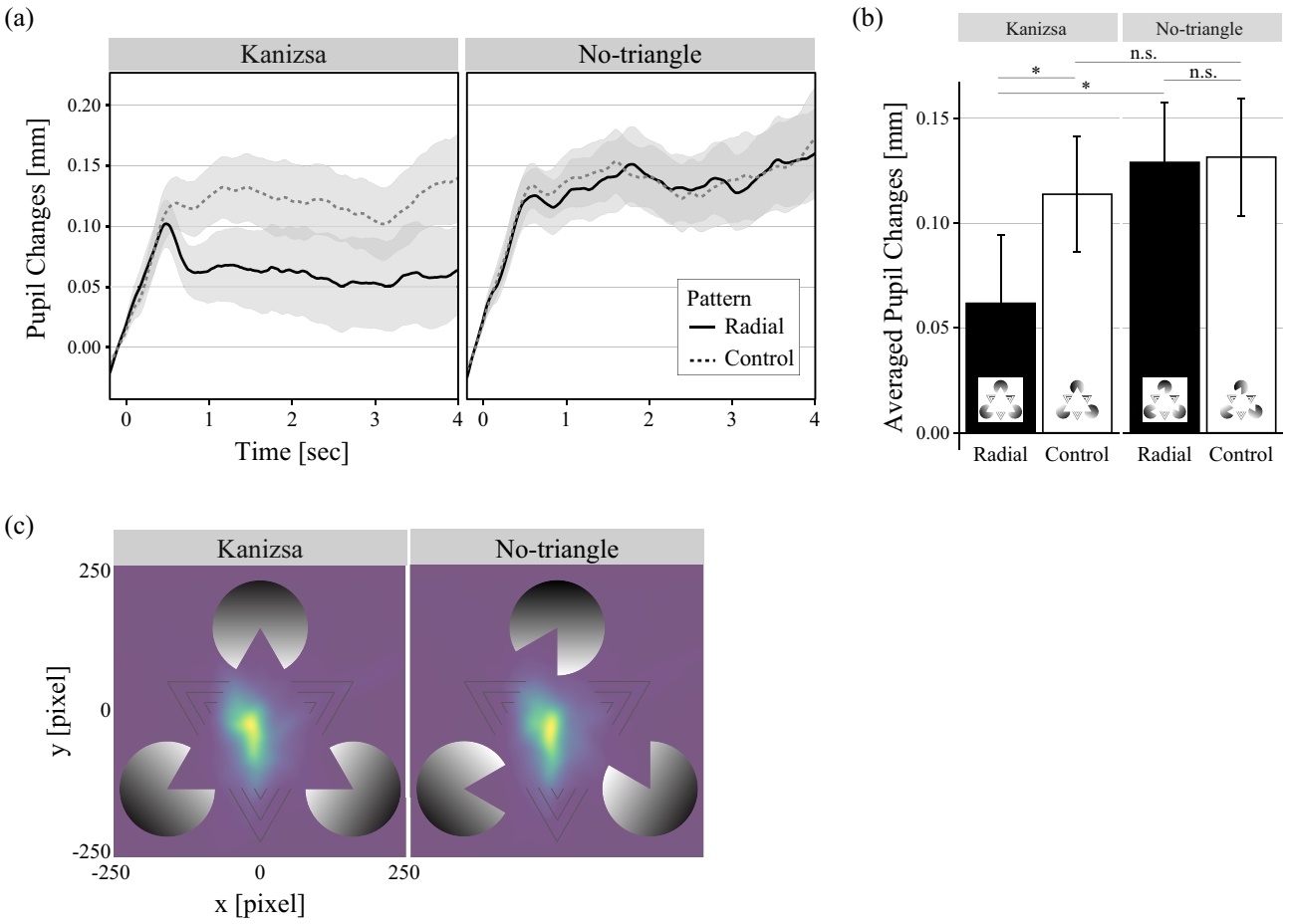

Figure 4.2 The pupillary response to the Kanizsa triangle.

Pupillary responses in Experiment 2. (a) The horizontal axis indicates the time (in seconds), while the vertical axis indicates the grand-averaged change in pupil dilation from the baseline (-200 ms to 0 ms, shows the time range of the baseline). Shaded areas represent the standard error of the mean. (b) The results of the averaged pupil diameter for each pattern and shape condition. (c) The gaze heatmap in the Kanizsa triangle and no-triangle with radial patterns. The asterisks (*) indicate a statistical significance of $p < 0.05$. Error bars indicate the standard error of the mean.

4.3.2 Experiment 2

A one way ANOVA repeated-measures on the adjusted luminance to the Kanizsa triangle indicated that the Kanizsa triangle with a radial pattern was evaluated as brighter compared to the triangle with a control pattern ($F(1,20) = 50.87$, $p < 0.001$, $\eta_p^2 = 0.7178$), as shown in 4.3. Additionally, the adjusted luminance for both the radial and control patterns was higher than for the uniform pattern of the reference stimulus ($t(20) = 6.3528$, $p < 0.001$, $t(20) = 2.1638$, $p = 0.04276$, respectively). We subsequently analyzed the

association between the adjusted brightness and the average pupil constriction for the Kanizsa triangle measured in Experiment 1 by using a simple linear regression model. The brightness for the Kanizsa triangle with the radial and control patterns was marginally correlated to pupil constriction ($t(20) = -1.756$, $p = 0.0872$).

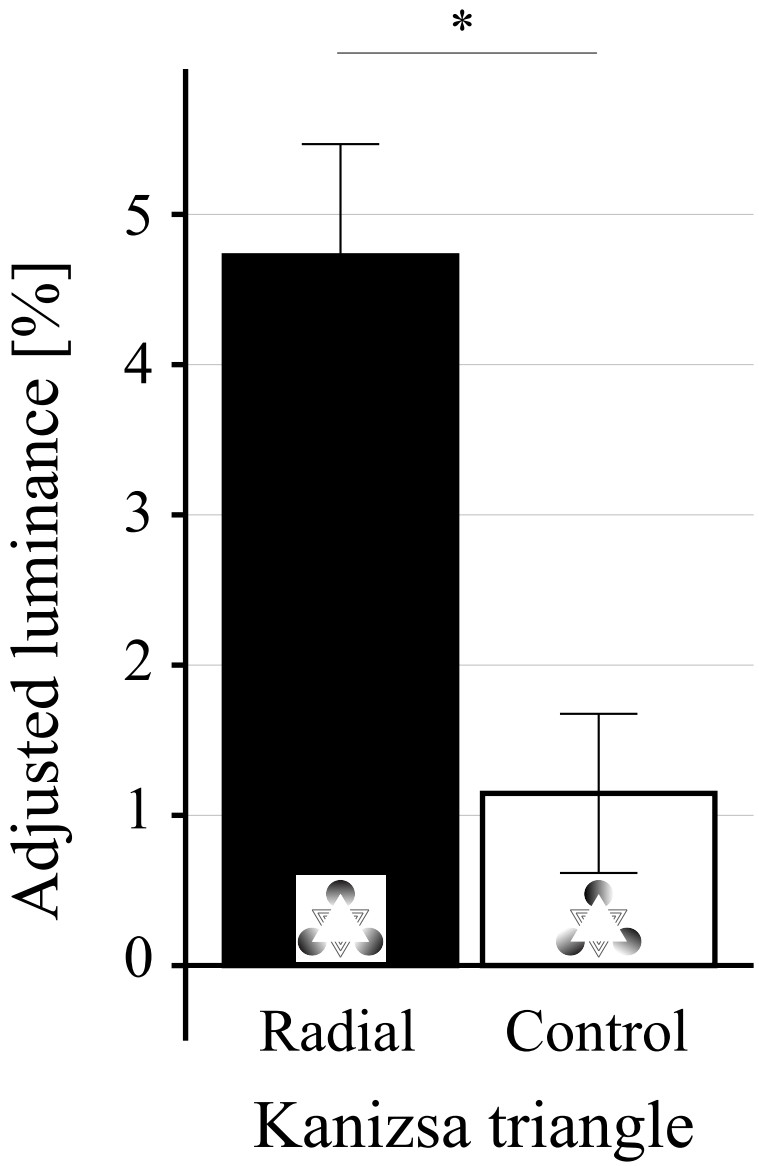

Figure 4.3 The adjusted luminance to the Kanizsa triangle.

The vertical axis shows the adjusted luminance compared to the uniform Kanizsa triangle. The asterisks (*) indicate a statistical significance of $p < 0.05$. Error bars indicate the standard error of the mean.

4.4 Discussion

In the current study, we used the Kanizsa triangle with luminance gradation elements, which resulted in the brightness enhancement and glare perception compared to the Kanizsa triangle with a control pattern (i.e., an illusory counter with a rotated version of the luminance gradation). Because these stimuli have the same luminance in any visual angle, we could exclude the effect of stimulus configuration. The present settings replicated the effect of a large pupil constriction in glare illusion by the Kanizsa triangle with a radial pattern (Bombeke et al., 2016; Laeng and Endestad, 2012; Suzuki et al., 2019a). Therefore, the pupil constriction to glare illusion is prompted by the brightness enhancement which is considered additionally to the effect of 'self-luminosity', and we deny the argument that the pupil changes related to glare illusion were determined by the localized luminance projected around the fovea in the visual field.

Interestingly, the pupil constriction effect disappeared in both the Kanizsa triangle with a control pattern (i.e., no glare perception with an illusory contour) and the no-triangle condition with a radial pattern (i.e., no illusory contour but with a converging luminance gradation onto the center). Although the Kanizsa triangle with the control pattern yielded a brightness enhancement via subjective contour, it did not affect pupil constriction as also shown in Bruno et al. study (2012). This is because the brightness enhancement to the Kanizsa triangle with the control pattern was very small as the results of brightness matching. However, the large pupil constriction was observed exclusively in the the Kanizsa triangle with a radial pattern, even though the pattern raised the brightness by almost $4-5\%$ which seemed still small, since the previous study reported that the glare illusion enhances the brightness of $20-35\%$ (Yoshida et al., 2008)).

We originally hypothesized that the self-luminosity perception prompted the large pupil constriction via different pathways from the surface-white, gray or black perception because several studies suggested that the self-luminosity perception in the glare illusion was involved in an extrastriate visual cortex and ventral-occipital cortical area but not a retinal processing (Bonato and Cataliotti, 2000; Leonards et al., 2005; Lu et al., 2006). Our additional experiment indeed indicated that the large pupil constriction to glare illusion did not depend on whether the luminance gradation slope was steep. Since the brightness enhancement effect to the steep slope of the luminance gradation is expected to be higher than to the gentle slope, the effect of brightness to the large pupil constrictions in any slope conditions of glare illusion were small. Therefore, the pupil constriction to the Kanizsa triangle with a radial pattern might be provided by the self-luminosity perception. If the large pupil constriction to the glare illusion is triggered by the self-luminosity, the cortical pathway to SC and PON via visual cortex involves the modulation of pupil constriction. The current findings suggest that the pathway from the visual cortex to the PON via the SC is involved in self-luminosity perception.

The pupil response reflects several cognitive and mental states; for instance, cognitive effort, attentional shifts, and unconscious and preconscious memory processing (e.g., Gomes et al., 2015; Kahneman and Beatty, 1966; Mathôt et al., 2013; Suzuki et al., 2018). The present study supports the possibility that the intrinsic pathway to the pupillary response for the 'anticipation' of probable dazzling sunlight is imitated by the glare illusion with self-luminosity perception.

4.5 Supplemental experiment on the effect of luminance gradation

In this experiment, we presented participants with different angles of illusory brightness stimuli individually on a computer screen. Participants answered whether they perceived self-luminosity for each of these illusions (as displayed in Figure 4.4a) after a few seconds of presentation while we monitored the eye movements with an infrared eye-tracker.

Participants. Twenty-two volunteers (17 men; 5 women; age range 20 - 25) took part in this experiment. Five participants were excluded from the analysis because the percentage of rejected trials was above 50%. All participants were undergraduate and graduate students who had a normal or corrected-to-normal vision. Additionally, they had normal color vision as established by the use of the Ishihara pseudo-isochromatic plates (Ishihara, 1996). All experimental procedures were in accordance with the ethical principles outlined in the Declaration of Helsinki and approved by the Committee for Human Research at the Toyohashi University of Technology. The experiment was conducted in accordance with the approved guidelines of the committee and all participants provided written informed consent.

Stimulus and apparatus. Figure 4.4a shows the glare, halo, and uniform stimuli used in Experiment. The xy coordinates of the each line in the CIE1931 color space were 0.3127 and 0.3290. The luminance graduation in the peripheral region of the stimulus was changed from the xy value mentioned above to an archroma color, accompanied by a changing Y value. The five angle conditions (58deg, 54deg, 42deg, and 38deg) were set to the luminance gradation from 0.72, 4.63, 13.05, and 16.21 cd/m^2 to 59.56, 55.38, 46.73, and 44.36 cd/m^2 for each stimulus. The uniform condition had a homogeneous pattern of elements in inducers of the stimulus and an averaged luminance gradation of 30.04 cd/m^2. The luminance of the background and central region of stimulus were 30.04 cd/m^2 and 59.56 cd/m^2, respectively. The luminance of the stimuli was calibrated using a spectro-radiometer (SR–3AR, TOPCON, Tokyo, Japan). All stimuli were presented on an LCD monitor (Display++, Cambridge Research Systems Ltd., Kent, UK) with a resolution of 1920 x 1080 and a refresh rate of 120 Hz. The diameter of each peripheral circle was 2.35 degree and 8 circles were located in 6 degrees from the center of the stimulus. The halo was

made from completely identical elements, but each circle was rotated by 180 degrees. The fixation point was located at 0.3 degrees from the center. Each participant's chin was fixed at a viewing distance of 700 mm. The task was conducted in a darkroom and executed in MATLAB2016a (The MathWorks, Natick, MA, USA) using Psychtoolbox (Brainard, 1997).

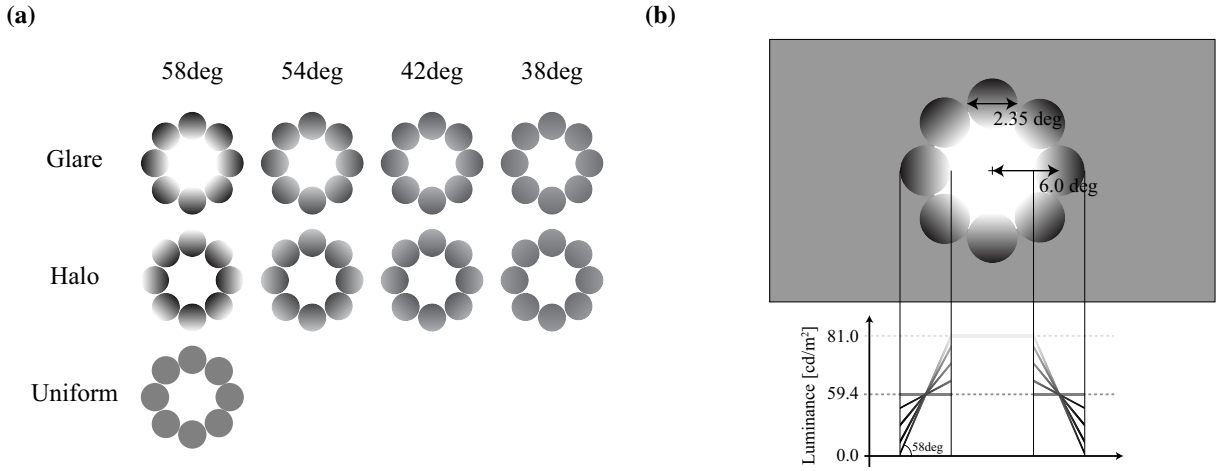

Figure 4.4 Experimental stimuli.

Procedure. The eye tracker was calibrated prior to each session using a standard five-point calibration, following which a session was conducted for approximately 8 min. Each trial began with a fixation point presented for 1,000 ms prior to the presentation of the stimulus and, consequently, each glare and halo stimulus was presented for 4,000 ms. Each trial was separated by an inter-stimulus interval (ISI) of 2,000 ms. The experiment consisted of 280 trials, divided into four sessions. Each of the 9 stimuli (4 types of angle $\times$ 2 gradient patterns + 1 uniform pattern) was presented randomly (number of trials = 20 per condition). Participants rested their chin at a fixed viewing distance of 70 cm.

Recording and analysis of pupil size. Pupil size and eye movements were measured by a Senso Motoric Instruments RED500 (SMI, Berlin, Germany) eye-tracking system at a sampling rate of 250 Hz. This equipment can measure eye movement at a resolution of about 0.01 degrees. The pupil data during eye blinks were interpolated using cubic-spline interpolation. Trials in which the pupils could not be detected during the beginning/ending of the trial were excluded from the analysis. Trials with additional artifacts, revealed by using peak changes on the velocity of the pupil response, were excluded from the analysis (the average rejected trials to each condition were 2.64 $\pm$ 2.70 trials out of 20 trials

per participant). The device outputted pupil size in mm. Baseline pupil size was computed as the average of the data collected during the fixation period prior to stimulus onset from –200 ms to 0 ms (i.e., presentation onset). In the time-course analysis, the pupil data in each trial were normalized by subtracting the pupil size at stimulus onset from the baseline pupil size, followed by the smoothing of each data point with ± 30 ms. Across conditions, the pupillary response was averaged from the presentation period of stimulus onset until 4,000 ms and evaluated by a repeated-measures ANOVA.

Statistical analysis. Two-way ANOVAs were performed using pupil change as the average during the whole epoch using the pattern (glare, halo, and uniform) and angle (58, 54, 42, and 38 degrees) as within-subject factors. The level of statistical significance was set to $p < 0.05$ for all analyses. Pairwise comparisons for main effects were corrected for multiple comparisons using the modified Bonferroni (Shaffer) method. Effect sizes (partial η^2; η_p^2) were determined for the ANOVA. Greenhouse-Geisser corrections were performed when the results of Mauchly's sphericity test were significant. Statistical analysis was performed using R software (Ihaka and Gentleman, 1996).

Results. Figure 4.5a illustrates the grand-averaged time course of pupil changes among participants during the whole presentation time and for each pattern (glare, halo, and uniform) and angle conditions. The pupil constricted after stimulus onset as a function of the PLR sustained for 1 s. We averaged pupil responses from 0 ms to 4,000 ms for each pattern and angle condition, as shown in Figure 4.5b. A two-way repeated-measures ANOVA on the average pupil changes revealed a significant main effect of the pattern conditions ($F(1, 21) = 28.61$, $p < 0.001$, $\eta_p^2 = 0.577$). Using multiple comparisons for each angle condition, a larger pupil constriction was observed for the glare compared to the halo ($p < 0.01$). However, the main effect of the angle and the interaction between pattern and angle were not significant ($F(2.108, 44.268) = 0.6215$, $p = 0.55$, $\eta_p^2 = 0.0287$, $F(2.465, 51.774) = 0.4388$, $p = 0.688$, $\eta_p^2 = 0.0205$, respectively)), indicating that the gradation angle did not affect pupil constriction to a great extent. Following this, we aggregated the angle condition to compare the results of the uniform stimuli, as displayed in Figure 4.5c. A one-way repeated-measures ANOVA on the averaged pupil changes across all conditions showed a significant main effect of the pattern ($F(21,1.868) = 14.53$, $p < 0.001$, $\eta_p^2 = 0.409$). Multiple comparisons of the pattern conditions showed that a larger pupil constriction was elicited by the glare condition compared to the halo and uniform conditions ($t(21)=5.3486$, $p = 0.0001$, $t(21) = 3.3941$, $p = 0.0027$). Pupil constriction for the uniform condition was larger than that for the halo condition ($t(21) = 2.1825$, $p = 0.0406$). Because participants looked at the fixation point at the center of the screen, this result seems consistent with the difference of physical averaged luminance between the glare and control conditions in the surrounding portion where the participants focused on. However, the pupil changes cannot be fully explained by the stimulus configuration because large pupil constriction was observed even for the lowest angle condition

of 38 degrees.

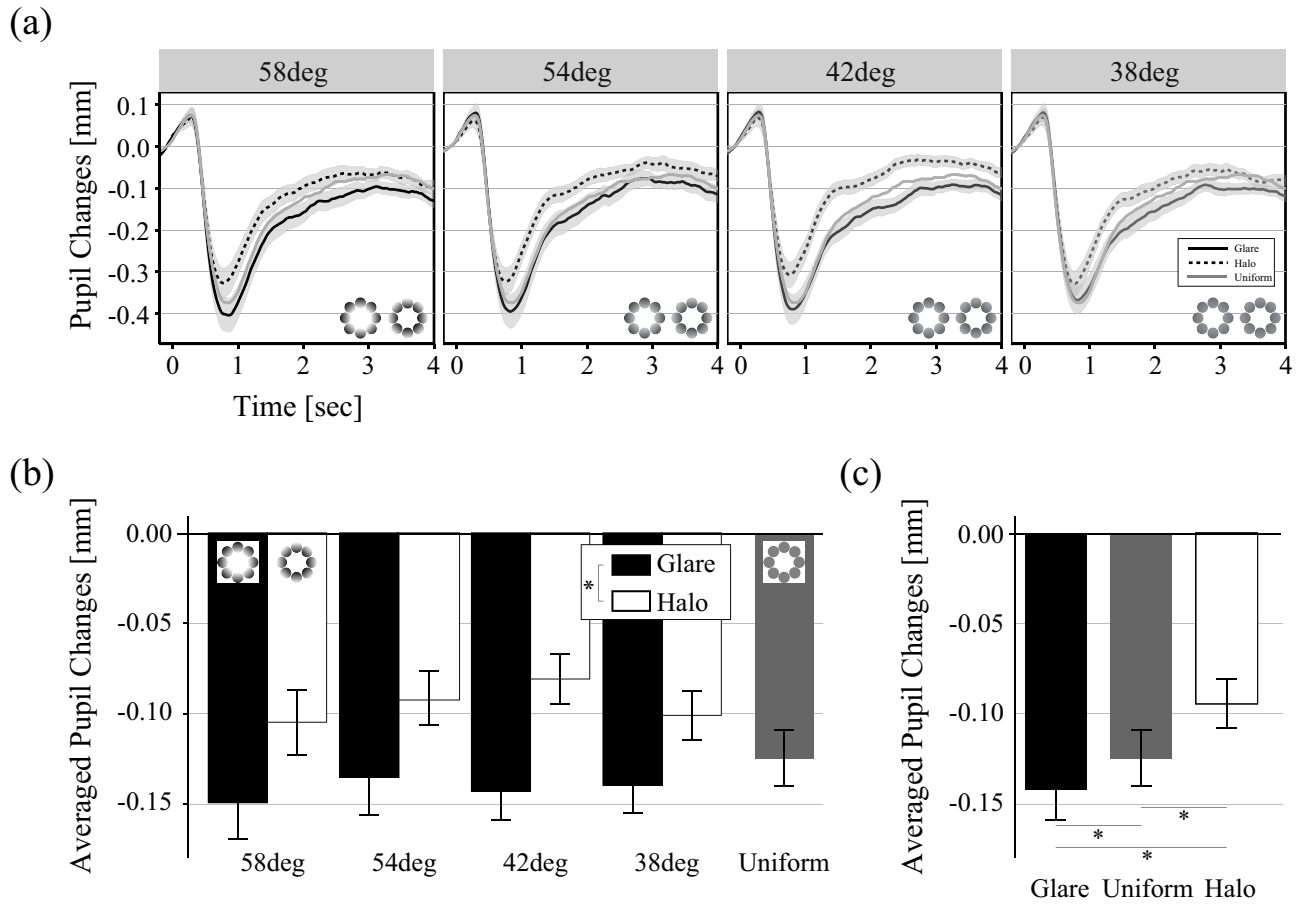

Figure 4.5 Pupillary response to the varied angle of glare illusion.

Pupillary responses in Experiment 1. (a) The horizontal axis indicates the time (in seconds), while the vertical axis indicates the grand-averaged change in pupil dilation from the baseline (the gray shaded area, from -200 ms to 0 ms, shows the time range of the baseline). The black solid and dotted lines show the results for the glare and halo patterns, respectively. The gray solid line indicates the results for the uniform pattern. (b) The average pupil changes in 4 s of viewing. (c) The averaged pupil constriction for different patterns (i.e., glare, halo, and control). The asterisks (*) indicate a statistical significance of $p < 0.05$. Error bars indicate the standard error of the mean.

Subsequently, we calculated the peak pupil constriction and the averaged velocity of pupil changes from the peak pupil constriction for each pattern and angle condition (Figure 4.6). A two-way repeated-measures ANOVA on the peak pupil constriction showed that a significant main effect of the pattern ($F(1, 16) = 30.99$, $p < 0.001$, $\eta_p^2 = 0.659$). However, the main effect of the angle and interaction between angle and pattern were not significant ($F(3, 48) = 1.448$, $p = 0.241$, $\eta_p^2 = 0.083$, $F(3, 48) = 0.748$, $p = 0.529$, η_p^2

= 0.0447). Additionally, a two-way repeated-measures ANOVA on the velocity of pupil changes revealed a significant main effect of the pattern (F(2.948, 61.917) = 1.513, p = 0.221, η_p^2 = 0.0672). Multiple comparisons of the pattern conditions showed that the constriction velocity for the glare at 58 deg was faster than that for the halo (F(1, 21) = 6.4982, p = 0.0187, η_p^2 = 0.2363). The main effect of the angle and the interaction between the pattern and angle were not significant (F(2.948, 61.917) = 1.513, p = 0.221, η_p^2 = 0.0672 , F(2.643, 55.501) = 0.6844, p = 0.548, η_p^2 = 0.0316 , respectively).

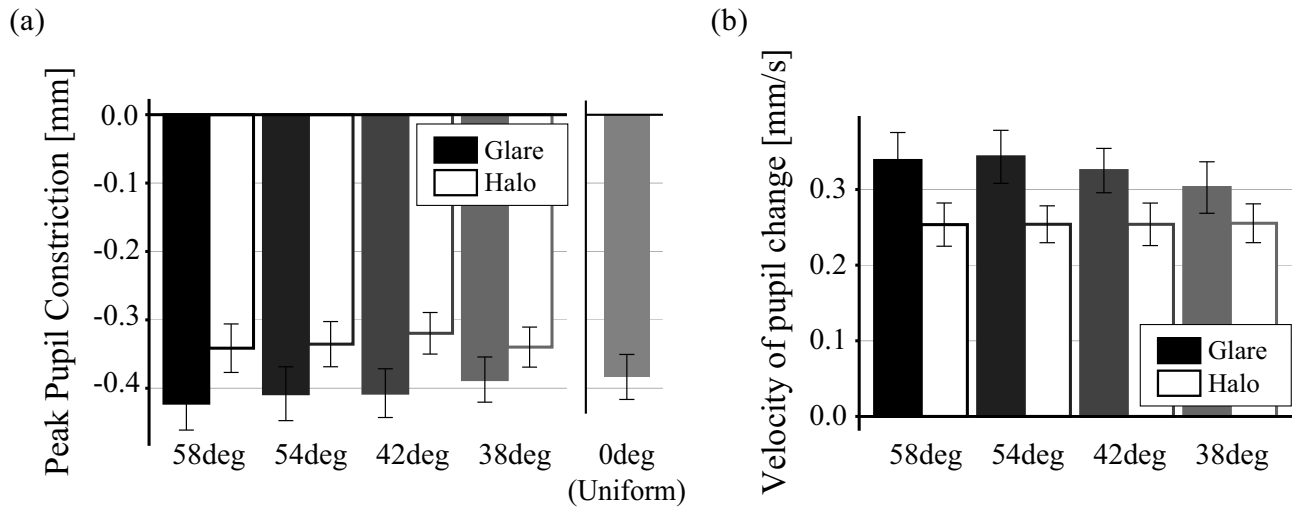

Figure 4.6 The peak pupil constriction and the velocity of pupil changes.

The maximum peak pupil constriction for each pattern and angle condition. The vertical axis indicates the grand-averaged change in peak pupil constriction from the baseline. (b) The averaged velocity of pupil changes from the peak constriction.

Because we expected that the mode of color appearance of self-luminosity for the glare illusion was related to pupil constriction, we calculated the correlation between pupil size and participants claiming that they perceived the luminosity from the presented stimulus at the end of each trial (as shown in Figure 4.7.

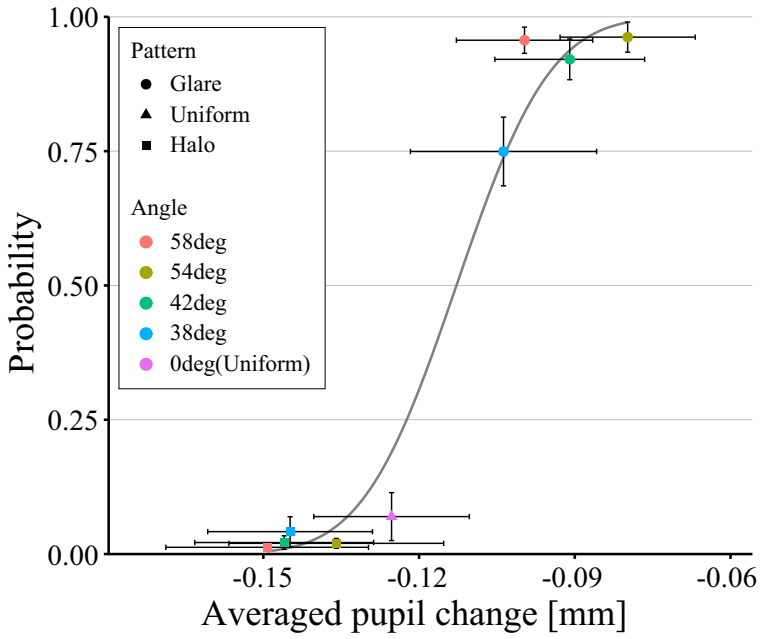

Figure 4.7 Psychometric fitting with response to self-luminosity.

The vertical axis indicates the probability of participants claiming they perceived the luminosity from the presented stimulus, while the horizontal axis shows the averaged pupil response for each stimulus.

Chapter 5

EEG and Pupil Measurement on Illusory Glare Perception

The glare illusion enhances the perceived brightness of a central white area surrounded by a luminance gradient, without any actual change in light intensity. In this study, we measured the varied brightness and neurophysiological responses of electroencephalography (EEG) and pupil size with the several luminance contrast patterns of the glare illusion to address the question of whether the illusory brightness changes to the glare illusion process in the early visual cortex. We hypothesized that if the illusory brightness enhancement was created in the early stages of visual processing, the neural response would be similar to how it processes an actual change in light intensity. To test this, we observed the sustained visual cortical response of steady-state visual evoked potentials (SSVEPs), while participants watched flickering dots displayed in the central white area of both the varied luminance contrast of glare illusion and a control stimulus (no glare condition). We found the SSVEP amplitude was lower in the glare illusion than in the control condition, especially under high luminance contrast conditions. Furthermore, we found the probable mechanisms of the inhibited SSVEP amplitude to the high luminance contrast of glare illusion based on the greater pupil constriction, thereby decreasing the amount of light entering the pupil. Thus, the brightness enhancement in the glare illusion is already represented at the primary stage of visual processing linked to the larger pupil constriction.

5.1 Introduction

In daily life, the perception of luminance from an object is an important function of human visual processing. The visual system must discriminate important information from a massive amount of inputs. It does this via a process called feature-selective attention. Feature-selective attention ensures that the visual system is attuned to the most salient stimuli, for example, social threats, people and memory selection. Previous studies have shown that modulation of feature-selective attention by manipulating stimulus property is reflected in the amplitude of steady-state visual evoked potentials (SSVEPs) (Fesi et al., 2014; Muller et al., 2006; Stormer et al., 2013). SSVEPs are measured as an oscillatory electroencephalography (EEG) signal, and tagged by flickering stimuli at the electrodes of the visual area (e.g., Müller et al., 1998; Regan, 1989). In addition to responding to attentional shift, SSVEP amplitude also increases linearly with increasing luminance contrast between a flickering random dot kinematogram and its background. For example, Andersen et al. reported that a stimulus with higher luminance contrast enhanced SSVEP amplitude via bottom-up biased visual processing (Andersen et al., 2012).

The aim of the current study was to measure SSVEPs to determine how brightness is perceived in the primary visual cortex. In general, we estimate brightness from the context surrounding an object, regardless of whether it has physical characteristics of a light source. In psychology, the term brightness refers to the perceived intensity of light coming from a given portion of an object (e.g., Purves et al., 2014). One way to study how the brain processes brightness is by using illusions, which alter our perception of brightness. The glare illusion is a generalized example in which we perceive brighter regardless of the actual luminance of the object (see Figure 5.1) (Zavagno, 1999). It is produced using a pattern of luminance gradations that converge onto a central white area, which is perceived as emitting light. The glare illusion enhances perceived luminance by 20 - 40% in comparison to a control condition (Yoshida et al., 2008). Agostini and Galmonte showed that the perceived luminance contrast between the square patch stimulus -which is put on the central white region of the glare illusion- and its background white region was significantly increased by the glare illusion (Agostini and Galmonte, 2002).

As mentioned in previous chapter, the brightness enhancement yields the larger pupil constriction when the self-luminosity perception is impressed by the glare illusion. Since we propose from earlier study that there is the pathway from the visual cortex to the PON via SC involved in the self-luminosity perception to modulate the pupil constriction, we are interested in the correlation between the cortical response and pupil size involved the processing of the glare illusion. Hence, we hypothesized that if the visual cortex processes the illusory brightness enhancement similar to how it processes an actual change in light intensity, then the SSVEP amplitude should be increased by the glare illusion; this assumption supports the report of an 'actual' luminance contrast effect on the SSVEP amplitude (Andersen et al.,

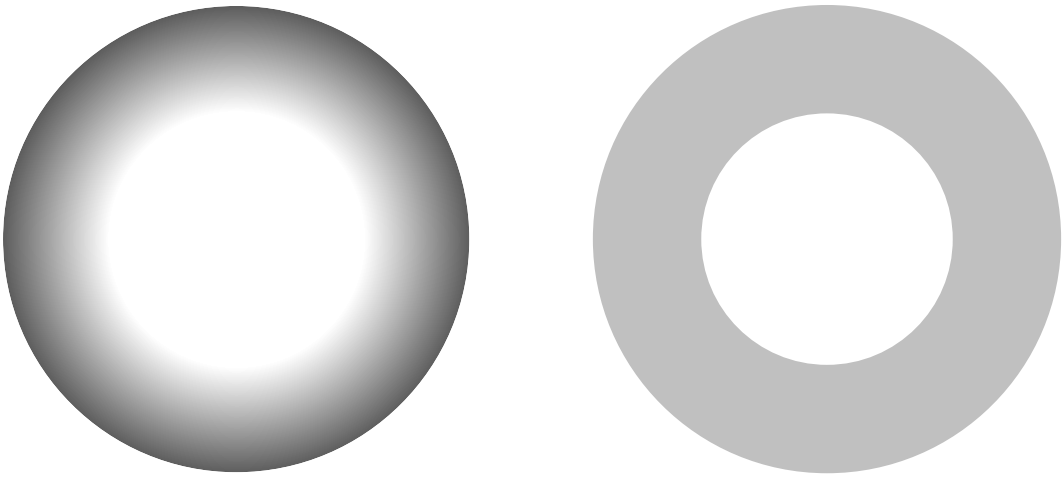

Figure 5.1 Glare illusion.

The glare illusion consists of a luminance gradation in the periphery. The central region of the glare illusion (left) typically appears brighter than the corresponding control stimulus (right) despite both having the same luminance.

2012). Another possibility is that the SSVEP amplitude would decrease because of the amount of light entering the eyes via pupil constriction. Most importantly, several previous studies showed that the brightness enhancement in the glare illusion, resulted in constriction of the pupil compared to its control condition (Laeng and Endestad, 2012; Suzuki et al., 2019a; Zavagno et al., 2017). They suggested that a top-down pathway is involved in the processing of the glare illusion as an adaptive response to protect from "dazzling". Since the pupillary response is mainly a function of retinal illuminance due to the amount of light energy entering the eye from the ambient environment (i.e., the pupil constricts in a bright room whereas it dilates in a dark room), the number of photons captured by the retina also decreases when the pupil is constricted by the bright illusion.

To test this hypothesis, we monitored changes in participants' brain activity while they watched flickering dots on the center region of a monitor, surrounded by either the glare illusion or its control condition (Experiment 1). The SSVEP amplitude was compared between the glare illusion and its control condition across five luminance contrast conditions, in line with the Andersen et al. (2012) study. To explore one possible mechanism responsible for the modulation of SSVEP amplitude by the glare illusion, we then measured pupil response while presenting the same stimuli as those used in Experiment 1 (Experiment 2). Since the two experiments involved the same participants, we were able to relate these responses to one another and correlate the change in pupil size to the change in SSVEP amplitude caused by the glare illusion.

5.2 Methods

5.2.1 Participants

Ten voluntary participants (nine men, one woman; age range 21–24 years) took part in Experiment 1 and 2. Data from one participant having the same luminance. Data from one participant were excluded from our analyses in Experiment 1 because a peak response of SSVEPs was not confirmed. All participants had normal or corrected to normal vision. All experimental procedures were in accordance with the ethical principles outlined in the Declaration of Helsinki and approved by the Committee for Human Research at the Toyohashi University of Technology, and the experiment was conducted in accordance with the approved guidelines of the committee. All participants provided written informed consent. Participant data and experimental scripts are available from https://github.com/suzuki970/Experimental_data/tree/master/P01.

5.2.2 Experiment 1

Stimulus and apparatus

We used the glare illusion (glare condition), which has luminance gradations converging onto a central white area. The uniform stimulus (control condition) was a control to each of the glare stimuli used in Experiment 1 and 2 (see Figure 5.2A). While the central region was surrounded by a luminance gradation in the glare illusion, the averaged luminance of the gradation was used to surround the circle in the control condition. The xy coordinates of the colors in the CIE1931 color space were x = 0.3127 and y = 0.3290. The luminance of the gradient pattern changed linearly from five luminance conditions (48, 54, 60, 66 and 72 cd/m^2) to 10 cd/m^2 as shown in Figure 5.2A. In that time, the luminance of the central region followed each luminance condition (48, 54, 60, 66 and 72 cd/m^2). The background luminance was 20 cd/m^2.

Forty dots (20 cd/m^2 in each) flickered within the central white region at a frequency of 7.5 Hz, which elicited SSVEPs during all trials. The luminance contrast ratio between the central region and dots was calculated from the Weber contrast: 0.58, 0.63, 0.67, 0.7 and 0.72. These luminance contrasts were used as the Contrast condition in this study. The location of the dots varied randomly in four directions: up, down, left, and right at 7.5 Hz. The luminance of the stimuli was calibrated using a chromameter (ColorCAL II, Cambridge Research System, Kent, UK).

All stimuli were presented on a cathode-ray tube (CRT) monitor (EIZO, FlexScan964, Ishikawa, Japan) with a resolution of 1280 × 1024 and refresh rate of 60 Hz. The task was executed in MATLAB 2014b (The MathWorks, Natick, MA) using Psychtoolbox 3 (Brainard, 1997). The task was carried out

in a shielded darkroom. The chin of each participant was fixed at a viewing distance of 600 mm from the monitor. All stimuli were presented at a visual angle of 6.47 degrees in the center of the monitor. The diameter of the stimulus from the center to the boundary of the inner circle was 2.5 degrees. Each dot subtended 0.29 degrees and was drawn in random position within the inner circle accompanied by the glare or control condition. The dots randomly moved up, down, left, or right by 0.05 degrees at 7.5 Hz flickering.

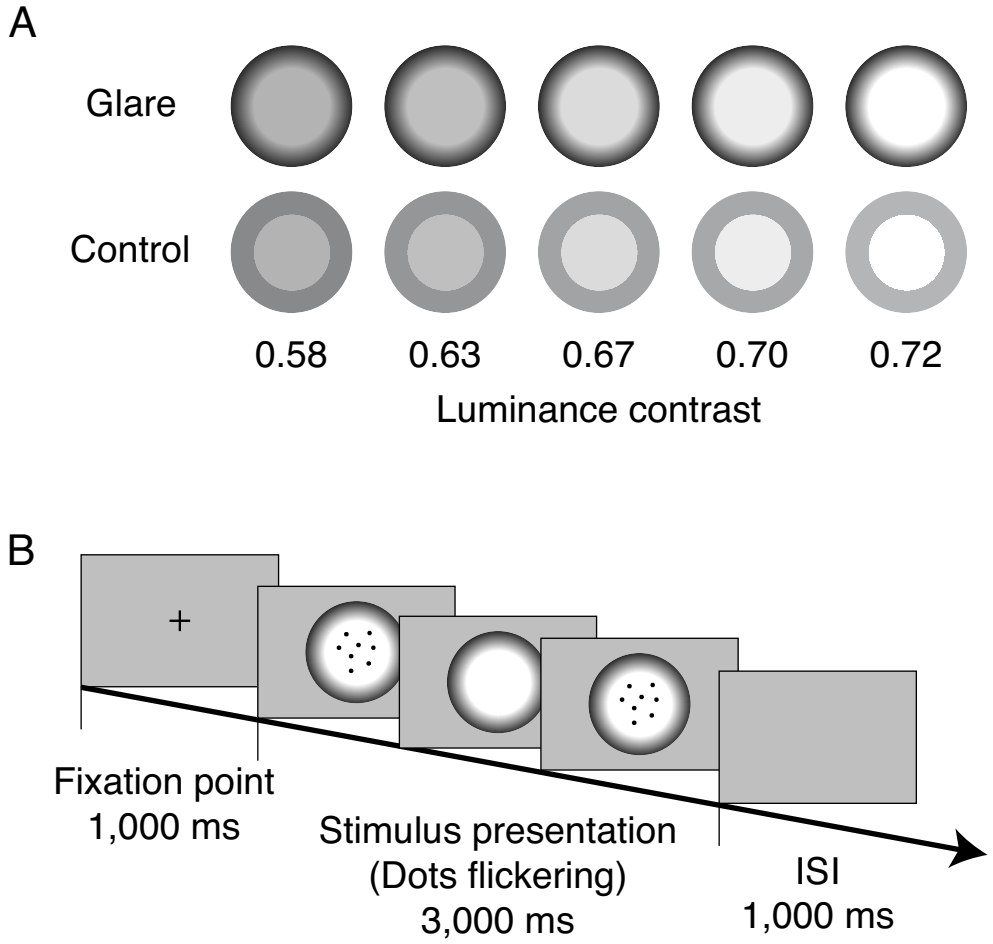

Figure 5.2 Experimental stimuli and design of Experiments 1 and 2.

(A) Examples of glare stimuli (above) and control stimuli (below) in five luminance contrast conditions used in Experiment 1 and 2. (B) The identical experiment design was used in both Experiment 1 and 2. Each trial included the presentation of the fixation point for 1000 ms and the presentation of the stimulus (glare or control condition) for 3000 ms. Each trial was separated by an inter-stimulus interval (ISI) of 1000 ms. Participants were instructed to focus on the flickering dots.

Procedure

Each trial consisted of the presentation of the fixation point for 1000 ms and the presentation of the stimulus for 3000 ms (see Figure 5.2, panel (B) for a design). Trials were separated by an inter-stimulus interval (ISI) of 1000 ms. The whole experiment consisted of 320 trials (5 contrasts $\times$ 2 patterns $\times$ 30 trials + 20 task trials), divided into four sessions. Each of the 10 stimuli (5 contrasts $\times$ 2 patterns) were presented randomly (number of trials = 30 per condition). In a subset of task trials (approximately 1 in every 15 trials), participants were instructed to respond by pressing the keypad when a black rectangle appeared in the center of the stimuli to confirm that they were paying attention to the stimulus.

EEG recording and analysis

Brain activity was measured using the BioSemi 64+6 channel ActiveTwo system (BioSemi Inc., Amsterdam, The Netherlands) at a sampling rate of 512 Hz. Electrodes were applied in accordance with the extended International 10–20 system. Extra electrodes were applied horizontally and vertically to the eye for bipolar monitoring of eye blinks. The EEG signal was sampled at 512 Hz and referenced to two additional electrodes (CMS: common mode sense and DRL: driven right leg). Recorded EEG data were band-pass filtered from 1 to 32 Hz. Epochs were defined from –200 ms to 3000 ms from the onset of the stimulus presentation. Baseline EEG data were averaged from –200 ms to 0 ms and subtracted from epoched EEG data. The baseline-corrected data from 500 to 3000 ms were used for analyses. We excluded the period from 0 ms to 500 ms because of the effect of visual onset. Epochs containing amplitudes greater than ± 80 μ V were defined as artifact epochs and rejected from further analyses. Epochs containing extreme values (limit = ± 80 μ V), abnormal trends (max slope = 50; R 2 limit = 0.3), improbable data (single channel limit = 5; all channel limit = 5) and abnormally distributed data (single channel limit = 5; all channel limit = 5) were also excluded from further analyses.

EEG epochs from 500 to 3000 ms poststimulus onset were averaged among the trials and subjected to a Fourier transformation analysis. The topographical map of the grandaveraged SSVEP amplitudes at each electrode location showed peak activity in the occipital area (Figure 5.3B). The electrode with the greatest SSVEP amplitude was selected from 15 electrodes located in the occipital area (O1, Oz, O2, Iz, POz, P3, P5, P7, PO3, PO7, P4, P6, P8, PO4, and PO8) for each individual participant. The SSVEP amplitude was then normalized in accordance with the formula of Andersen et al. for each participant (Andersen et al., 2011). To assess the time course of activity, we applied Morlet wavelet time-frequency analyses to the data from 500 ms to 3000 ms by using ft_freqanalysis from the FieldTrip toolbox for (Oostenveld et al., 2011) after the EEG data were averaged in each condition across the trials. The wavelet width (i.e., number of averaged time series) was 13 (averaged time window = 65 ms), and

the frequency of interest (FOI) shifted from 6 to 16 Hz at 0.25 Hz intervals.

Statistical analysis

We calculated the grand-averaged SSVEP amplitude of the peak value at 7.5 Hz in Experiment 1. A two-way ANOVA was performed using the averaged SSVEP amplitude in each Contrast (i.e., 0.58, 0.63, 0.67, 0.7 and 0.72) and Pattern (i.e., glare and control condition) as within-subject factors. The level of statistical significance was set to $p < 0.05$ for all analyses. Pairwise comparisons for main effects were corrected for multiple comparisons using the modified Bonferroni (Shaffer) method. Effect sizes (partial η^2; η_p^2) were determined for the ANOVA. Greenhouse-Geisser corrections were performed when Mauchly's sphericity test results were significant. Statistical analyses were performed using R software (Ihaka and Gentleman, 1996).

5.2.3 Experiment 2

Stimuli and experimental procedure.

The stimuli and experimental paradigms used in Experiment 2 were identical to those used in Experiment 1 displayed in Figure 5.2B. Stimuli were presented on a liquid crystal display (LCD) monitor (Viewpixx3D, VPixx Technologies, Saint-Bruno-de-Montarville, QC, Canada) with a resolution of 1920 × 1080 and a refresh rate of 120 Hz. The xy coordinates and Y value were completely aligned with Experiment 1 using a chromameter for calibration. As in Experiment 1, 40 dots flickered at 7.5 Hz in the central white region. Each of 10 conditions (5 contrasts × 2 patterns) were presented randomly (number of trials = 20 per each condition). The experiment consisted of 220 trials (5 contrasts × 2 patterns × 20 trials + 20 task trials), divided over four sessions.

Pupil measurement

Pupil size and eye movement were measured during the task using an eye-tracking system (EyeLink 1000, SR Research, Oakland, Canada) at a sampling rate of 500 Hz. Eye movement was observed in the participants' left eye with an infrared light video camera at a resolution of no more than 0.1 degrees. Trials in which the pupil could not be detected were excluded from analyses. The device outputs pupil size in arbitrary units. In the time course analysis, each trial was normalized by subtracting the pupil size at stimulus onset from the baseline pupil size, following which each data point was smoothed using ±5 sampling. Baseline pupil size was computed as an average of data collected during the fixation period prior to stimulus onset from –200 ms to 0 ms (i.e., presentation onset). Across the conditions, the pupillary

response was averaged from 500 ms to 3000 ms after stimulus onset and evaluated by a repeated-measures analysis of variance (ANOVA) so that it was aligned with the time window analyzed in Experiment 1.

Statistical analysis

A two-way ANOVA was performed on the grand-averaged pupil changes from 500 ms to 3000 ms in each Contrast (0.58, 0.63, 0.68, 0.70, 0.72) and Pattern (glare and control conditions) as within-subject factors. To assess the correlation between the SSVEP amplitude in Experiment 1 and the pupil constriction across Contrast and Pattern conditions, we used a linear regression model in R using the lm function (R Core Team, 2016) In the time serial correlation analysis, p-values were corrected with false discovery rate (FDR) for multiple comparisons using the Benjamini and Hochberg method (Benjamini and Hochberg, 1995).

5.3 Results

5.3.1 Experiment 1

We first analyzed the topographical map of the grand-averaged SSVEP amplitudes at 7.5 Hz as shown in Figure 5.3A. Since the peak activity was observed in the occipital area as expected, the averaged spectra among 15 occipital electrodes (see methods) were calculated using a Fourier transform in each Pattern condition (Figure 5.3B). We confirmed that large SSVEP amplitudes reflected the fundamental flickering frequency of 7.5 Hz. Figure 5.4A shows the grand-averaged SSVEP amplitude of the peak value at 7.5 Hz for each Pattern and Contrast condition. A two-way repeated-measures ANOVA revealed a significant interaction of the averaged SSVEP amplitudes between Pattern and Contrast conditions ($F(2.774, 22.189) = 3.52$, $p = 0.0345$, $\eta_p^2 = 0.306$). The simple effect for the interaction of the Contrast at control condition showed that the SSVEP amplitude significantly increased monotonically as a function of the luminance contrast ($F(4,8) = 3.4174$, $p = 0.0380$, $\eta_p^2 = 0.2993$), as expected from the results of a previous study (Andersen et al., 2012). However, post-hoc modified Bonferroni (Shaffer) corrected t-tests for the luminance at control only showed the significance between contrast ratio 0.63 and 0.72 ($t(8) = 3.9065$, $p = 0.0045$). Most importantly, the SSVEP amplitude in the glare illusion condition increased up to a luminance contrast of 0.67 as in the control condition, whereas it decreased for the highest luminance contrast ratios of 0.7 and 0.72. The post-hoc tests for the interaction showed that the SSVEP amplitudes in the glare condition at contrast ratios of 0.7 and 0.72 were smaller than in the control condition ($F(1,8) = 6.5771$, $p = 0.034$, $\eta_p^2 = 0.4512$ and $F(1,8) = 15.6407$, $p = 0.0042$, $\eta_p^2 = 0.6616$, respectively). The main effects of Contrast and Pattern were not significant ($F(2.768, 22.145) = 1.416$, $p = 0.265$, $\eta_p^2 = 0.15$; $F(1, 8) = 3.399$, $p = 0.102$, $\eta_p^2 = 0.298$). Figure 5.4B shows the Morlet wavelet time-frequency representation

for the luminance contrast ratio of 0.72. In Experiment 2, we assessed the correlation with the pupil constriction across time using the peak SSVEP amplitudes at 7.5 Hz from the wavelet analysis.

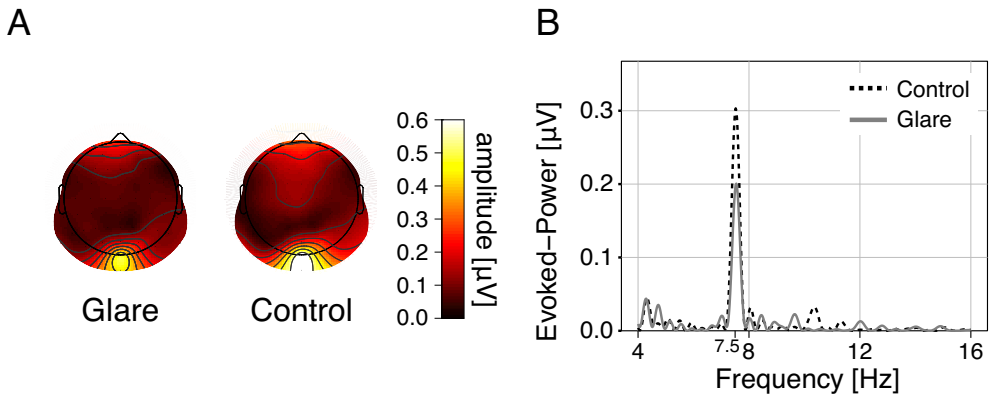

Figure 5.3 Results of SSVEP amplitude and topographical map.

(A) Topographical map of steady-state visual evoked potential (SSVEP) amplitudes in each Pattern (glare versus control) averaged among Contrast conditions. (B) The grand-averaged SSVEP amplitude was observed at the fundamental frequency of the flickering dots (7.5 Hz). The dashed and solid lines show the result of averaged SSVEP amplitude among Contrast conditions in both the control and glare conditions.

5.3.2 Experiment 2

A two-way repeated-measures ANOVA on the averaged pupil changes from 500 ms to 3000 ms (i.e., the same window used in Experiment 1) as shown in Figure 5.5A revealed a significant main effect of Contrast condition ($F(4, 32) = 43.38$, $p < 0.001$, $\eta_p^2 = 0.844$). The interaction between Pattern and Contrast was also marginally significant ($F(4, 32) = 2.292$, $p = 0.0811$, $\eta_p^2 = 0.223$) (Rosnow and Rosenthal, 1989). Post-hoc multiple comparisons for the Contrast condition were significant in all the luminance contrast pairs (ps < 0.05). Similarly, the post-hoc tests for the interaction showed that pupil constriction increased as a function of luminance contrast for both glare ($F(4,32) = 34.0078$, $p < 0.001$, $\eta_p^2 = 0.8096$) and control conditions ($F(4,32) = 27.7667$, $p < 0.001$, $\eta_p^2 = 0.7763$). Crucially, we also found the significant interaction of Pattern at luminance contrast of 0.72 ($F(1,8) = 10.4289$, $p = 0.0121$, $\eta_p^2 = 0.5659$) suggesting that, consistent with recent findings, the 'glare' effect of greater pupil constriction was observed at luminance contrast of 0.72, though not at the other luminance contrasts ($p > 0.05$).

We subsequently calculated the correlation between the time series of SSVEP amplitude at 7.5 Hz in Experiment 1 (Figure 5.5B in top panel) and the pupil constriction in Experiment 2 (Figure 5.5B in middle panel) in every 2.7 ms from 0 ms to 3,000 ms (i.e., from stimulus onset to offset). We first

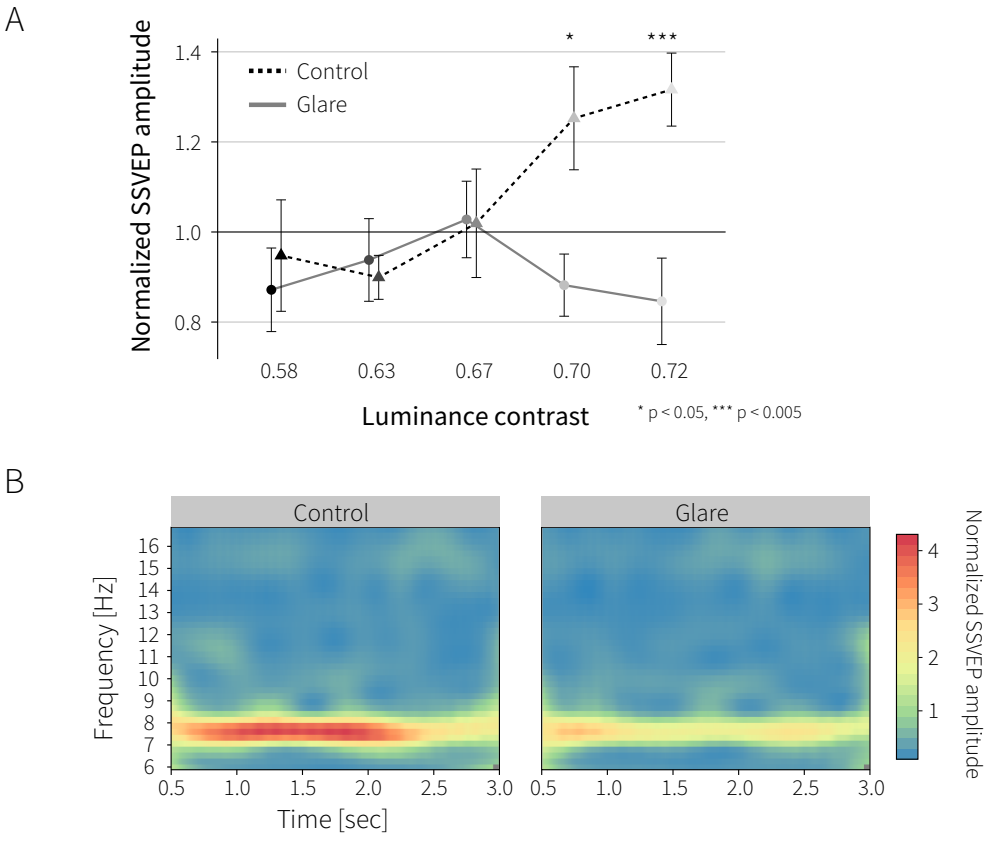

Figure 5.4 Results of averaged SSVEP amplitude in each Contrast.

(A) The grand-averaged SSVEP amplitude at the frequency of interest of 7.5 Hz for both glare and control conditions for each luminance contrast. The abscissa and ordinate indicate the luminance contrast and the normalized SSVEP amplitude among subjects respectively. Error bars indicate the standard error of the mean. (B) The time course SSVEP amplitude for glare and control in the contrast of 0.72 as examples.

assessed the correlation across Contrast in each Pattern using a simple linear regression model; the SSVEP amplitudes in both glare and control conditions were then entered as the dependent variables in each model. As expected, there was a strong inverse relationship between the SSVEP amplitude and extent of pupil change returning toward the baseline pupil size (Figure 5.5B in bottom panel), indicating that brighter stimuli produced the larger SSVEP amplitudes and greater pupil constriction. The correlation between the averaged SSVEP amplitude and pupil constriction from 500 ms to 3000 ms also showed significant inverse relation (for glare, $y = –0.011x + 0.209$, $t(8) = –5.269$, $p < 0.001$, $R = –0.6264$ and for control, $y = –0.013x + 0.249$, $t(8) = –3.688$, $p = 0.0006$, $R = –0.4902$). The confidence of these results was confirmed by a Bayesian Pearson's rho correlation in favor of H_1 (difference), but also for H_0 (i.e., no difference), using the statistical software JASP (https://jasp-stats.org/; Team, 2018). A Bayesian analysis reveals whether the evidence is more in favor of H_1 when the obtained Bayesian Factor (BF_{10}) is greater than 3 (Dienes, 2014). These analyses revealed that the stimulus luminance change resulted in strong evidence for the larger SSVEP amplitudes and greater pupil constriction to brighter stimulus ($BF_{10} = 5260.46$ for glare and $BF_{10} = 53.17$ for control).

Next, the correlation analysis in each Contrast and Pattern was separately tested to account for the individual differences between participants across the conditions. We found that averaged SSVEP amplitude and pupil constriction inversely correlated in all conditions from luminance contrast of 0.58 to 0.72 (for glare, $R = –0.65$, $p = 0.058$, $BF_{10} = 1.955$; $R = –0.463$, $p = 0.21$, $BF_{10} = 0.815$; $R = –0.753$, $p = 0.019$, $BF_{10} = 4.376$; $R = –0.768$, $p = 0.016$, $BF_{10} = 5.079$; $R = –0.743$, $p = 0.022$, $BF_{10} = 3.991$ and for control, $R = –0.266$, $p = 0.489$, $BF_{10} = 0.503$; $R = –0.637$, $p = 0.065$, $BF_{10} = 1.807$; $R = –0.416$, $p = 0.265$, $BF_{10} = 0.705$; $R = –0.518$, $p = 0.153$, $BF_{10} = 0.998$; $R = –0.378$, $p = 0.316$, $BF_{10} = 0.634$). A Bayesian analysis for the correlation revealed that the larger pupil constriction in the luminance contrast condition of 0.68, 0.70 and 0.72 for glare pattern resulted in moderate evidence for the elevation of SSVEP amplitude.

Most importantly, we further assessed the correlation between the SSVEP amplitude and pupil constriction each Contrast across Pattern as shown in Figure 5.6 to account for the inhibition of the SSVEP amplitude in point of the greater pupil constriction to the glare illusion at the luminance contrast of 0.72. When the greater pupil constriction relates to the larger SSVEP amplitude, those responses should be inversely correlated. On the contrary, if the greater pupil constriction prompts the inhibition of SSVEP amplitude, the correlation of those responses at the luminance contrast of 0.72 would be weaker than the other luminance contrast condition. The analysis revealed that the SSVEP amplitude and pupil constriction were inversely correlated at the luminance contrast of 0.58, 0.63, 0,67 and 0.70 with moderate or strong evidence (i.e., $BF_{10} > 3$) ($R = –0.4604$, $p = 0.0545$, $BF_{10} = 4.608$; $R = –0.5491$, $p = 0.0183$, $BF_{10} = 7.867$; $R = –0.5904$, $p = 0.0099$, $BF_{10} = 11.901$; $R = –0.5653$, $p = 0.0145$, $BF_{10} = 5.042$) while

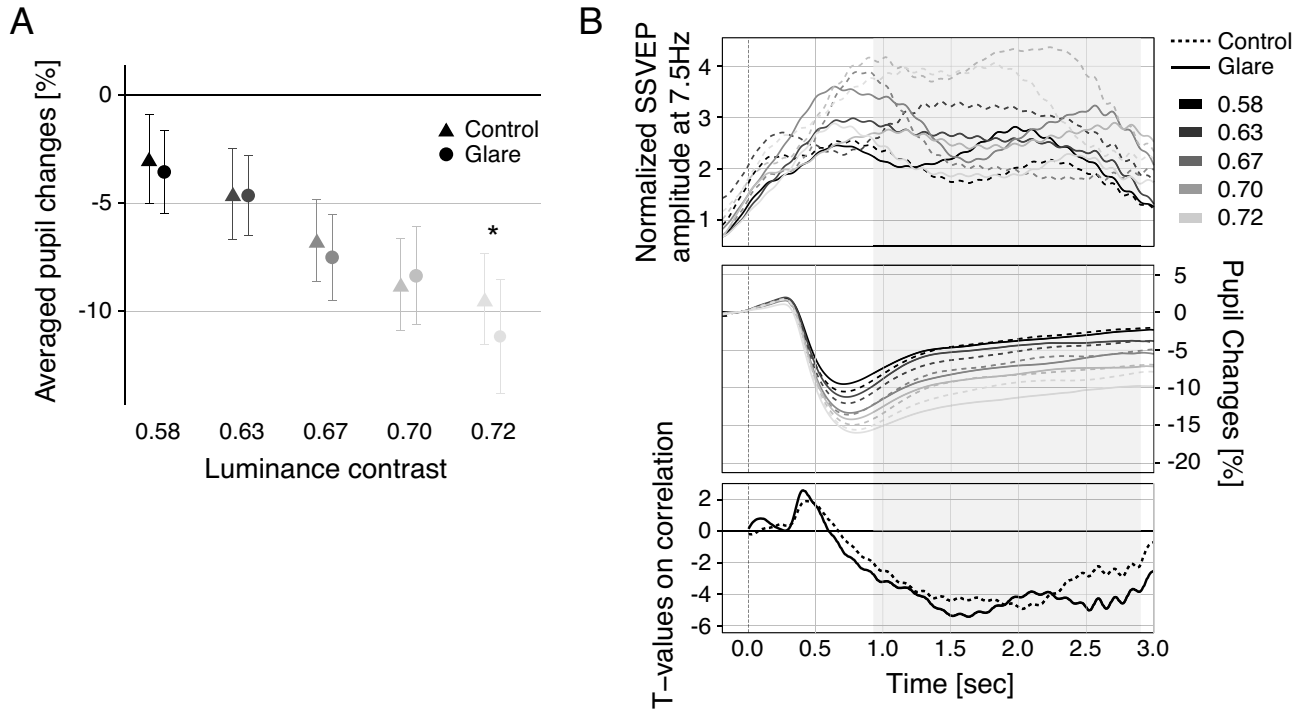

Figure 5.5 Pupil response.

(A) The averaged pupil changes from 500 ms to 3000 ms of viewing for each Pattern and Contrast condition. The asterisks (*) indicate a statistical significance of $p < 0.05$. Error bars represent the standard error of the mean. (B) The time course of the SSVEP amplitudes and pupil responses for each Pattern and Contrast condition. The horizontal axis indicates the time from -200 ms to 3000 ms (i.e., from baseline area to stimulus offset). The grand-averaged SSVEP amplitude at the frequency of interest of 7.5 Hz from a time-frequency analysis shown in the top panel, as well as the time course of pupil response in the middle panel. The dashed and solid lines show the result of control and glare condition, respectively. The color gradations indicate each Contrast condition. The bottom panel shows t-values on the correlation across Contrast in each Pattern between the SSVEP amplitude (top panel) and the pupil constriction (middle panel) in each time period using a simple regression model. The gray-shaded areas show a significant correlation of $p < 0.05$. The p values were corrected for multiple comparisons with an expected FDR of 0.05.

an inconclusive or 'anecdotal' evidence (i.e., $BF_{10} < 3$) at the luminance contrast of 0.72 was found (R = –0.4463, p = 0.0634, $BF_{10} = 2.010$) as well as the time course of correlation analysis in Figure 5.6. As we expected, the correlation between the pupil response and SSVEP amplitude at luminance contrast of 0.72 responses was weaker than the other luminance contrast condition, most likely because the greater pupil constriction with the 'glare' effect existed only at the luminance condition of 0.72 linked to the inhibited SSVEP amplitude. Thus, the weak correlation revealed the effect of greater pupil constriction on the inhibition of the SSVEP amplitude produced by the glare illusion.

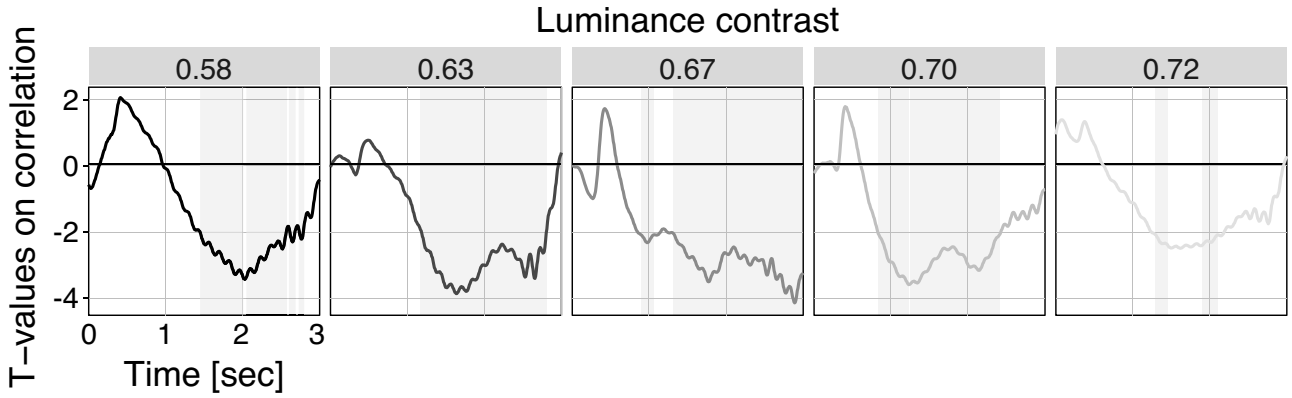

Figure 5.6 Time course correlations between the SSVEP amplitude and pupil response.

T-values on the correlation between the SSVEP amplitude and the pupil response in each Contrast across Pattern. The luminance contrast values are shown on the top of the graphs. The gray-shaded areas indicate the significant correlation area of FDR corrected $p < 0.05$.

5.4 Discussion

In the current study, we observed SSVEP amplitudes (Experiment 1) and pupil changes (Experiment 2) while participants viewed flickering dots at the center of the stimulus in glare illusion and control conditions to address the question of whether the illusory brightness enhancement was created in the early stages of visual processing related to the pupil changes. As expected, the SSVEP amplitude in the control condition (i.e., in the absence of gradients causing illusory glare) increased in proportion to the luminance contrast, consistent with the previous demonstration of Andersen et al. (2012). Thus, we successfully replicated results from a previous study showing that SSVEP amplitude reflects localized luminance contrast between the flickering stimulus and background luminance. Similar results were observed in the glare condition up to a luminance contrast of 0.67, whereas, for the higher luminance contrast of 0.7 and 0.72, the SSVEP amplitude decreased compared to control conditions. Moreover, the

glare illusion at the luminance contrast of 0.72 resulted in greater pupil constriction, which was consistent with one of our hypotheses that the SSVEP amplitude would decrease if pupil constriction restricted the amount of light entering the eyes, as evidenced by a simple regression model to these responses.

As expected, the larger SSVEP amplitude and greater pupil constriction were provided as a function of the actual luminance change, and no relationship of those responses in the control condition within constant luminance contrast between participants was found. This appears consistent with the ideas that although the SSVEP amplitude and pupil constriction reflect the localized luminance contrast change, the SSVEP amplitudes under the constant luminance condition are not related to pupil size (Thigpen et al., 2018). On the contrary, the SSVEP amplitude and pupil constriction to the glare illusion were inversely correlated under each certain luminance contrasts of 0.67, 0.70 and 0.72. Since the correlation was calculated in each constant luminance and pattern condition, the inverse correlation indicates simply an individual difference. A likely explanation for the individual differences is that the extent of pupil constriction reflects how each participant perceives brightness while viewing the glare illusion. We note that there are, in general, substantial individual differences of "a sensitivity to the light" because the perceived intensity of light is determined by the combination of the luminance and the chromatic channels; one probable account for the individual differences may be due to the spectral absorption of the eye lens and of macular pigments (Nayatani et al., 1988; Whitehead, 2006).

The SSVEP amplitude was enhanced by higher luminance contrast between flickering stimulus and background luminance, indicating that the neural response to actual luminance changes was processed in the early visual cortex, as described by the previous study (Andersen et al., 2012). Given that the glare illusion we used in this study is enough to enhance brightness as demonstrated by our additional experiment (see `https://github.com/suzuki970/Experimental_data/tree/master/P01/Additional%20information`), the SSVEP amplitudes seen in the glare condition were inconsistent with the hypothesis that the SSVEP amplitude would increase as a function of the illusory brightness enhancement in the glare condition. However, the results support our other hypothesis that the SSVEP amplitude reflects the number of photons captured by the retina because the decrease in SSVEP amplitude to the glare illusion at the luminance contrast of 0.72 was accompanied by pupil constriction. Bombeke and colleagues also suggested that the pupil-size differences modulate the feedforward response of V1 (Bombeke et al., 2016). The current findings indicate the weak correlation between the SSVEP amplitude and pupil constriction across both glare and control condition at the luminance contrast of 0.72, whereas the SSVEP amplitude and pupil constriction were inversely correlated at the other luminance contrast condition, which we failed to observe the larger pupil constriction effect on the illusory glare. As mentioned earlier, the inverse correlation between the SSVEP amplitude and pupil response across glare and control condition seemed to indicate the individual differences because those glare and control patterns at luminance contrast condition from

0.58 to 0.7 yielded no significant changes in pupillary diameter within participants. Thus, when larger pupil constriction and the decrease in the SSVEP amplitude are provided by the glare illusion at the luminance contrast of 0.72, those responses affected positively the correlation and then resulted in the weak correlation.

The pupil constriction effect due to illusory glare has been demonstrated by several previous studies (Bombeke et al., 2016; Laeng and Endestad, 2012; Laeng et al., 2018; Suzuki et al., 2019a; Zavagno et al., 2017), as well as pictures of the sun (Binda et al., 2013b; Naber and Nakayama, 2013). We should note that the phenomenon of pupil constriction to the bright illusion was replicated only in the highest luminance contrast condition, even though some significant brightness enhancement existed in the lower luminance contrast conditions of the glare illusion as shown in our additional experiment. Tamura et al. observed that the brightness enhancement in the glare illusion depends on the luminance contrast between the central area of the glare illusion and background (Tamura et al., 2016); the lower luminance contrast condition produces only a slight brightness enhancement. Thus, the experience of 'glare' or 'dazzling' effect due to the luminance gradation of the stimulus may elicit the larger pupil constriction. However, we need to point out a potential limitation of the stimulus used in this study. The circle shape of the glare illusion was not consistent with the previous works which reported the pupil changes to the bright illusion (Laeng and Endestad, 2012; Laeng et al., 2018), as well as other similar stimuli (e.g., Kanizsa, 1979; Kitaoka, 2005; Zavagno, 2005). Thus, the configuration of stimulus shape, size, luminance gradation and contrast may be important to elicit the larger pupil constriction in the glare illusion than its control stimulus.

5.5 Conclusions

The present findings elucidate the relationship between visual cortical response indexed by SSVEPs and pupillometry in the glare illusion. The glare illusion enhances brightness perception due to a luminance gradient surrounding a central white area of the stimulus, without any real change in light intensity. Our study suggests that brightness perception also modulates the SSVEPs via modulation of pupil changes. The inhibition of SSVEPs in the glare illusion could be extended to studies of glare involving psychological dazzling and discomfort (Bargary et al., 2014; Colombo et al., 2012; Lin et al., 2015; Maniglia et al., 2018), or even used to evaluate the mimicking of glare perception in Irlen syndrome, without an actual light source (Evans and Stevenson, 2008). In conclusion, this study provides evidence that SSVEP amplitude is modulated by the glare illusion, which at high luminance contrast causes greater pupillary constriction.

5.6 Additional experiment

Following Experiment 1 and 2, we conducted a two-alternative forced choice (2AFC) task to confirm perceived brightness enhancement in our luminance condition. The equipment and stimulus property were identical to that used in Experiment 2, except for the luminance contrast condition. Seven luminance contrasts were used (42, 48, 54, 60, 66, 72 and 78 cd/m^2).

Procedure At the beginning of the trial, the fixation point was presented prior to the stimulus presentation for 1,000 ms. Then, two stimuli were displayed side-by-side: the target stimulus and the reference stimulus at 7.35 degrees from the center of the monitor on either side of the center. The side (left, right) of the target and reference stimuli was determined randomly in each trial but the number of the trials for each stimulus was kept constant (number of trials = 16). The reference stimulus could be one of 7 luminance patterns of control stimulus (42, 48, 54, 60, 66, 72 and 78 cd/m^2). The target stimulus was picked from one of 5 luminance patterns of glare stimulus (48, 54, 60, 66, and 72 cd/m^2) or one of 7 luminance patterns of control stimulus as a control condition. Participants were asked to engage in a 2AFC task in which the reference or target stimulus appearing brighter (right or left). The whole experiment therefore consisted of 672 trials (7 references $\times$ 5 targets $\times$ 16 trials + 7 control stimulus $\times$ 16 trials), divided into four sessions.

Results The probability with which the participants chose the reference stimulus was calculated. The average probability in each target luminance contrast was fit with a psychometric function which implements the maximum-likelihood method using the Palamedes Toolbox (Prins and Kingdom, 2009). Analysis of the 2AFC task revealed that the brightness perception was clearly enhanced by the glare illusion in every contrast condition used in the prior experiment as shown in Figure 5.7. We estimated the 'illusory' brightness to the glare illusion in Contrast of 0.58, 0.63 and 0.57 from Point of Subjective Equality (PSE): 0.685, 0.712 and 0.732 respectively. The results indicated that the perceived brightness enhancement also occurred in the low luminance contrast condition.

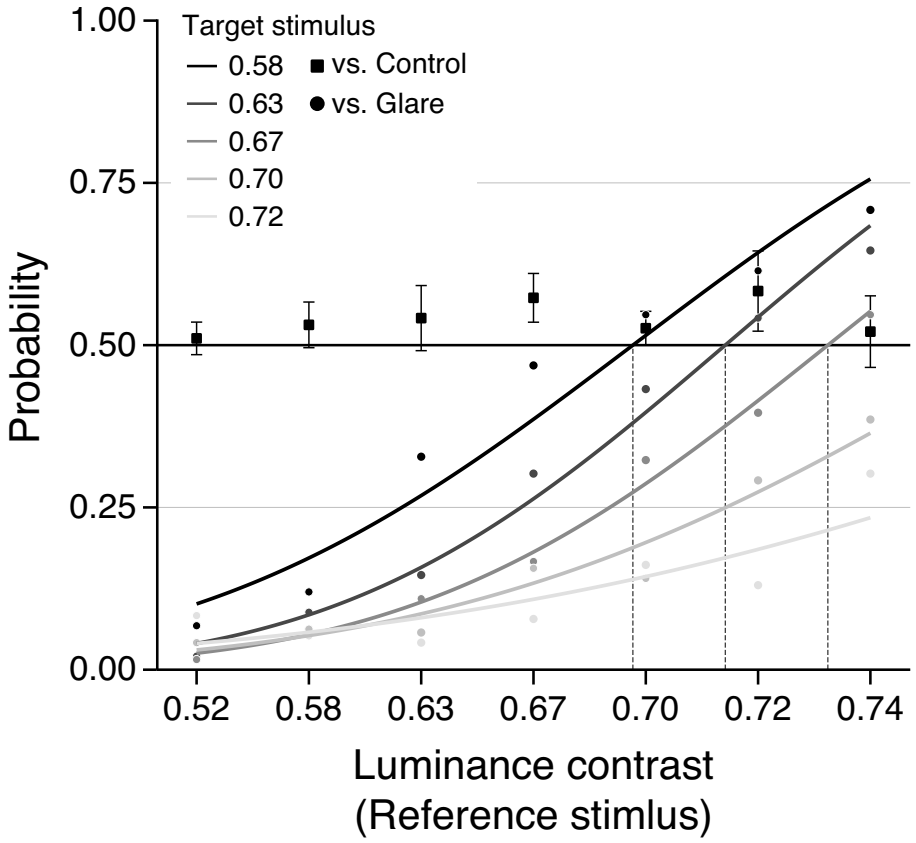

Figure 5.7 Results of Brightness estimation.

The vertical line indicates the probability the participants selected the target stimulus. The squares and circles show the result for the reference of control and glare stimulus respectively. In the result for the glare stimuli, the average probability in each target luminance contrast was fit with a psychometric function. Dots lines indicate the PSE in each luminance pattern.

Chapter 6

General Discussion and Conclusions

"The eyes, which are the windows of the soul." — Plato, in the Phaedrus

Pupil dilation/constriction informs us of the processing of our cognitive effort, emotion, mental, and attentional state via the LC-NE system (Beatty, 1982; Bradley et al., 2008; Einhäuser et al., 2008; Laeng and Sulutvedt, 2013; Mathôt et al., 2017; Suzuki et al., 2018). In addition to previous findings indicating that large pupil constriction is prompted by glare illusion (Laeng and Endestad, 2012), we originally considered the pupil response to the level of brightness and the luminosity perception in glare illusion to be indexed as the objective marker of pupillary changes. In the current study, we observed pupil responses to the varied pattern of glare illusion; the parameter in the color of luminance gradation, the central luminance, and the shape in glare illusion were manipulated and resulted in modulating the brightness changes and evoking the luminosity perception.

6.1 Pupil control circuit for glare illusion

Here, we illustrate a probable schematic of brain processing for glare illusion related to pupil constriction (Figure 6.1). Pupil constriction is controlled by the sphincter muscles with increasing parasympathetic nervous system activities. The visual input into the retina is translated into an electric signal and projected to the PON, primary visual cortex, and SC. Whether pupil constriction occurs depends on the intensity of luminance of the visual stimulus which is referred to as the PLR (Figure 6.1 blue line). From the serial experiment in the previous chapters, the PLR to glare illusion and control stimulus occurred in a manner consistent with brightness perception (Chapters 2, 3, and 4), and the difference of pupil constriction between glare and control stimulus was sustained from stimulus onset to offset. Therefore, the pathway evoking large pupil constriction to glare illusion is relatively processed in the early stage of visual processing, similar to the PLR circuit. This is a very rational process because it demands immediate

processing; i.e., the situation where we actually perceive a glare (e.g., from the sun) might lead to crucial eye damage.

6.2 The presence of feedback to V1 from pupil constriction

Even though pupil constriction to illusory glare functions might be a reaction to protect the eyes, the constriction effect was not temporary contrary to the PLR. This indicates that the high sympathetic activity should remain to constrict the pupils as we showed the time course of pupillary changes in any experiments. Because EEG (SSVEP) measurement implied that pupil constriction caused by glare illusion is related to the primary visual cortex (V1) evidenced from the time-course analysis in Chapter 5, there is a pathway to modulate the visual input owing to pupil constriction (Figure 6.1 red line). As we mentioned in Chapter 4, the perception of self-luminosity also plays an important role to modulating pupil constriction. Leonards et al.(2005) reported that self-luminosity involves an extrastriate visual cortex and ventral-occipital cortical area (Leonards et al., 2005). Therefore, the perception of self-luminosity for the glare illusion is processed in the extrastriate cortex, and then the feedback signal in the form of pupil constriction affects the SSVEP amplitude. Additionally, there might be a circuit via SC and frontal cortex to process the colored glare illusion (i.e., large pupil constriction for the blue glare illusion) based on the memory-related visual processing or inherited mechanism discussed in Chapter 3. This theoretical evidence may contribute to understanding the neural mechanisms of glare illusion. Moreover, our hypothesis, based on the ecology of vision, that the visual system adapts to dazzling light as an inherited trait, might benefit from the theoretical understanding of the processing of glare illusion in the brain.

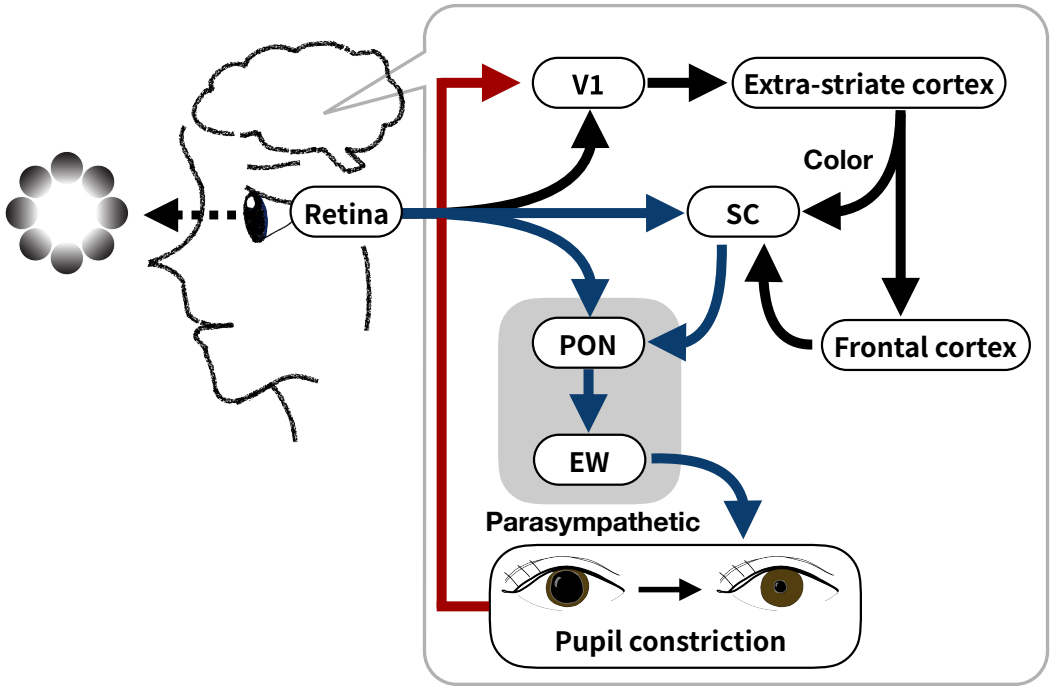

Figure 6.1 A probable model for processing the glare illusion.

Schematic circuit of pupil constriction caused by glare illusion. Abbreviations: PON, pretectal olivary nucleus; EW, Edinger-Westphal nucleus; SC, superior colliculus; V1, primary visual cortex.

6.3 Conclusions

In the present study, we focused on the pupil response to bright illusion in terms of brightness and luminosity. Further, we investigated the relation of pupil response to the EEG response and the effect on the pupil size owing to the stimulus visual angle. Here, we summarize the findings and contribution of our study.

Pupil response on brightness Several studies have reported a brightness effect on pupil changes by using bright illusion (e.g., an image of the sun and a picture of the natural scene) (Binda et al., 2013b; Laeng and Endestad, 2012; Naber and Nakayama, 2013; Suzuki et al., 2019a). We proposed that the extent of glare-related pupil constrictions for the participants in our experiments were correlated to each individual's subjective brightness adjustments.

Blue glare illusion effect The blue glare illusion yields a stronger perception of enhanced perceived brightness compared to all the other colors in a variety of patterns, and the pupil measurements capture this effect effectively. Therefore, we originally proposed that blue may not only enhance the subjective sense of brightness but that pupil constriction for the color blue could represent an adaptive response of the visual system to a probable dangerous situation of dazzling sunlight.

We also found the pupil response to the 'blue' glare effect occurred to black/brown iris but not to blue/hazel iris colors people. Since an iris color relates to a macular pigment density as a marker for the adaptation to the homogeneous environment, we propose that the pupillary constriction represents the adaptation response to probable dazzling sunlight imitated by the glare illusion similar to the function of MP to filter the blue light projecting to the retina.

Pupil response on self-luminosity Self-luminosity, the perception of light emission from an object, is a mode of color appearance evoked by glare illusion (Zavagno and Caputo, 2001, 2005). We investigated whether luminosity contributes to pupil constriction by using the Kanizsa triangle with a luminance gradation as elements generating the illusory contour. We claim that pupil constriction reflects the brightness judgment with the mode of self-luminosity, although the brightness change produced by the subjective illusory contour with the Kanizsa triangle does not affect pupil size.

Correlation between EEG and pupillary response The sustained visual cortical response of SSVEPs reflects the activity in V1 modulated by the stimulus luminance contrast, attention, and other cognitive factors. We found that the inhibition of SSVEPs with the large pupil constriction in the case of bright glaze illusion has a high luminance contrast, thereby decreasing the amount of light projected to the retina. Hence, the brightness enhancement in the glare illusion is already represented at the primary stage of visual processing which is linked to large pupil constriction.

References

Adelson, E. H. (1993). Perceptual organization and the judgment of brightness. *Science*, 262(5142):2042–2044.

Adelson, E. H. (1995). Checker shadow illusion. http://persci.mit.edu/home.

Adelson, E. H. and Pentland, A. P. (1996). The perception of shading and reflectance. *Perception as Baysian Inference*, pages 409–423.

Agostini, T. and Galmonte, A. (2002). A new effect of luminance gradient on achromatic simultaneous contrast. *Psychonomic Bulletin & Review*, 9(2):264–269.

Andersen, S. K., Fuchs, S., and Müller, M. M. (2011). Effects of Feature-selective and Spatial Attention at Different Stages of Visual Processing. *Journal of Cognitive Neuroscience*, 23(1):238–246.

Andersen, S. K., Muller, M. M., and Martinovic, J. (2012). Bottom-Up Biases in Feature-Selective Attention. *Journal of Neuroscience*, 32(47):16953–16958.

Arnold, A. C., Gallagher, P. E., and Diz, D. I. (2012). Brain renin–angiotensin system in the nexus of hypertension and aging. *Hypertension Research*, 36(1):5–13.

Aston-Jones, G. and Cohen, J. D. (2005). An integrative theory of locus coeruleus-norepinephrine function: adaptive gain and optimal performance. *Annual Review of Neuroscience*, 28(1):403–450.

Barbur, J. L., Harlow, A. J., and Sahraie, A. (1992). Pupillary responses to stimulus structure, colour and movement. *Ophthalmic and Physiological Optics*, 12(2):137–141.

Barbur, J. L., Moro, S., Harlow, J. A., Lam, B. L., and Liu, M. (2004). Comparison of pupil responses to luminance and colour in severe optic neuritis. *Clinical Neurophysiology*, 115(11):2650–2658.

Barbur, J. L., Weiskrantz, L., and Harlow, J. A. (1999). The unseen color aftereffect of an unseen stimulus: Insight from blindsight into mechanisms of color afterimages. *Proceedings of the National Academy of Sciences*, 96(20):11637–11641.

Bargary, G., Jia, Y., and Barbur, J. L. (2014). Mechanisms for Discomfort Glare in Central Vision. *Investigative Ophthalmology & Visual Science*, 56(1):464–471.

Bates, D., Mächler, M., Bolker, B., and Walker, S. (2015). Fitting Linear Mixed-Effects Models Using lme4. *Journal of Statistical Software*, 67(1):1–48.

Beatty, J. (1982). Task-evoked pupillary responses, processing load, and the structure of processing resources. *Psychological Bulletin*, 91(2):276–292.

Beatty, J. and Lucero-Wagoner, B. (2000). The pupillary system. In Cacioppo, J. T., Tassinary, L. G., and Berntson, G., editors, *Handbook of psychophysiology*, pages 142–162.

Benjamini, Y. and Hochberg, Y. (1995). Controlling the false discovery rate: a practical and powerful approach to multiple testing. *Journal of the Royal Statistical Society. Series B (Methodological)*, 57(1):289–300.

Bergamin, O., Schoetzau, A., Sugimoto, K., and Zulauf, M. (1998). The influence of iris color on the pupillary light reflex. 236(8):567–570.

Bijleveld, E., Custers, R., and Aarts, H. (2009). The Unconscious Eye Opener. *Psychological Science*, 20(11):1313–1315.

Binda, P., Pereverzeva, M., and Murray, S. O. (2013a). Attention to Bright Surfaces Enhances the Pupillary Light Reflex. *Journal of Neuroscience*, 33(5):2199–2204.

Binda, P., Pereverzeva, M., and Murray, S. O. (2013b). Pupil constrictions to photographs of the sun. *Journal of Vision*, 13(6):8–8.

Bombeke, K., Duthoo, W., Mueller, S. C., Hopf, J.-M., and Boehler, C. N. (2016). Pupil size directly modulates the feedforward response in human primary visual cortex independently of attention. *NeuroImage*, 127(C):67–73.

Bonato, F. and Cataliotti, J. (2000). The effects of figure/ground, perceived area, and target saliency on the luminosity threshold. *Perception & Psychophysics*, 62(2):341–349.

Bone, R. A. and Landrum, J. T. (2004). Heterochromatic flicker photometry. *Archives of Biochemistry and Biophysics*, 430(2):137–142.

Bradley, J. C., Bentley, K. C., Mughal, A. I., Bodhireddy, H., Young, R. S. L., and Brown, S. M. (2010). The Effect of Gender and Iris Color on the Dark-Adapted Pupil Diameter. *Journal of Ocular Pharmacology and Therapeutics*, 26(4):335–340.

Bradley, M. M., Miccoli, L., Escrig, M. A., and Lang, P. J. (2008). The pupil as a measure of emotional arousal and autonomic activation. *Psychophysiology*, 45(4):602–607.

Brainard, D. H. (1997). The Psychophysics Toolbox. *Spatial vision*, 10(4):433–436.

Brown, H. and Friston, K. J. (2012). Free-energy and illusions: the cornsweet effect. *Frontiers in Psychology*, 3(FEB):43.

Brown, T. M., Tsujimura, S.-i., Allen, A. E., Wynne, J., Bedford, R., Vickery, G., Vugler, A., and Lucas, R. J. (2012). Melanopsin-Based Brightness Discrimination in Mice and Humans. *Current Biology*, 22(12):1134–1141.

Bullough, J. D., Fu, Z., and Van Derlofske, J. (2002). Discomfort and Disability Glare from Halogen and HID Headlamp Systems. *Advanced Lighting Technology for Vehicles*, 1:1–5.

Canny, J. F. (1986). A Computational Approach to Edge Detection. *IEEE Trans. Pattern Anal. Mach. Intell.*, PAMI-8(6):679–698.

Ciulla, T. A., Curran-Celantano, J., Cooper, D. A., Hammond, B. R., Danis, R. P., Pratt, L. M., Riccardi, K. A., and Filloon, T. G. (2001). Macular pigment optical density in a midwestern sample. *Ophthalmology*, 108(4):730–737.

Clark, A. (2015). Radical Predictive Processing. *The Southern Journal of Philosophy*, 53(1):3–27.

Colombo, E. M., Issolio, L. A., Barrionuevo, P. A., and Comastri, S. A. (2012). Veiling luminance as a descriptor of brightness reduction caused by transient glare. *Journal of the Optical Society of America A*, 29(10):2230–2236.

Corney, D., Haynes, J.-D., Rees, G., and Lotto, R. B. (2009). The Brightness of Colour. *PLOS ONE*, 4(3):e5091–12.

Corney, D. and Lotto, R. B. (2007). What Are Lightness Illusions and Why Do We See Them? *PLOS Computational Biology*, 3(9):e180–11.

Cornsweet, T. (1970). *Visual perception*. New York: Academic Press.

Dain, S. J., Cassimaty, V. T., and Psarakis, D. T. (2004). Differences in FM100-Hue test performance related to iris colour may be due to pupil size as well as presumed amounts of macular pigmentation. *Clinical and Experimental Optometry*, 87(4-5):322–325.

Davison, P., Akkali, M., Loughman, J., Scanlon, G., Nolan, J., and Beatty, S. (2011). Macular pigment: Its associations with color discrimination and matching. *Optometry and Vision Science*, 88(7):816–822.

Dienes, Z. (2014). Using Bayes to get the most out of non-significant results. *Frontiers in Psychology*, 5(e33400):781.

Duffy, D. L., Montgomery, G. W., Chen, W., Zhao, Z. Z., Le, L., James, M. R., Hayward, N. K., Martin, N. G., and Sturm, R. A. (2007). A three-single-nucleotide polymorphism haplotype in intron 1 of OCA2 explains most human eye-color variation. *American Journal of Human Genetics*, 80(2):241–252.

Einhäuser, W., Koch, C., and Carter, O. L. (2010). Pupil dilation betrays the timing of decisions. *Frontiers in Human Neuroscience*, 4.

Einhäuser, W., Stout, J., Koch, C., and Carter, O. (2008). Pupil dilation reflects perceptual selection and predicts subsequent stability in perceptual rivalry. *Proceedings of the National Academy of Sciences*, 105(5):1704–1709.

Ellis, C. J. (1981). The pupillary light reflex in normal subjects. *The British journal of ophthalmology*, 65(11):754–759.

Evans, B. J. W. and Stevenson, S. J. (2008). The Pattern Glare Test: a review and determination of normative values. *Ophthalmic and Physiological Optics*, 28(4):295–309.

Fahle, M. W., Stemmler, T., and Spang, K. M. (2011). How Much of the "Unconscious" is Just Pre - Threshold? *Frontiers in Human Neuroscience*, 5:120.

Fairchild, M. D. (2013). *Color Appearance Models*. John Wiley & Sons.

Faul, F., Erdfelder, E., Lang, A.-G., and Buchner, A. (2007). G*Power 3: A flexible statistical power analysis program for the social, behavioral, and biomedical sciences. *Behavior Research Methods*, 39(2):175–191.

Fesi, J. D., Thomas, A. L., and Gilmore, R. O. (2014). Cortical responses to optic flow and motion contrast across patterns and speeds. *Vision Research*, 100(C):56–71.

Flannagan, M. J., Sivak, M., and Traube, E. C. (1994). Discomfort glare and brightness as functions of wavelength.

Gamlin, P. D. R. (2006). The pretectum: connections and oculomotor-related roles. In Büttner-Ennever, J. A., editor, *Neuroanatomy of the Oculomotor System*, pages 379–405. Elsevier.

Gamlin, P. D. R., Zhang, H., Harlow, A., and Barbur, J. L. (1998). Pupil responses to stimulus color, structure and light flux increments in the rhesus monkey. *Vision Research*, 38(21):3353–3358.

Gao, H. and Pei, Y. (2009). Effects of sunlight glare on drivers' psychophysiological characteristics. *ICCTP 2009: Critical Issues in Transportation Systems Planning, Development, and Management*.

Gilchrist, A. (2006). *Seeing Black and White*. Oxford University Press.

Gilchrist, A., Kossyfidis, C., Bonato, F., Agostini, T., Cataliotti, J., Li, X., Spehar, B., Vidal, A., and Economou, E. (1999). An anchoring theory of lightness perception. *Psychological Review*, 106(4):795–834.

Goldwater, B. C. (1972). Psychological significance of pupillary movements. *Psychological Bulletin*, 77(5):340–355.

Gomes, C. A., Montaldi, D., and Mayes, A. (2015). The pupil as an indicator of unconscious memory: Introducing the pupil priming effect. *Psychophysiology*, 52(6):754–769.

Granholm, E. and Steinhauer, S. R. (2004). Pupillometric measures of cognitive and emotional processes. *International Journal of Psychophysiology*, 52(1):1–6.

Hammond, B. R., Fuld, K., and Snodderly, D. M. (1996). Iris color and macular pigment optical density. *Experimental Eye Research*, 62(3):293–298.

Hammond Jr, B. R., Fletcher, L. M., and Elliott, J. G. (2013). Glare Disability, Photostress Recovery, and Chromatic Contrast: Relation to Macular Pigment and Serum Lutein and Zeaxanthin. *Investigative Opthalmology & Visual Science*, 54(1):476–6.

Hanada, M. (2015). Effects of Colors on the Feeling of Being Dazzled Evoked by Stimuli with Luminance Gradients. *Perceptual and Motor Skills*, 121(1):219–232.

Hermann, L. (1870). Eine Erscheinung simultanen Contrastes. *Pflügers Archiv für die gesamte Physiologie*, (3):13–15.

Hohwy, J. (2013). *The Predictive Mind*. Oxford University Press.

Hotta, H. and Uchida, S. (2010). Aging of the autonomic nervous system and possible improvements in autonomic activity using somatic afferent stimulation. *Geriatrics & Gerontology International*, 10(9671):S127–S136.

Huey, E. B. (1898). Preliminary Experiments in the Physiology and Psychology of Reading. *The American Journal of Psychology*, 9(4):575–586.

Ihaka, R. and Gentleman, R. (1996). R: A Language for Data Analysis and Graphics. *Journal of Computational and Graphical Statistics*, 5(3):299–314.

Ishigughi, A. (1987). Illusory gray spots and diagonal lines on the Hermann grid. *Japanese Psychological Research*, 29(3):112–119.

Ishihara, S. (1996). Ishihara's tests for colour blindness (38 plates ed.). Handaya, Japan.

Kahneman, D. and Beatty, J. (1966). Pupil Diameter and Load on Memory. *Science*, 154(3756):1583–1585.

Kanizsa, G. (1979). *Organization in vision*. essays on gestalt perception. Praeger Publishers, New York.

Kardon, R., Anderson, S. C., Damarjian, T. G., Grace, E. M., Stone, E., and Kawasaki, A. (2009). Chromatic Pupil Responses. *OPHTHA*, 116(8):1564–1573.

Katz, D. (1935). *The World of Colour*. Kegan Paul, London.

Kawada, A., Yaguchi, H., Shioiri, S., and Miyake, Y. (1993). Individual differences of the contribution of chromatic channels to brightness. *Journal of the Optical Society of America A*, 10(6):1373–1379.

Kimura, E. and Young, R. S. L. (1995). Nature of the pupillary responses evoked by chromatic flashes on a white background. *Vision Research*, 35(7):897–906.

Kingdom, F. (1997). Simultaneous contrast: the legacies of Hering and Helmholtz. *Perception*, 26(6):673–677.

Kingdom, F. and Moulden, B. (1988). Border effects on brightness: a review of findings, models and issues. *Spatial Vision*, 3(4):225–262.

Kitaoka, A. (2005). *Trick Eyes*. http://www.ritsumei.ac.jp/˜akitaoka/light.html.

Klingner, J., Tversky, B., and Hanrahan, P. (2011). Effects of visual and verbal presentation on cognitive load in vigilance, memory, and arithmetic tasks. *Psychophysiology*, 48(3):323–332.

Laeng, B., Brennen, T., Elden, Å., Gaare Paulsen, H., Banerjee, A., and Lipton, R. (2007). Latitude-of-birth and season-of-birth effects on human color vision in the Arctic. *Vision Research*, 47(12):1595–1607.

Laeng, B. and Endestad, T. (2012). Bright illusions reduce the eye's pupil. *Proceedings of the National Academy of Sciences of the United States of America*, 109(6):2162–2167.

Laeng, B., Færevaag, F. S., Tanggaard, S., and von Tetzchner, S. (2018). Pupillary Responses to Illusions of Brightness in Autism Spectrum Disorder. *i-Perception*, 9(3):204166951877171–11.

Laeng, B., Sirois, S., and Gredebäck, G. (2012). A Window to the Preconscious? *Perspectives on Psychological Science*, 7(1):18–27.

Laeng, B. and Sulutvedt, U. (2013). The Eye Pupil Adjusts to Imaginary Light. *Psychological Science*, 25(1):188–197.

Lee, J. and Stromeyer, C. F. (1989). Contribution of human short-wave cones to luminance and motion detection. *The Journal of Physiology*, 413(1):563–593.

Leonards, U., Troscianko, T., Lazeyras, F., and Ibanez, V. (2005). Cortical distinction between the neural encoding of objects that appear to glow and those that do not. *Brain research. Cognitive brain research*, 24(1):173–176.

Libet, B., Gleason, C. A., Wright, E. W., and Pearl, D. K. (1983). Time of conscious intention to act in relation to onset of cerebral activity (readiness-potential). *Brain*, 106(3):623–642.

Lin, C.-L., Jung, M., Wu, Y. C., She, H.-C., and Jung, T.-P. (2015). Neural Correlates of Mathematical Problem Solving. *International Journal of Neural Systems*, 25(02):1550004–17.

Loewenfeld, I. E. (1993). The Pupil: Anatomy, physiology, and clinical applications.

Long, F., Yang, Z., and Purves, D. (2006). Spectral statistics in natural scenes predict hue, saturation, and brightness. *Proceedings of the National Academy of Sciences*, 103(15):6013–6018.

Loskutova, E., Nolan, J., Howard, A., and Beatty, S. (2013). Macular Pigment and Its Contribution to Vision. *Nutrients*, 5(6):1962–1969.

Lotto, R. B., Williams, S. M., and Purves, D. (1999). An empirical basis for Mach bands. *Proceedings of the National Academy of Sciences*, 96(9):5239–5244.

Lu, H., Zavagno, D., and Liu, Z. (2006). The Glare Effect Does Not Give Rise to a Longer-Lasting Afterimage. *Perception*, 35(5):701–707.

Lucas, R. J., Douglas, R. H., and Foster, R. G. (2001). Characterization of an ocular photopigment capable of driving pupillary constriction in mice. *Nature Neuroscience*, 4(6):621–626.

Lüdtke, H., Kriegbaum, C., Leo-Kottler, B., and Wilhelm, H. (1999). Pupillary light reflexes in patients with Leber's hereditary optic neuropathy. *Graefe's archive for clinical and experimental ophthalmology = Albrecht von Graefes Archiv fur klinische und experimentelle Ophthalmologie*, 237(3):207–211.

MacLachlan, C. and Howland, H. C. (2002). Normal values and standard deviations for pupil diameter and interpupillary distance in subjects aged 1 month to 19 years. *Ophthalmic and Physiological Optics*, 22(3):175–182.

Maniglia, M., Thurman, S. M., Seitz, A. R., and Davey, P. G. (2018). Effect of Varying Levels of Glare on Contrast Sensitivity Measurements of Young Healthy Individuals Under Photopic and Mesopic Vision. *Frontiers in Psychology*, 9:3703–7.

Mathôt, S. (2013). A simple way to reconstruct pupil size during eye blinks. pages 1–5.

Mathôt, S., Grainger, J., and Strijkers, K. (2017). Pupillary Responses to Words That Convey a Sense of Brightness or Darkness. *Psychological Science*, 28(8):1116–1124.

Mathôt, S., van der Linden, L., Grainger, J., and Vitu, F. (2013). The Pupillary Light Response Reveals the Focus of Covert Visual Attention. *PLOS ONE*, 8(10):e78168–10.

McCourt, M. E. (1982). A spatial frequency dependent grating-induction effect. *Vision Research*, 22(1):119–123.

Miyamoto, K. and Murakami, I. (2015). Pupillary light reflex to light inside the natural blind spot. *Scientific Reports*, 5(1):1–12.

Muller, M. M., Andersen, S., Trujillo, N. J., Valdes-Sosa, P., Malinowski, P., and Hillyard, S. A. (2006). Feature-selective attention enhances color signals in early visual areas of the human brain. *Proceedings of the National Academy of Sciences*, 103(38):14250–14254.

Müller, M. M., Picton, T. W., Valdes-Sosa, P., Riera, J., Teder-Sälejärvi, W. A., and Hillyard, S. A. (1998). Effects of spatial selective attention on the steady-state visual evoked potential in the 20–28 Hz range. *Cognitive Brain Research*, 6(4):249–261.

Naber, M., Frässle, S., and Einhäuser, W. (2011). Perceptual rivalry: reflexes reveal the gradual nature of visual awareness. *PLOS ONE*, 6(6):e20910.

Naber, M., Frassle, S., Rutishauser, U., and Einhauser, W. (2013). Pupil size signals novelty and predicts later retrieval success for declarative memories of natural scenes. *Journal of Vision*, 13(2):11–11.

Naber, M. and Nakayama, K. (2013). Pupil responses to high-level image content. *Journal of Vision*, 13(6).

Nakano, Y., Ikeda, M., and Kaiser, P. K. (1988). Contributions of the opponent mechanisms to brightness and nonlinear models. *Vision Research*, 28(7):799–810.

Nayatani, Y., Takahama, K., and Sobagaki, H. (1988). Physiological causes of individual variations in color-matching functions. *Color Research & Application*, 13(5):289–297.

Oostenveld, R., Fries, P., Maris, E., and Schoffelen, J. M. (2011). FieldTrip: Open Source Software for Advanced Analysis of MEG, EEG, and Invasive Electrophysiological Data. *Computational Intelligence and Neuroscience*, 2011(1):1–9.

Pamplona, V. F., Oliveira, M. M., and Baranoski, G. V. G. (2009). Photorealistic models for pupil light reflex and iridal pattern deformation. *ACM Transactions on Graphics*, 28(4):1–12.

Park, J. C. and McAnany, J. J. (2015). Effect of stimulus size and luminance on the rod-, cone-, and melanopsin-mediated pupillary light reflex. *Journal of Vision*, 15(3):13–13.

Parry, N. R. A., McKeefry, D. J., Kremers, J., and Murray, I. J. (2016). A dim view of M-cone onsets. *Journal of the Optical Society of America A*, 33(3):A207–7.

Patterson, E. J., Bargary, G., and Barbur, J. L. (2015). Understanding disability glare: light scatter and retinal illuminance as predictors of sensitivity to contrast. *Journal of the Optical Society of America A*, 32(4):576–10.

Prins, N. and Kingdom, F. A. A. (2009). Palamedes: Matlab routines for analyzing psychophysical data. Technical report.

Proença, H. and Alexandre, L. A. (2005). UBIRIS: A noisy iris image database.

Purves, D., Lotto, R. B., Williams, S. M., Nundy, S., and Yang, Z. (2001). Why we see things the way we do: Evidence for a wholly empirical strategy of vision. *Philosophical Transactions of the Royal Society B: Biological Sciences*, 356(1407):285–297.

Purves, D., Monson, B. B., Sundararajan, J., and Wojtach, W. T. (2014). How biological vision succeeds in the physical world. *Proceedings of the National Academy of Sciences*, 111(13):4750–4755.

Purves, D., Shimpi, A., and Lotto, R. B. (1999). An empirical explanation of the cornsweet effect. *Journal of Neuroscience*, 19(19):8542–8551.

Purves, D., Williams, S. M., Nundy, S., and Lotto, R. B. (2004). Perceiving the Intensity of Light. *Psychological Review*, 111(1):142–158.

R Core Team (2016). R: A Language and Environment for Statistical Computing. Technical report, Vienna, Austria.

Rebbeck, T. R., Kanetsky, P. A., Walker, A. H., Holmes, R., Halpern, A. C., Schuchter, L. M., Elder, D. E., and Guerry, D. P. (2002). P gene as an inherited biomarker of human eye color. *Cancer Epidemiology Biomarkers and Prevention*, 11(8):782–784.

Regan, D. (1989). Human brain electrophysiology: Evoked Potentials and Evoked Magnetic Fields in Science and Medicine. Elsevier.

Rosnow, R. L. and Rosenthal, R. (1989). Statistical Procedures and the Justification of Knowledge in Psychological Science. *American Psychologist*, 44(10):1276–1284.

Samuels, E. and Szabadi, E. (2008). Functional Neuroanatomy of the Noradrenergic Locus Coeruleus: Its Roles in the Regulation of Arousal and Autonomic Function Part I: Principles of Functional Organisation. *Current Neuropharmacology*, 6(3):235–253.

Sara, S. J. (2009). The locus coeruleus and noradrenergic modulation of cognition. *Nature Reviews Neuroscience*, 10(3):211–223.

Sirois, S. and Brisson, J. (2014). Pupillometry. *Wiley Interdisciplinary Reviews: Cognitive Science*, 5(6):679–692.

Sivak, M., Schoettle, B., Minoda, T., and Flannagan, M. J. (2005a). Blue Content of LED HeadLamps and Discomfort Glare.

Sivak, M., Schoettle, B., Minoda, T., and Leukos, M. F. (2005b). Short-wavelength content of LED headlamps and discomfort glare. *The Illuminating Engineering Society of North America*.

Spencer, D. E. and Moon, P. (1944). On the Stiles-Crawford Effect. *JOSA*, 34(6):319–329.

Spitschan, M., Jain, S., Brainard, D. H., and Aguirre, G. K. (2014). Opponent melanopsin and S-cone signals in the human pupillary light response. *Proceedings of the National Academy of Sciences*, 111(43):15568–15572.

Sterpenich, V., D'Argembeau, A., Desseilles, M., Balteau, E., Albouy, G., Vandewalle, G., Degueldre, C., Luxen, A., Collette, F., and Maquet, P. (2006). The Locus Ceruleus Is Involved in the Successful Retrieval of Emotional Memories in Humans. *Journal of Neuroscience*, 26(28):7416–7423.

Stormer, V. S., Winther, G. N., Li, S. C., and Andersen, S. K. (2013). Sustained Multifocal Attentional Enhancement of Stimulus Processing in Early Visual Areas Predicts Tracking Performance. *Journal of Neuroscience*, 33(12):5346–5351.

Stringham, J. M., Garcia, P. V., Smith, P. A., Hiers, P. L., McLin, L. N., Kuyk, T. K., and Foutch, B. K. (2015). Macular Pigment and Visual Performance in Low-Light Conditions. *Investigative Opthalmology & Visual Science*, 56(4):2459–2468.

Sturm, R. A. and Frudakis, T. N. (2004). Eye colour: Portals into pigmentation genes and ancestry. *Trends in Genetics*, 20(8):327–332.

Sulutvedt, U., Mannix, T. K., and Laeng, B. (2018). Gaze and the Eye Pupil Adjust to Imagined Size and Distance. *Cognitive Science*, 15(3):529–18.

Suzuki, Y., Minami, T., Laeng, B., and Nakauchi, S. (2019a). Colorful glares: Effects of colors on brightness illusions measured with pupillometry. *Acta Psychologica*, 198:102882.

Suzuki, Y., Minami, T., and Nakauchi, S. (2018). Association between pupil dilation and implicit processing prior to object recognition via insight. *Scientific Reports*, 8(1):1–10.

Suzuki, Y., Minami, T., and Nakauchi, S. (2019b). Pupil Constriction in the Glare Illusion Modulates the Steady-State Visual Evoked Potentials. *Neuroscience*, 416:221–228.

Tamietto, M., Castelli, L., Vighetti, S., Perozzo, P., Geminiani, G., Weiskrantzf, L., and de Gelder, B. (2009). Unseen facial and bodily expressions trigger fast emotional reactions. *Proceedings of the National Academy of Sciences of the United States of America*, 106(42):17661–17666.

Tamura, H., Nakauchi, S., and Koida, K. (2016). Robust brightness enhancement across a luminance range of the glare illusion. *Journal of Vision*, 16(1):10–13.

Team, J. (2018). JASP (Version 0.9)[Computer software].

Thigpen, N. N., Bradley, M. M., and Keil, A. (2018). Assessing the relationship between pupil diameter and visuocortical activity. *Journal of Vision*, 18(6):7–12.

Tsujimura, S., Wolffsohn, J. S., and Gilmartin, B. (2001). A linear chromatic mechanism drives the pupillary response. *Proceedings of the Royal Society B: Biological Sciences*, 268(1482):2203–2209.

Tsujimura, S.-i. and Tokuda, Y. (2011). Delayed response of human melanopsin retinal ganglion cells on the pupillary light reflex. *Ophthalmic and Physiological Optics*, 31(5):469–479.

Wang, C.-A. and Munoz, D. P. (2015). A circuit for pupil orienting responses: implications for cognitive modulation of pupil size. *Current Opinion in Neurobiology*, 33:134–140.

Watson, A. B. and Yellott, J. I. (2012). A unified formula for light-adapted pupil size. *Journal of Vision*, 12(10):12–12.

Weiskrantz, L., Cowey, A., and Mare, C. L. (1998). Learning from the pupil: A spatial visual channel in the absence of V1 in monkey and human. *Brain*, 121(6):1065–1072.

Whitehead, A. J. (2006). Macular Pigment. *Archives of Ophthalmology*, 124(7):1038.

Winn, B., Whitaker, D., Elliott, D. B., and Phillips, N. J. (1994). Factors affecting light-adapted pupil size in normal human subjects. *Investigative Ophthalmology & Visual Science*, 35(3):1132–1137.

Woelders, T., Leenheers, T., Gordijn, M. C. M., Hut, R. A., Beersma, D. G. M., and Wams, E. J. (2018). Melanopsin- and L-cone-induced pupil constriction is inhibited by S- and M-cones in humans. *Proceedings of the National Academy of Sciences of the United States of America*, 115(4):792–797.

Wood, M. (2012). Lightness-The Helmholtz-Kohlrausch effect. *Out of the Wood*, pages 20–22.

Woodhouse, J. M. and Campbell, F. W. (1975). The role of the pupil light reflex in aiding adaptation to the dark. *Vision Research*, 15(6):649–653.

Wook Hong, S. and Shevell, S. K. (2004). Brightness contrast and assimilation from patterned inducing backgrounds. *Vision Research*, 44(1):35–43.

Wyatt, H. J. (1995). The form of the human pupil. *Vision Research*, 35(14):2021–2036.

Yarbus, A. L. (1967). *Eye Movements and Vision*. Plenum Press, New York.

Yoshida, A., Ihrke, M., Mantiuk, R., and Seidel, H.-P. (2008). *Brightness of the glare illusion*. ACM, New York, New York, USA.

Zavagno, D. (1999). Some new luminance-gradient effects. *Perception*, 28(7):835–838.

Zavagno, D. (2005). The phantom illumination illusion. *Perception & Psychophysics*, 67(2):209–218.

Zavagno, D. and Caputo, G. (2001). The Glare Effect and the Perception of Luminosity. *Perception*, 30(2):209–222.

Zavagno, D. and Caputo, G. (2005). Glowing greys and surface-white: the photo-geometric factors of luminosity perception. *Perception*, 34(3):261–274.

Zavagno, D., Daneyko, O., and Sakurai, K. (2011). What can pictorial artifacts teach us about light and lightness? *Japanese Psychological Research*, 53(4):448–462.

Zavagno, D., Tommasi, L., and Laeng, B. (2017). The Eye Pupil's Response to Static and Dynamic Illusions of Luminosity and Darkness. *i-Perception*, 8(4):1–15.